Turning Tears into Sweets: CandyCollect for Pediatric Salivary Pathogen Sampling

Wan-chen Tu

A dissertation
submitted in partial fulfillment of the
requirements for the degree of

Doctor of Philosophy

University of Washington
2025

Reading Committee:
Ashleigh B. Theberge, Chair
Paul K. Drain
Robert E. Synovec

Program Authorized to Offer Degree:
Chemistry

University of Washington

Abstract

Turning Tears into Sweets: CandyCollect for Pediatric Salivary Pathogen Sampling

Wan-chen Tu

Chair of the Supervisory Committee:
Ashleigh B. Theberge
Department of Chemistry

Open microfluidic channels are gaining widespread use in biotechnology, biology, and diagnostics due to their broad applicability and user-friendly design, which enables easy addition or removal of components. Chapter 1 reviews capillary-driven open microfluidic systems and the implementation of open microfluidic channels in helping human specimen sampling. Chapter 2 introduces an improved open microfluidic system with enhanced capillary pumping capabilities. Chapter 3 describes the use of the CandyCollect device—a lollipop-inspired, open microfluidic tool for collecting salivary pathogens—in an initial human subject study. This remote, at-home study demonstrated the CandyCollect device's ability to effectively capture commensal salivary bacteria, including *Streptococcus mutans* and *Staphylococcus aureus*, from healthy adults. Chapter 4 presents the first clinical data using CandyCollect devices to sample pediatric patients diagnosed with Group A Streptococcus (GAS) pharyngitis. In summary, this dissertation spans from the foundational design principles of open microfluidic systems to their practical application in enhancing human pathogen sampling.

TABLE OF CONTENTS

LIST OF FIGURES

ACKNOWLEDGEMENTS

The past five years at UW have been an incredibly rewarding journey, made more meaningful by the wonderful, supportive, and caring people around me. I truly cannot imagine what my time here would have been like without you.

To Ashleigh, I am incredibly grateful to have you as my advisor. You have been a truly transformative experience. Thank you for supporting me and believing in me, even when I doubt myself. Your authenticity and integrity make you a role model for so many of us me, which inspires me to be a better scientist and mentor —thank you. To Sanitta, it's been a pleasure working with you on the CandyCollect project and beyond. To Erwin, thank you for always bringing your blood-related knowledge and fresh ideas to the table. To Jean, thank you for teaching me the fundamentals of microfluidics.

I'm deeply appreciate the entire Theberge/BCME Lab for shaping my graduate experience. It has been a privilege to work with—and learn from—such a diverse and talented group of scientists. A special thank you to Anika McManamen—having you as my first lab partner and friend made all the difference. Your support helped me navigate the anxiety and uncertainty of those first two years. Xiaojing, thank you for your endless patience and kindness in training me and answering my countless questions. I am also grateful to Ulri and Tammi for your guidance during my first year. To my lab co-authors—especially Jodie, Ingrid, and Sophie—thank you for the joy of co-leading projects together. I've learned so much through our collaboration. Thanks also to DB, Carlos, and Damon for your teamwork on the blood filtration project. To Lauren, Filip, Ariel, Maddie, Jamison, Albert, Amanda, Yuting, Jian Wei, and Dostie—I had so much fun working with you and we have so many memorable moments both in and out of the lab. To the many

undergraduate students, I have had the pleasure of working with you over the years—thank you for your dedication and effort. Special thanks to Meg, Damielle, Vicky, Grant, Eden, Mason, Molly, and many others.

I'm also grateful to my collaborators—Ellen, Greg, and Tristan. Your insights and expertise have deeply enriched my research experience. Many thanks to my committee members—Professors Robert Synovec, Bo Zhang, Matt Bush, Paul Drain, and Suzie Pun—for your thoughtful feedback and valuable perspectives.

Heartfelt thanks to Judy, Betty, and Greg—our wonderful nannies—for your care for Emilia. You have been my partners on the other major project of my life, and I couldn't be more grateful for the peace of mind your support has given me while I worked in the lab.

To my friends and family in Taiwan and Seattle, thank you for your unwavering encouragement. To Mom and Dad, thank you for supporting my education from the very beginning and always providing a welcoming home. To the Chiou family, thank you for making me feel I am not far from home.

To myself, thank you for not giving up, even when things get tough.

DEDICATION

To my parents, to my sister, and to my husband, who gave me the space to explore and choose my own path.

To Emilia

Chapter 1 | Introduction

1.1 Capillary flow in open-microfluidic channels

Microfluidics is a relatively recent scientific and interdisciplinary field that has developed rapid advancements over the past few decades and involves the manipulation and control of fluids in microchannels with dimensions less than 1 mm.[1–6] Compared to conventional closed microfluidic systems, open microfluidic systems offer numerous advantages, including enhanced accessibility, simplified fabrication, and ease of use. [7] This is primarily because open systems remove at least one structural component, such as the floor, ceiling, or walls, thus exposing the fluidic environment to the external surroundings. In open channels, fluid manipulation can be achieved via pipetting or via surface tension-driven methods, effectively eliminating the need for actuation components, such as valves or pumps; this not only simplifies operation but also facilitates easier and more cost-effective fabrication.[8,9] A particular subset of these systems, known as "open-microfluidic capillary systems", further refines this approach by controlling fluid within devices that maintain open air–liquid interfaces using capillary forces.[1–3,6,10] Open microfluidic capillary systems are generally straightforward to produce and compatible with a wide array of manufacturing methods, including soft lithography, 3D printing, micromilling, and injection molding.[1] Their versatility has enabled broad application in various domains such as cell culture, sample collection and preparation, enzyme-linked immunosorbent assay (ELISA), gel electrophoresis, and point-of-care diagnostics.[1,3,11,12]

Despite these advantages, a key limitation of capillarity-based systems lies in the progressive decline of flow velocity—and consequently, flow rate—over time. According to the Lucas–Washburn–Rideal (LWR) law, this decline is inversely proportional to the square root of

time.[13,14] To address this limitation, Lee et al. (2020) demonstrated that a capillary tree structure can sustain a relatively high velocity within the root channel.[15] To further extend the duration of sustained flow and expand the potential applications of such systems, we integrated absorbent paper pads at the extremities of the capillary tree branches. This design enhancement is discussed in detail in Chapter 2.

1.2 Microfluidic point-of-care device

Point-of-care (PoC) diagnostics hold significant potential for the early detection and monitoring of a wide range of diseases, including cancer, diabetes, and cardiovascular conditions.[16–19] The COVID-19 pandemic starkly highlighted the vulnerabilities associated with an overreliance on centralized laboratory testing infrastructures. This crisis accelerated the global push to validate alternative specimen types—such as anterior nasal swabs replacing nasopharyngeal swabs—and prompted a broader reevaluation of diagnostic workflows. As a result, there has been a tangible shift from conventional sample collection at centralized healthcare facilities toward decentralized approaches, including self-collection at home or in PoC environments.[16,20] This decentralization is particularly important for increasing diagnostic access in underserved and remote communities, as well as for enabling real-time health monitoring.

To achieve operational efficiency and cost-effectiveness, portable PoC devices increasingly leverage microfluidic technology, particularly microchannels that allow precise manipulation of minute fluid volumes. These microfluidic platforms offer several key advantages: (1) they significantly reduce the required sample volume—by many orders of magnitude—compared to traditional assays, (2) they simplify fluid handling, allowing for the addition or removal of reagents without the need for an expert operator, and, and (3) the ability to perform

complex biological assays using minimal infrastructure.[1–3,21] Open microfluidic PoC devices can enable user-friendly sample collection, processing, and storage—presenting critical advantages for applications in low-resource settings, telemedicine, micro-sampling, and at-home sampling. Microfluidic devices have been successfully validated for collecting and processing a wide array of biological fluids, including blood, including blood,[22,23] plasma,[24,25] sweat,[26,27] and saliva.[28] Many of these platforms are further integrated with downstream analytical capabilities, such as nucleic acid extraction,[29] and immunoassays,[30] enabling comprehensive diagnostic workflows from the in-clinic or at-home settings.

1.3 Sampling tools for saliva collection

Saliva is an accessible, non-invasive biological specimen that has garnered increasing attention for its potential in disease diagnostics and health monitoring. One notable advantage of saliva sampling is its easy collection process, which may be performed by healthcare professionals, by individuals themselves, or by guardians on behalf of children. The procedure is quick, painless, and does not require specialized equipment or invasive tools, making it highly suitable for routine, large-scale, or at-home diagnostic applications.

It has been reported that human saliva contains approximately 20–30% of the proteins present in blood,[31–33] along with a diverse array of biological constituents including commensal microbes, bacterial pathogens, and viral agents[34,35] These findings suggest that saliva is a viable alternative specimen for disease screening, diagnosis, and monitoring.[35,36] Further, biomolecules in saliva can be used to identify a variety of cancers,[37] illicit and prescription drug use,[38,39] and hereditary disorders and hormonal irregularities[40] as well as measure cortisol levels for diagnosing Cushing's syndrome.[41] Infectious disease screening is another prominent application

of salivary diagnostics. Saliva has been used effectively to detect infections caused by the human immunodeficiency virus (HIV),[42] herpesviruses,[34] hepatitis viruses,[43] and other pathogenic viruses and bacteria.[34,35] Additionally, normative studies have established baseline concentrations of various biomarkers in saliva collected from healthy individuals, thereby creating a foundation for future diagnostic reference ranges.[44]

To support these diagnostic applications, a variety of saliva collection tools have been commercialized, enabling sample acquisition both in-clinical and at-home settings. Common technologies include the draining method (SalivaBio Saliva Collection Aid), the spitting method (e.g., SpeciMAX Stabilized Saliva Collection Kit, Greiner Bio-One), the suction method (e.g., Salivette, SalivaBio Oral Swab), and the swab method (e.g., Eswab, ORAcollect™•Dx, V-Chek test card and Whistling, Self-LolliSponge). [45–51]

Although saliva analysis can be less invasive, many sampling methods include a throat swab of the oropharyngeal area of the patient's mouth which can be very unsettling or uncomfortable. This discomfort can reduce user compliance and potentially compromise the quality of the collected sample, leading to inaccurate or inconclusive diagnostic outcomes.[52] To address these limitations and promote a more user-centered approach to saliva-based diagnostics, our group previously developed the CandyCollect device—a novel, lollipop-inspired, open-microfluidic sampling tool designed specifically for the painless and user-friendly collection of salivary pathogens. Initial laboratory studies demonstrated the device's capability to effectively capture *Streptococcus pyogenes*, the bacterium responsible for strep throat. Building on this proof of concept, this dissertation presents a comprehensive evaluation of CandyCollect's versatility and diagnostic potential. Chapter 3 describes its application in nationwide, at-home

human research studies for detecting commensal oral bacteria, including *Streptococcus mutans* and *Staphylococcus aureus*, while Chapter 4 details the first clinical data collected from pediatric patients diagnosed with Group A Streptococcus (GAS) pharyngitis. Together, these studies demonstrate the feasibility of CandyCollect as a scalable and comfortable alternative for salivary pathogen collection.

1.4 Overview of the dissertation

The works presented in this dissertation demonstrate a comprehensive exploration of open microfluidic systems, beginning with their fundamental principles and advancing through to a diverse range of practical applications. These investigations not only highlight the versatility and innovation inherent in open microfluidic technologies but also provide deeper insight into their real-world impacts, particularly in improving human health, enhancing accessibility to diagnostic tools.

1.5 References

1. Berthier E, Dostie AM, Lee UN, Berthier J, Theberge AB. Open Microfluidic Capillary Systems. *Anal Chem*. 2019;91(14):8739-8750. doi:10.1021/acs.analchem.9b01429
2. Jean Berthier KAB and EB. *Open Micorfluidics*.; 2016.
3. Jean Berthier ABT and EB. *Open-Channel Microfluidics Fundamental and Applications*.; 2019.
4. Zeng Y, Khor JW, van Neel TL, et al. Miniaturizing chemistry and biology using droplets in open systems. *Nat Rev Chem*. 2023;7(6):439-455. doi:10.1038/s41570-023-00483-0
5. Zimmermann M, Schmid H, Hunziker P, Delamarche E. Capillary pumps for autonomous capillary systems. *Lab Chip*. 2007;7(1):119-125. doi:10.1039/b609813d
6. Zimmermann M, Bentley S, Schmid H, Hunziker P, Delamarche E. Continuous flow in open microfluidics using controlled evaporation. *Lab Chip*. 2005;5(12):1355-1359. doi:10.1039/b510044e

7. Duffy DC, McDonald JC, Schueller OJA, Whitesides GM. Rapid prototyping of microfluidic systems in poly(dimethylsiloxane). *Anal Chem*. 1998;70(23):4974-4984. doi:10.1021/ac980656z
8. Walker GM, Beebe DJ. A passive pumping method for microfluidic devices. *Lab Chip*. 2002;2(3):131-134. doi:10.1039/b204381e
9. Berthier E, Warrick J, Yu H, Beebe DJ. Managing evaporation for more robust microscale assays: Part 2. Characterization of convection and diffusion for cell biology. *Lab Chip*. 2008;8(6):860-864. doi:10.1039/b717423c
10. Zimmermann M, Schmid H, Hunziker P, Delamarche E. Capillary pumps for autonomous capillary systems. *Lab Chip*. 2007;7(1):119-125. doi:10.1039/b609813d
11. Gutzweiler L, Gleichmann T, Tanguy L, Koltay P, Zengerle R, Riegger L. Open microfluidic gel electrophoresis: Rapid and low cost separation and analysis of DNA at the nanoliter scale. *Electrophoresis*. 2017;38(13-14):1764-1770. doi:10.1002/elps.201700001
12. Gosselin D, Gougis M, Baque M, et al. Screen-Printed Polyaniline-Based Electrodes for the Real-Time Monitoring of Loop-Mediated Isothermal Amplification Reactions. *Anal Chem*. 2017;89(19):10124-10128. doi:10.1021/acs.analchem.7b02394
13. Lucas Ueber das Zeitgesetz des kapillaren Aufstiegs von Flüssigkeiten.
14. Xvii V, Edward Washburn Synopsis BW. *Second Series MGrck, Ig2I P H YSICAL REVIEW. THE DYNAMICS OF CAPILLARY FLOK*.
15. Lee JJ, Berthier J, Kearney KE, Berthier E, Theberge AB. Open-Channel Capillary Trees and Capillary Pumping. *Langmuir*. 2020;36(43):12795-12803. doi:10.1021/acs.langmuir.0c01360
16. Yang SM, Lv S, Zhang W, Cui Y. Microfluidic Point-of-Care (POC) Devices in Early Diagnosis: A Review of Opportunities and Challenges. *Sensors*. 2022;22(4). doi:10.3390/s22041620
17. Mejía-Salazar JR, Cruz KR, Vásques EMM, de Oliveira ON. Microfluidic point-of-care devices: New trends and future prospects for ehealth diagnostics. *Sensors (Switzerland)*. 2020;20(7). doi:10.3390/s20071951
18. Pandey CM, Augustine S, Kumar S, et al. Microfluidics Based Point-of-Care Diagnostics. *Biotechnol J*. 2018;13(1). doi:10.1002/biot.201700047
19. Mao X, Huang TJ. Microfluidic diagnostics for the developing world. *Lab Chip*. 2012;12(8):1412-1416. doi:10.1039/c2lc90022j
20. Sachdeva S, Davis RW, Saha AK. Microfluidic Point-of-Care Testing: Commercial Landscape and Future Directions. *Front Bioeng Biotechnol*. 2021;8. doi:10.3389/fbioe.2020.602659
21. Yager P, Edwards T, Fu E, et al. Microfluidic diagnostic technologies for global public health. *Nature*. 2006;442(7101):412-418. doi:10.1038/nature05064

22. Leuthold LA, Heudi O, Déglon J, et al. New microfluidic-based sampling procedure for overcoming the hematocrit problem associated with dried blood spot analysis. *Anal Chem*. 2015;87(4):2068-2071. doi:10.1021/ac503931g
23. Delahaye L, Veenhof H, Koch BCP, Alffenaar JWC, Linden R, Stove C. *FOCUS SERIES: ALTERNATIVE SAMPLING STRATEGIES Alternative Sampling Devices to Collect Dried Blood Microsamples: State-of-the-Art*.; 2021.
24. Hauser J, Lenk G, Ullah S, Beck O, Stemme G, Roxhed N. An Autonomous Microfluidic Device for Generating Volume-Defined Dried Plasma Spots. *Anal Chem*. 2019;91(11):7125-7130. doi:10.1021/acs.analchem.9b00204
25. Brakewood W, Lee K, Schneider L, Lawandy N, Tripathi A. A capillary flow-driven microfluidic device for point-of-care blood plasma separation. *Frontiers in Lab on a Chip Technologies*. 2022;1. doi:10.3389/frlct.2022.1051552
26. Choi J, Kang D, Han S, Kim SB, Rogers JA. Thin, Soft, Skin-Mounted Microfluidic Networks with Capillary Bursting Valves for Chrono-Sampling of Sweat. *Adv Healthc Mater*. 2017;6(5). doi:10.1002/adhm.201601355
27. Zhang Y, Chen Y, Huang J, et al. Skin-interfaced microfluidic devices with one-opening chambers and hydrophobic valves for sweat collection and analysis. *Lab Chip*. 2020;20(15):2635-2645. doi:10.1039/d0lc00400f
28. Ma H, Khazaee Nejad S, Vargas Ramos D, et al. Lab-on-a-lollipop (LoL) platform for preventing food-induced toxicity: all-in-one system for saliva sampling and electrochemical detection of vanillin. *Lab Chip*. Published online August 29, 2024. doi:10.1039/d4lc00436a
29. Ali N, Rampazzo RDCP, Costa ADiT, Krieger MA. Current Nucleic Acid Extraction Methods and Their Implications to Point-of-Care Diagnostics. *Biomed Res Int*. 2017;2017. doi:10.1155/2017/9306564
30. Alexa R. Meyer, Michael A. Gorin. First point- of-care PSA test for prostate cancer detection. *Clin Genitourin Cancer*. 2019;16:331-332. doi:10.1016/j.clgc.2019.01.006
31. Bandhakavi S, Stone MD, Onsongo G, Van Riper SK, Griffin TJ. A dynamic range compression and three-dimensional peptide fractionation analysis platform expands proteome coverage and the diagnostic potential of whole saliva. *J Proteome Res*. 2009;8(12):5590-5600. doi:10.1021/pr900675w
32. Yeh CK, Christodoulides NJ, Floriano PN, et al. *Current Development of Saliva/Oral Fluid-Based Diagnostics*. http://www.mc.uky.edu/microbiology/miller.asp
33. Pfaffe T, Cooper-White J, Beyerlein P, Kostner K, Punyadeera C. Diagnostic potential of saliva: Current state and future applications. *Clin Chem*. 2011;57(5):675-687. doi:10.1373/clinchem.2010.153767
34. Slots J, Slots H. Bacterial and viral pathogens in saliva: Disease relationship and infectious risk. *Periodontol 2000*. 2011;55(1):48-69. doi:10.1111/j.1600-0757.2010.00361.x

35. Corstjens PLAM, Abrams WR, Malamud D. Detecting viruses by using salivary diagnostics. *Journal of the American Dental Association*. 2012;143:12S-18S. doi:10.14219/jada.archive.2012.0338
36. Hofman LF. *Innovative Non-or Minimally-Invasive Technologies for Monitoring Health and Nutritional Status in Mothers and Young Children Human Saliva as a Diagnostic Specimen 1*. Vol 131.; 2001.
37. Hu S, Arellano M, Boontheung P, et al. Salivary proteomics for oral cancer biomarker discovery. *Clinical Cancer Research*. 2008;14(19):6246-6252. doi:10.1158/1078-0432.CCR-07-5037
38. 23 OraSure Technologies.
39. Aps JKM, Martens LC. Review: The physiology of saliva and transfer of drugs into saliva. *Forensic Sci Int*. 2005;150(2-3):119-131. doi:10.1016/j.forsciint.2004.10.026
40. Eliaz Kaufman, Ira B. Lamster. The diagnostic applications of saliva--a review. *Crit Rev Oral Biol Med*. 2002;13(2):197-212.
41. Doi M, Sekizawa N, Tani Y, et al. *Late-Night Salivary Cortisol as A Screening Test for the Diagnosis of Cushing's Syndrome in Japan*. Vol 55.; 2008.
42. Wesolowski LG, Mackellar DA, Facente SN, et al. Post-marketing surveillance of OraQuick whole blood and oral fluid rapid HIV testing. 2006;20:1661-1666.
43. Raggam RB, Wagner J, Michelin BDA, et al. Reliable detection and quantitation of viral nucleic acids in oral fluid: Liquid phase-based sample collection in conjunction with automated and standardized molecular assays. *J Med Virol*. 2008;80(9):1684-1688. doi:10.1002/jmv.21245
44. Mohamed R, Campbell J, Cooper-White J, Dimeski G, Punyadeera C. The impact of saliva collection and processing methods on CRP, IgE, and Myoglobin immunoassays. *Clin Transl Med*. 2012;1(1). doi:10.1186/2001-1326-1-19
45. De Meyer J, Goris H, Mortelé O, et al. Evaluation of Saliva as a Matrix for RT-PCR Analysis and Two Rapid Antigen Tests for the Detection of SARS-CoV-2. *Viruses*. 2022;14(9):1931. doi:10.3390/v14091931
46. Ottaviano E, Parodi C, Borghi E, et al. Saliva detection of SARS-CoV-2 for mitigating company outbreaks: a surveillance experience, Milan, Italy, March 2021. *Epidemiol Infect*. 2021;149:e171. doi:10.1017/S0950268821001473
47. Melo Costa M, Benoit N, Dormoi J, et al. Salivette, a relevant saliva sampling device for SARS-CoV-2 detection. *J Oral Microbiol*. 2021;13(1). doi:10.1080/20002297.2021.1920226
48. NAVAZESH M. Methods for Collecting Saliva. *Ann N Y Acad Sci*. 1993;694(1):72-77. doi:10.1111/j.1749-6632.1993.tb18343.x

49. Sobczak Ł, Goryński K. Evaluation of swabs from 15 commercially available oral fluid sample collection devices for the analysis of commonly abused substances: Doping agents and drugs of abuse. *Analyst*. 2020;145(22):7279-7288. doi:10.1039/d0an01379j
50. Topkas E, Keith P, Dimeski G, Cooper-White J, Punyadeera C. Evaluation of saliva collection devices for the analysis of proteins. *Clinica Chimica Acta*. 2012;413(13-14):1066-1070. doi:10.1016/j.cca.2012.02.020
51. Golatowski C, Gesell Salazar M, Dhople VM, et al. Comparative evaluation of saliva collection methods for proteome analysis. *Clinica Chimica Acta*. 2013;419:42-46. doi:10.1016/j.cca.2013.01.013
52. Kaitz M, Sabato R, Shalev I, Ebstein R, Mankuta D. Children's noncompliance during saliva collection predicts measures of salivary cortisol. *Dev Psychobiol*. 2012;54(2):113-123. doi:10.1002/dev.20580

Chapter 2 **| *Enhanced capillary pumping using open-channel capillary trees with integrated paper pads***

Reproduced in part from Jodie C. Tokihiro, Wan-chen Tu,* Jean Berthier,* Jing J. Lee, Ashley M. Dostie, Jian Wei Khor, Madeleine Eakman, Ashleigh B. Theberge,[#] Erwin Berthier,[#] "Enhanced capillary pumping using open-channel capillary trees with integrated paper pads." Physics of Fluids 35, 082120 (2023). https://doi.org/10.1063/5.0157801*

** Equal contribution*
[#] Co-corresponding authors

JCT: Data curation (equal); Formal analysis (equal); Investigation (equal); Methodology (equal); Project administration (equal); Validation (equal); Visualization (equal); Writing – original draft (equal); Writing – review & editing (equal). WCT: Data curation (equal); Formal analysis (equal); Investigation (equal); Methodology (equal); Project administration (equal); Validation (equal); Visualization (equal); Writing – original draft (equal); Writing – review & editing (equal). JCB: Conceptualization (equal); Data curation (equal); Formal analysis (equal); Methodology (equal); Supervision (equal); Validation (equal); Writing – original draft (equal); Writing – review & editing (equal). JJL: Data curation (equal); Formal analysis (equal); Investigation (equal); Methodology (equal); Software (equal); Writing – original draft (equal). AMD: Data curation (equal); Investigation (equal); Writing – original draft (equal). JWK: Conceptualization (equal); Formal analysis (equal); Writing – review & editing (equal). ME: Investigation (equal); Writing – review & editing (equal). ABT: Conceptualization (equal); Formal analysis (equal); Funding acquisition (equal); Project administration (equal); Supervision (equal); Writing – review & editing (equal). EB: Conceptualization (equal); Formal analysis (equal); Funding acquisition (equal); Supervision (equal); Writing – review & editing (equal).

Abstract

The search for efficient capillary pumping has led to two main directions for investigation: first, assembly of capillary channels to provide high capillary pressures, and second, imbibition in absorbing fibers or paper pads. In the case of open microfluidics (i.e., channels where the top boundary of the fluid is in contact with air instead of a solid wall), the coupling between capillary channels and paper pads unites the two approaches and provides enhanced capillary pumping. In this work, we investigate the coupling of capillary trees—networks of channels mimicking the branches of a tree—with paper pads placed at the extremities of the channels, mimicking the

small capillary networks of leaves. It is shown that high velocities and flow rates (7 mm/s or 13.1 µL/s) for more than 30 seconds using 50% (v/v) isopropanol, which has a 3-fold increase in viscosity in comparison to water; 6.5 mm/s or 12.1 µL/s for more than 55 seconds with pentanol, which has an 3.75-fold increase in viscosity in comparison to water; >3.5 mm/s or 6.5 µL/s for more than 150 seconds with nonanol, which has an 11-fold increase in viscosity in comparison to water) can be reached in the root channel, enabling higher sustained flow rates than that of capillary trees alone.

2.1 Introduction

Simple and autonomous microfluidic systems can be designed by use of capillary forces. In such systems, bulky active pumps[1,2] are not needed. However, a major drawback in a capillarity-based system is the decrease of the flow velocity—and the flow rate—with time. According to the Lucas-Washburn-Rideal (LWR) law, the decrease of the velocity is proportional to the inverse of the square root of time.[3–5] To overcome this drawback, different capillary pump designs have been developed.

Whereas many passive designs have been developed for capillary-driven flows in closed channels[6-9], few have been yet proposed in the case of open channels. The electrowetting-based pumping device proposed by Satoh *et al.* is one of the first pumping designs in open geometries, but requires the addition of electric actuation.[10] The most current open-pumping systems rely on evaporation. Evaporation from a rectangular open-channel has been documented by Kolliopoulos *et al.*[11] and Lynn *et al.*[12] and pumping has been set from a reservoir or fibrous pads by Zimmermann *et al*.[13] However, these methodologies are restricted to low boiling point liquids and entail long experiment durations. The search for efficient open channel pumping based solely

on geometrical features is currently progressing. Srinivasan has proposed a geometrical diffuser for zero gravity pumping in space vanes[14] and Guo *et al.* have developed an interesting system combining capillarity in closed channels and additional pumping from paper pads has been documented.[15]

In this work, the pumping mechanism involves the use of networks of small channels where the capillary pressure is high, or matrices of fibers (often paper pads) with a high wicking power. These capillary pumps are placed behind the "region of interest" where the biological or chemical processes are performed and can be used in multiple applications including separation methods or sample processing.

Capillary trees for capillary pumping in closed (confined) channels have been developed in the past.[16] Examples include triple tree line capillary pumps used for performing immunoassays,[17] microstructures for simple and advanced capillary pumping,[18] and multilayers of microfluidic paper to generate the capillary flow.[19, 20] On the other hand, it was shown that microporous and fibrous structures, such as paper pads or porous membranes, provide efficient pumping properties due to their high wicking power.[21-23]

In the capillary-driven microfluidics field, open systems are of special interest.[24–26] These systems remove at least one 'wall' of the microfluidic channel (often the top wall), providing easy access to the flowing liquid in the channels. We have previously found that a capillary tree can be used to maintain a high value of velocity in the root channel—the channel of interest for a given application—in open microfluidic devices.[27]

In this work, we show that these open capillary tree channels can easily be connected to paper pads (mimicking the small capillary networks of leaves). We have chosen to use an open

channel instead of a closed capillary tree due to fabrication limitations such as difficulty in adjusting a cover plate over the trees with minimal to no leakage of the flowing solvent.

In itself, an “infinite” capillary tree with decreasing channels has been shown to be favorable for pumping, but practically, it is impossible to design and fabricate such a device. In addition, paper alone is limited by the high friction of the liquid in the microporous media. Hence, the additive structure constituted by the paper pads replaces the downscaling of the trees and enhances the global pumping effect, first coming from the capillary tree and then from the fibrous paper “leaves”. The paper pads are placed in milled receptacles at the end of the branched channels. We used a geometric design of capillary trees where the root channel is successively divided in a cascade of daughter channels and the cross sections of the daughter channels are progressively decreased in a ratio of 0.85. With this design, a high flow rate in the root channel can be achieved and sustained with such designs using bifurcations and paper pads (Figure 2.1). The multiplication of the tree branches avoids the velocity decrease in the root channel predicted by the Lucas-Washburn law in the case of a constant cross-section channel. The flow rate decreases in the branches after each bifurcation, but the flow rate in the root channel is twice that of the first branches and four times that in the second branches, and so on. On the other hand, the multiplication of the pads in parallel palliates the friction effect in each pad on the flow rate in the root channel.

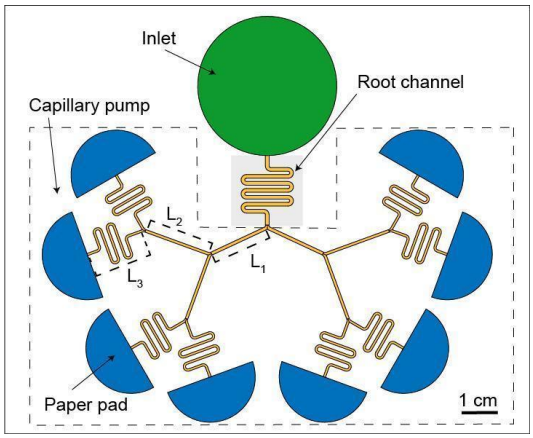

Figure 2.1. Diagram of an open channel microfluidic device utilizing a capillary tree channel and paper pads.

A closed form model for the flow dynamics is derived here, coupling the formulation of the capillary tree flow with the paper pads. In this manuscript, it will be shown that high capillary velocities are obtained even in the case of highly viscous fluids, pentanol, and nonanol. While there are publications where paper pads are used to drive flow[15,23], to the best of our knowledge, this is the first study to couple paper pads to bifurcating trees, specifically in open channel systems. We show here that by combining homothetic capillary tree channels with paper pads in an open microfluidic device, such designs maintain a high liquid velocity (7 mm/s or 13.1 µL/s) for more than 30 seconds using 50% (v/v) isopropanol, which has a 3-fold increase in viscosity in comparison to water; 6.5 mm/s or 12.1 µL/s for more than 55 seconds with pentanol, which has an 3.75-fold increase in viscosity in comparison to water; >3.5 mm/s or 6.5 µL/s for more than 150 seconds a fluid that has a viscosity that is 11 times higher than water in the root channel for more than one minute.

2.2. Materials and Methods

2.2.1. Fabrication of capillary tree channels

The device consists of winding serpentine-shaped channels (the root channel), a large inlet in which the liquid is introduced using a pipette, three levels of branches, and semicircle paper pads at the extremity of the last set of channel branches (Figure 2.1). The dimensions of the channels are listed in Appendix Table A2; an engineering drawing is included in Appendix A; and the computer-aided design files are included in the electronic Appendix A. The widths and depths of the channels are homothetically reduced by a factor of 0.85 after each bifurcation. The turns in the winding channels do not affect the capillary flow in the absence of capillary filaments,[28] as the rounded bottom avoids the formation of filaments observed in channels of rectangular cross section.[29] The average wall friction length of the root channel is estimated to be $\lambda\sim$ 259 μm from our preceding work.[27,30] It was shown that the average friction length produces the value of the average wall friction τ by the formula $\tau = \mu V/\lambda$[21], where μ is the liquid viscosity.

The device was designed using a computer aided design (CAD) software (Solidworks 2017, Waltham, MA) and the design files were converted to G-code using a computer aided manufacturing (CAM) software (Fusion 360). Channels were milled in poly(methyl methacrylate) (PMMA) sheets (3.175 mm thick, #8560K239; McMaster-Carr, Sante Fe Springs, CA). To create round bottom channels, endmills with a cutter diameter of 1/32" (TR-2-0312-BN) and 1/64" (TR-2-0150-BN) were used (Performance Micro Tool, Janesville, WI). The devices were fabricated via micromilling on a Datron Neo computer numerical control (CNC) mill (Datron, Germany). The channel bottom is estimated to have a few microns of roughness which is one magnitude below

the roughness values that were observed by Lade et al.[31] that would produce fluctuations in flow velocity.

2.2.2. Paper pads

Whatman #1 paper (Whatman Grade 1 Qualitative Filter Paper, #28450-160, VWR Scientific, San Francisco, CA) was cut into half circle shapes using a Plotter cutter (Graphtec). A tight contact between the paper pads and the outlets of the last tree channels is essential to maintaining the capillary flow of the fluid. The main characteristics of the paper pads are listed in the Supplemental Material Table SIII. The capillary pressure depends on the liquid that is used and the values are in alignment with the experimental results.

2.2.3. Solvents

The physical properties of the solvents are indicated in the Appendix Table A1. To mitigate evaporation of the solvents, pentanol and nonanol, which are low volatile solvents, (boiling points are 139°C and 213°C for pentanol and nonanol, respectively), were used. Both pentanol and nonanol have been colored with either Solvent Yellow 7 or with Solvent Green 3 (Sigma-Aldrich) at concentrations of 0.50 mg/mL and 1.43 mg/mL, respectively. Aqueous isopropyl alcohol (IPA) (VWR Scientific) was used at a concentration 50% (v/v) and colored with 0.60 % yellow or 1.2 % blue food coloring. (McCormick). Note that the surface tensions of the aqueous IPA solutions decrease with the concentration while the viscosity increases, but the capillary force ($\gamma\cos\vartheta$) stays nearly constant above a concentration of 20% (v/v).

2.2.4. Capillary trees with integrated paper pads flow experiments

To obtain fluid travel distance and velocity data, 2 mL of the yellow-dyed fluid was pipetted into the reservoir of the device. Once the fluid front reached the end of level 1, a 200 µL refill of the yellow fluid was added. After the yellow fluid wetted the paper pad, 500 µL of the blue-dyed fluid was pipetted into the fluid reservoir with a 200 µL refill after the blue fluid front reached the end of level 1. Data was reported up to the point with when the paper pad was saturated at 90 s for IPA50, 57s for pentanol, 154 s for nonanol, for trials 1-3, respectively (Figure 2.3 and Fig. AIIII)).

2.2.5. Imaging and Analysis

Videos of the progression of the solvent flow in the device were recorded using a Nikon-D5300 ultra-high resolution single lens reflective (SLR) camera. The images of the videos were extracted automatically by the code. The location of the tip of the 50% IPA flow was pinpointed using MATLAB software, while the travel distance of the pentanol and nonanol flows were measured manually using Fiji (ImageJ) software. For the manual analysis, the scale was set for an individual trial with the “Set Scale” tool. The fluid front was pinpointed with the “Segmented Line” tool and the “Measure” function was used to calculate the total distance traveled along the capillary tree. Each data was from every 10 frames (yellow) or 30 frames (blue).

2.3 Results and Discussion

2.3.1. Theory

In the first phase, the flow advances in the capillary tree, dividing itself at each bifurcation. The device is designed so that the tree is symmetrical, thus all fluidic channels have the same

length. This motion has already been analyzed in our prior work.[27] We describe here a theoretical approach for open capillary channel bifurcating trees coupled to paper pads. The nomenclature and associated definitions used in this section can be found in Table 2.1.

TABLE 2.1. Nomenclature for theoretical approach

Symbol	Definjtion	[Unit]
Latin, lower case		
p	perimeter	[mm]
P_0	perimeter of root channel	[mm]
p_n	perimeter of branch n	[mm]
t	time	[s]
t_n	time at extremity of branch n	[s]
t_0	time at exit of the root channel	[s]
z	travel distance	[mm]
z_0	travel distance (root channel)	[mm]
z_n	travel distance in branch n	[mm]
z_p	travel distance in the paper pad	[mm]
Latin, upper case		
A_n	characteristic treelength (n branches)	[mm]
C	coefficient of the LW law	[mm^2/s]
K	permeability (paper pad)	[mm^2]
L	length of a branch	[mm]
L_0	length of root channel	[mm]
P	pressure	[Pa]
P_j	pressure at node j	[Pa]
P_{cap}	capillary pressure	[Pa]
S	cross-sectional area	[mm^2]
S_0	cross-sectional area (root channel)	[mm^2]
S_{p0}	cross-sectional area (paper pad entrance)	[mm^2]
V	velocity	[mm/s]
V_0	velocity (root channel)	[mm/s]
V_n	velocity (branch n)	[mm/s]

Greek, lower case		
α	homothetic factor	[non-dimensional]
β	geometrical angle of the circular pad	[rd]
γ	liquid-air surface tension	[mN/m]
λ	porosity (paper pad)	[non-dimensional]
μ	friction length	[mm]
τ	liquid viscosity	[mPa.s]
θ	time (for paper pads)	[s]
Θ*	Young angle	[rd]
ϕ	generalized Cassie angle	[rd]
Greek, upper case		
∇	gradient operator	[1/mm]
Σ_n	characteristic number for the tree	[non-dimensional]

Let us recall that the marching distance in the open root channel (the channel before the beginning of the bifurcations) is given by

$$z_0 = \sqrt{\frac{2\,\lambda\,\gamma\,cos\theta_0^*}{\mu}}\,\sqrt{t} \qquad (1)$$

where λ is the average wall friction length,[28] γ is the surface tension, μ is the viscosity, t is the time, ϑ^* is the generalized Cassie angle,[32] and index *0* refers to the root channel, so that θ_0^* is the generalized Cassie angle in the root channel. Using the pressure at each node (bifurcation) plus the homothetic relation for the channel perimeters, and cross sections and the mass conservation equation, one finds the expression of z_n for the marching distance in the channels after the n^{th} bifurcations:

$$z_n = A_n \left[-1 + \sqrt{1 + \frac{\alpha^n C}{A_n^2}\ (t - t_{n-1})}\right] \quad (2)$$

where $C = \frac{2\,\lambda\,\gamma\,cos\theta^*}{\mu}$, α is the homothetic ratio, t_{n-1} is the time at which the liquid enters the nth channel, and A_n is a geometrical factor which depends on the channel lengths L_0 to L_{n-1} and α. The algebra leading to this expression is lengthy and fully developed in Appendix A Section 1. Note that (2) differs from the Lucas-Washburn expression where $z \sim t^{1/2}$.

Figure 2.2 (Multimedia View) shows the flow of fluid in a device that combines a capillary tree and paper pads. When the flow reaches the paper pads, the wicking of the pads is governed by Darcy's law.[33,34]

$$V_p = -\frac{K}{\mu\phi}\ \nabla P = \frac{K}{\mu\phi}\ \frac{P_{cap} - P_j}{z_p}, \quad (3)$$

where P_{cap} is the capillary pressure of the paper, P_j is the pressure at the channel-paper pad junction, K is the permeability of the pad, and φ *is* its porosity. The index, *p,* refers to the paper, and the triplet (P_{cap}, K, φ) characterizes the paper strip.[35,36] The capillary pressure of the paper pad must be larger—in absolute value—than the pressure P_j at the last nodes so that the liquid continues to flow in the pads (V_p >0). This condition is easily satisfied even if the capillary pressure in the tree increases after each bifurcation: $P_{cap,n} = p_n\,\gamma cos\theta_n^*/S_n = \alpha^{-n} p_0\,\gamma cos\theta_0^*/S_0 = \alpha^{-n} P_{cap,0}$. If we remark that $\alpha^{-n} P_{cap,0} \sim 50$ Pa, and that the capillary pressure in most paper pads is of the order of 3000 Pa at least (Appendix), more than 25

bifurcations will still produce a capillary pressure inferior to that of the pad—considering α=0.85. The derivation of the flow motion in the pads (coupled to the tree) is detailed in the Appendix Section 2. Note that three assumptions are used in the model. First, that the paper pads are homogeneous (i.e., there is no region of higher or lower poverty). Hence, saturation is neglected, and the sharp front assumption is used.[37–39] This observation is confirmed by experiments.[23,37]

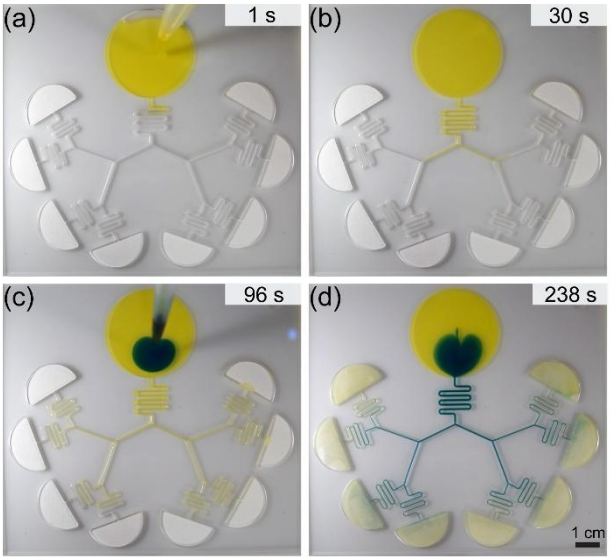

Figure 2.2. Still images of an open channel device filled with yellow and blue nonanol solutions. (a) Yellow liquid is pipetted in the inlet of the open channel. (b) Progression of the yellow liquid in the root channel and capillary tree. (c) Blue liquid is pipetted in the inlet after the yellow liquid reaches the paper pad. (d) Progression of blue liquid in the open channel. Scale bar is 1 cm. (Multimedia View)

Second, it is assumed that the dilatation of the paper fibers from the liquid is negligible, therefore, the porosity φ is constant everywhere in the pad. Third, the cellulose fibers do not absorb the wicking liquid, thus the mass conservation of the flowing liquid is independent of time.

Equation (3) can be solved using the expression of the pressure, P_j, found in the first phase

(flow in the tree) and assuming a circular or flat contact line in the conical (angle β) or rectangular pads (β = 0). The travel distance in the paper is then

$$z_p = \frac{a_n}{\left(1+\frac{a_n}{\delta}\right)}\frac{S_{p,0}}{S_0}\left(-1+\sqrt{1+\left(\frac{S_0}{S_{p,0}}\right)^2\frac{b\left(1+\frac{a_n}{\delta}\right)\tau}{a_n^2}}\right) \quad (4)$$

where

$a_n = 2^n \Sigma_n K \frac{p_0 L_0}{\lambda\ S_0}$, $\delta = \frac{S_0}{2\,\beta\,h_p}$, and $b = \frac{2K}{\mu\phi}P_{cap}$. Here, p_0 corresponds to the total perimeter of the cross section of the root channel, S_0 is the cross-section surface area, h_p is the thickness of the paper pad, β is the paper pad cone angle, τ is the time counted from the moment when the liquid reaches the pads, and $\Sigma_n = \left[1+\frac{L_1}{2\alpha^4 L_0}+\ldots+\frac{L_n}{(2\,\alpha^4)^n L_0}\right]$. Note that if β is zero, then δ is infinite, resulting in $\frac{a_n}{\delta}$ to cancel out in equation (4). The two first parameters a_n and δ have the dimension of length, while the unit for b is mm^2/s and Σ_n is dimensionless. The ratio $\frac{S_0}{S_{p,0}}$ is the ratio between the cross-sectional area of the root channel and that of the paper pad (at the junction with the tree). Using the mass conservation equation, the velocity in the root channel when the liquid wicks the paper is given by

$$V_{root} = 2^n V_p \phi \frac{S_p}{S_0} = \phi\left(\frac{S_{p,0}}{S_0}\ \frac{z_p}{\delta}\right)\frac{S_0}{S_{p,0}}\frac{b}{2a\,\Sigma_n\sqrt{1+\left(\frac{S_0}{S_{p,0}}\right)^2\frac{b\left(1+\frac{a_n}{\delta}\right)\tau}{a_n^2}}}\ . \quad (5)$$

where z_p is given by (4).

2.3.2. Comparison with experiments

The travel distance produced by equation (S13) (Appendix A Section 2) has been checked against the experiments using colored solutions of 50% IPA (v/v), pentanol, nonanol (Figure 2.3) flowing in the homothetic tree of ratio α = 0.85. A representative trial for each fluid is shown in Figure 2.3. Raw data for the travel distance for each fluid is presented in Appendix A Figure A2. The travel distances in the tree, as measured by the progression of the fluid front, are well matched by the theory. The theory assumes perfect flow with a circular fluid front in the semi-circular paper pad and perfect synchronization between the pads; however, in our experiments, the fluid front deviates from the theory due not-perfectly circular liquid front in the paper, not perfect synchronization between the flows in the in the different branches and occasional leaking in the space below the pads. Nonetheless, this does not preclude the data. Note that a velocity jump is predicted by the model at the tree/pad junction due to the sudden change of capillary pressure. However, this velocity jump is not high due to the friction along the whole capillary tree. For this reason and because of the connection between channel and pads, this jump is hardly seen in the experiments.

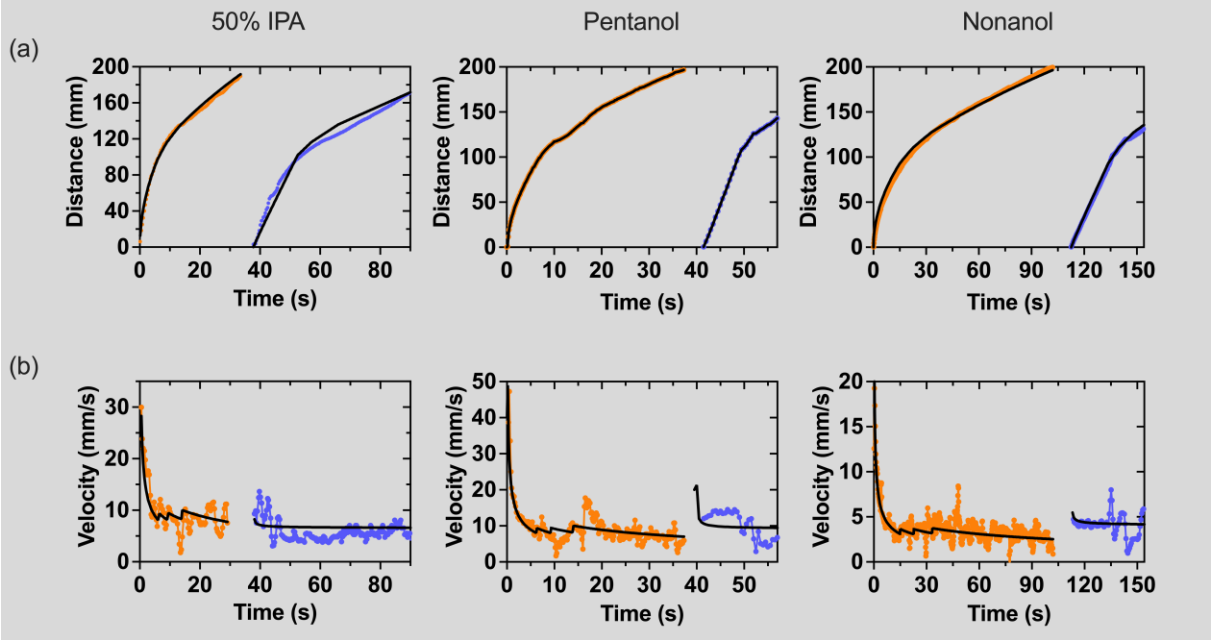

Figure 2.3. Travel distance and velocity over time for 50% (v/v) IPA solution, pentanol, nonanol solutions in an open channel capillary tree with paper pads. (a) Experimentally determined travel distances in the bifurcating capillary tree vs. time for the first phase of the flow (orange dots) and the second phase of the flow (blue dots) after the flow has reached the pads and blue colored solution has been added to the inlet. Travel distance was determined by measuring the distance of the fluid front in the device in the recorded videos. The black lines are the theoretical results. (b) Velocities in the root channel vs. time when the tip of the flow is in the capillary tree (orange dots) and in the paper pads (blue dots). Velocities were determined using equation (5).

In the case of 50% IPA, the coefficient, $\sqrt{\left(\frac{\gamma}{\mu}\right) 2\lambda \cos\theta^*}$, was found to be approximately 40 mm/s$^{1/2}$ (Appendix A Table A1). In the paper pads, a good fit was found for a capillary pressure of 3000 Pa. Root channel velocities on the order of 7 mm/s were obtained for 60 seconds (Figure 2.3) for 50% IPA. The contact of the liquid with the pads occurs at 35 seconds for both 50% IPA and pentanol, and 95 seconds for nonanol (Figure 2.3). Raw velocity data plots are presented in Appendix A Figure A3.

For the case of pentanol, which is a fluid with an "intermediary" viscosity of 3.75 mPa.s. the pentanol also has a good fit for the travel distances in the capillary tree is obtained for the value $\sqrt{\left(\frac{\gamma}{\mu}\right) 2\lambda\, cos\theta^*}$ = 40 mm/s$^{1/2}$.

The case of nonanol is of great interest due to its high viscosity of 0.011 Pa.s. A very good fit for the travel distances in the capillary tree is obtained for the value $\sqrt{\left(\frac{\gamma}{\mu}\right) 2\lambda\, cos\theta^*}$ = 23.7 mm/s$^{1/2}$, and a capillary pressure P_{cap} = 5500 Pa in the paper pad. Root channel velocities on the order of 3.5 mm/s were obtained for 150 seconds (Figure 2.3).

The fluctuations that were observed in the velocity measurements (Figure 2.3) are due to the discretization, *d*z/*d*t. The velocity is the derivative of the travel distance and derivation amplifies the fluctuations. The only physical variation is at the junction between the channel and the paper due to abrupt capillary pressure changes.

2.3.3 Discussion

Efficient capillary pumping has been the subject of many investigations. In this problem, three parameters must be considered: (1) the maximum velocity of the flow, (2) the maximum flow rate, and (3) the duration of the pumping. Prior research has focused on obtaining the highest possible velocities, but typically only for a short time and a moderate volumetric flow rate. For example, Reches *et al.* [40] has obtained interesting velocities of 2 cm/s for water in treated threads of wool, but along a length of 2 cm, corresponding to a duration time of 1 second. In Table 2.2, a review of the literature for various methods of capillary pumping is summarized. The table indicates that it is difficult to obtain high velocities (larger than 1 mm/s) for a long duration (larger than 30 seconds) in capillary-based systems.

Table 2.2. Literature review of capillary pumping

Reference Liquid	Velocity [mm/s]	Flow rate [µL/s]	Duration [s]	Channel characteristics
Water[a]	n/a	0.13	15	Large array of PCB pillars spaced 50 to 300 µm
Water[b]	15	n/a	20	Multilayer paper pads (Whatmann #1) 100 to 200 µm
Water[c]	n/a	0.07	n/a	Large array of pillars spaced 50 µm–- SI chips
Water[d]	0.3	n/a	1000	Paper pads width 1 to 3 cm (rectangular or circular sectors) Millipore nitrocellulose
Water[e]	10	n/a	10	Multilayer paper pads paper 175 µm, gap 36 µm (Whatmann #1)
Glycerol solutions [f]	0.4	n/a	<10	3D printed channels Width 300 µm acrylonitrile-butadiene-styrene
Parylene/ Water[g]	0.4	n/a	< 10	Channels 10 µm parylene
Water, (Wool, Threads)[h]	20	n/a	1	Fiber threads length 1 cm cotton, wool, polyester
<u>This study</u>				Milled capillary trees Width 1 mm to 300 µm
Nonanol	>3.5	6.5	>150	PMMA
50% IPA	7	13.1	>60	

Pentanol	6.5	12.1	>55

[a] Reference 41.

[b] Reference 19.

[c] Reference 42.

[d] Reference 21.

[e] Reference 43.

[f] Reference 31.

[g] Reference 44.

[h] Reference 40.

In our study it is assumed that the capillary tree is “symmetrical”, i.e., all branches at the same level of ramification are identical. The channels are relatively larger in size due to CNC milling constrictions; however, this theory is applicable to smaller dimensions up to 300 µm in width when employing other types of fabrication methods. High velocities are obtained with our device where the dimensions are at the upper side of the microscale limits. If we remark that the root channel velocity is approximately proportional to the square root of the friction length and that the friction length decreases proportionally with the channel dimension, a homothetical reduction of the channel dimension of a factor, n, will result in the reduction of the velocity of a factor $\sqrt{n}$. For example, if the channel cross-section is decreased by 4 (200 µm width), the velocity will be reduced by a factor of 2. Still, high velocities are obtained with the device for microscale channels. The progression of the liquid is the same for each path and is obtained by using the extended LWR law that states that the dynamics of the flow results from the balance between

the capillary force on the advancing meniscus and the wall friction along the path.[3–5,24,25] Intrinsically, capillary-driven flow velocities decrease as capillary length decreases. Here, our device enables longer capillary lengths in the root channel due to the multiplication of daughter branches while maintaining high flow velocities, allowing for applications in diagnostics and bioanalytical chemistry.[24] Note that the approach proposed here is also applicable to closed systems by using the friction length of the closed channels instead of open capillary channels.[24,25] In the microporous paper pads, the wicking liquid velocity is given by Darcy's law[33,34] and determined by three parameters: permeability, porosity, and capillary pressure.[35,36]

To validate the closed form model derived in this work, experiments were performed using nonanol, IPA, and pentanol solutions in open microfluidic channels. We chose these liquids because they wet native PMMA without surface treatment (θ = 13 - 47°, Appendix A Table A1). Further, evaporation of these liquids is slow compared to the time scale of the capillary flow. Hence, evaporation is not taken into account for this study.[3,45–47] High capillary velocities are obtained even in the case of highly viscous nonanol, which has a viscosity eleven times that of water (Appendix A Table A1). In the case of the less viscous IPA aqueous solution, velocities higher than 1 cm/s were obtained.

The device presented here is of interest for its ability to combine velocity, flow rate, and duration. In the future, the device can be optimized to achieve higher velocity. A longer length of the last branch of the capillary tree can enable a higher velocity in the root channel. The choice of the paper matrix is of great importance, especially the two parameters K/φ (Leverett parameter) and capillary pressure (P_{cap}). Longer pads would allow longer duration of the high velocity flow. Additionally, the device can be micromilled using different materials, such as

polystyrene, which enables wider application.[48] Devices can be oxygen plasma treated to allow flow of aqueous solutions (cell culture media, biological fluids, etc.).[26, 48]

2.4 Conclusion

In this work, the dynamics of the capillary flow circulating in a capillary tree with paper pads placed at the extremities of the capillary tree branches have been investigated. A model for the dynamics of the flow in the capillary tree has been coupled to a model for the flow in the paper pads. This coupling has been validated against experiments performed with milled open PMMA channels and paper pads. It is first shown that capillary trees with homothetically decreasing cross-sectional areas (in a ratio of 0.85) maintain the flow velocity in the root channel. Moreover, the presence of paper pads at the extremities of the branches prolongs the duration of the high flow rate pumping. The present analysis demonstrates the possibility of obtaining high velocities and flow rates (7 mm/s or 13.1 µL/s) for more than 30 seconds for IPA 50%, 6.5 mm/s or 12.1 µL/s for more than 55 seconds with pentanol and flow rates of >3.5 mm/s or 6.5 µL/s for more than 150 seconds for nonanol. These flow rates are nearly constant (save periodic jumps due to experimental fluctuations) if conical-shaped paper pads are used as suggested in the literature.[49, 50] For volatile fluids, the employment of evaporation could extend the duration of these high flow rates. Further, we envision many areas of future application including using our method to push the limits of viscous fluid flow in open channels as we can enable the sustained passive flow of complex biological fluids. This device has the potential to be applied to biological experiments such as *in vitro* cell culture or analytical methods involving biological fluids.

2.5 References

1. Gervais L, Hitzbleck M, Delamarche E. Capillary-driven multiparametric microfluidic chips for one-step immunoassays. *Biosens Bioelectron*. 2011; 15,27(1):64-70. doi: 10.1016/j.bios.2011.06.016.
2. R. Safavieh and D. Juncker. Capillarics: pre-programmed, self-powered microfluidic circuits built from capillary elements. *Lab Chip*. 2013; 13: 4180-4189. https://doi.org/10.1039/C3LC50691F
3. Lucas R. Ueber das Zeitgesetz des kapillaren Aufstiegs von Flüssigkeiten. *Kolloid-Z*. 1918; 23, 15. doi: 10.1007/BF01461107.
4. Washburn EW. The dynamics of capillary flow. Phys. Rev. 1921; 17, 273. Doi: 10.1103/PhysRev.17.273.
5. Rideal EK. CVIII. On the flow of liquids under capillary pressure. London, Edinburgh Dublin Philos. 1922; *Mag. J. Sci*. 44(264), 1152. doi: 10.1080/14786441008634082.
6. Juncker D, Schmid H, Drechsler U, Wolf H, Wolf M, Michel B, de Rooij N, Delamarche E. Autonomous Microfluidic Capillary System. *Anal. Chem.,* 2002, 74, 6139-6144. doi: 10.1021/ac0261449
7. Cesaro-Tadic S, Dernick G, Juncker D, Buurman G, Kropshofer H, Michel B, Fattinger C, Delamarche E. High-sensitivity miniaturized immunoassays for tumor necrosis factor α using microfluidic systems. *Lab on a Chip*. 2004; 4, 563-569. doi: 10.1039/B408964B
8. Zimmermann M, Schmid H, Hunziker P, Delamarche E. Capillary pumps for autonomous capillary systems. *Lab on a Chip*. 2007; 7(1):119–125. doi: 10.1039/B609813D
9. Vestad T, Marr DWM, Oakey J. Flow control for capillary-pumped microfluidic systems. *J. Micromech. Microeng*. 2004; 14:1503–1506. Doi: 10.1088/0960-1317/14/11/010.
10. Satoh W, Hosono H, Suzuki H. On-Chip Microfluidic Transport and Mixing Using Electrowetting and Incorporation of Sensing Functions. *Anal Chem*. 2005; 77, 6857-6863. doi: 10.1021/ac050821s.
11. Kolliopoulos P, Jochem KS, Francis LF, Kumar S. Capillary flow of evaporating liquid solutions in open rectangular microchannels. *Journal of Fluid Mechanics*. 2022; 938, A22. doi:10.1017/jfm.2022.140.
12. Lynn NS, Dandy DS. Passive microfluidic pumping using coupled capillary/evaporation effects. *Lab on a Chip*. 2009; 9(23):3422-9. doi:10.1039/b912213c.
13. Zimmermann M, Bentley S, Schmid H, Hunziker P, Delamarche E. Continuous flow in open microfluidics using controlled evaporation. *Lab on a Chip*. 2005; 5(12):1355–9. doi: 10.1039/B510044E
14. Srinivasan R. Estimating zero-g flow rates in open channels having capillary pumping vanes. *Int. J. Numer. Meth. Fluids*. 2003; 41, 389-417. doi: 10.1002/fld.446
15. Guo W, Hansson J, van der Wijngaart W. Capillary pumping independent of the liquid

surface energy and viscosity. *Microsyst. Nanoeng*. 2018; 4: 2. doi: 10.1038/s41378-018-0002-9

16. Olanrewaju A, Beaugrand M, Yafia M, Juncker D. Capillary microfluidics in microchannels: from microfluidic networks to capillaric circuits. *Lab Chip*. 2018; 18(16): 2323-2347. doi: 10.1039/c8lc00458g.
17. Pla-Roca M, Juncker D. PDMS microfluidic capillary systems for patterning proteins on surfaces and performing miniaturized immunoassays. *Methods Mol Biol*. 2011; 671:177-94. doi: 10.1007/978-1-59745-551-0_10.
18. Delamarche E, Juncker D, Schmid H. Microfluidics for processing surfaces and miniaturizing biological assays. *Adv. Mater. 2005*; 17, 2911–2933. doi: 10.1002/adma.200501129.
19. Channon RB, Nguyen MP, Scorzelli AG, Henry EM, Volckens J, Dandy DS, Henry CS. Rapid flow in multilayer microfluidic paper-based analytical devices. *Lab Chip*. 2018; 27, 18(5):793-802. doi: 10.1039/c7lc01300k.
20. Channon RB, Nguyen MP, Henry CS, Dandy DS. Multilayered Microfluidic Paper-Based Devices: Characterization, Modeling, and Perspectives. *Anal Chem*. 2019; 16, 91(14):8966-8972. doi: 10.1021/acs.analchem.9b01112.
21. Mendez S, Fenton EM, Gallegos GR, Petsev DN, Sibbett SS, Stone HA, Zhang Y, López GP. Imbibition in porous membranes of complex shape: quasi-stationary flow in thin rectangular segments. *Langmuir*. 2010; 19, 26(2):1380-5. doi: 10.1021/la902470b.
22. Wang X, Zhou J, Papautsky I. Vortex-aided inertial microfluidic device for continuous particle separation with high size-selectivity, efficiency, and purity. *Biomicrofluidics*. 2013; 21, 7(4):44119. doi: 10.1063/1.4818906.
23. Kokalj T, Park Y, Vencelj M, Jenko M, Lee LP. Self-powered Imbibing Microfluidic Pump by Liquid Encapsulation: SIMPLE. *Lab Chip*. 2014; 21, 14(22):4329-33. doi: 10.1039/c4lc00920g.
24. Berthier J, Brakke KA, Berthier E. Open Microfluidics (Wiley Publishers, 2016)
25. Berthier J, Berthier E, Theberge AB. Open-Channel Microfluidics: Fundamentals and Applications (Morgan and Claypool Publishers, 2019).
26. Berthier E, Dostie AM, Lee UN, Berthier J, Theberge AB. Open Microfluidic Capillary Systems. *Anal Chem*. 2019; 16, 91(14):8739-8750. doi: 10.1021/acs.analchem.9b01429.
27. Lee JJ, Berthier J, Kearney KE, Berthier E, Theberge AB. Open-Channel Capillary Trees and Capillary Pumping. *Langmuir.* 2020; 3, 36(43):12795-12803. doi: 10.1021/acs.langmuir.0c01360.
28. Lee JJ, Berthier J, Theberge AB, Berthier E. Capillary Flow in Open Microgrooves: Bifurcations and Networks. *Langmuir*. 2019; 13, 35(32):10667-10675. doi: 10.1021/acs.langmuir.9b01456.
29. Berthier J, Brakke KA, Gosselin D, Navarro F, Belgacem N, Chaussy D. Spontaneous capillary flow in curved, open microchannels. *Microfluid. Nanofluidics.* 2016: 20, 100. doi:

10.1007/s10404-016-1766-6
30. Berthier J, Brakke KA, Gosselin D, Huet M, Berthier E. Metastable capillary filaments in rectangular cross-section open microchannels. *AIMS Biophys*. 2014; 1(1), 31. 10.3934/biophy.2014.1.31.
31. Lade RK Jr, Hippchen EJ, Macosko CW, Francis LF. Dynamics of Capillary-Driven Flow in 3D Printed Open Microchannels. *Langmuir*. 2017; 28, 33(12):2949-2964. doi: 10.1021/acs.langmuir.6b04506.
32. Berthier J, Gosselin D, Berthier E. A generalization of the Lucas–Washburn–Rideal law to composite microchannels of arbitrary cross section. *Microfluid. Nanofluid*. 2015; 19, 497. doi: 10.1007/s10404-014-1519-3
33. Darcy H. Les Fontaines Publiques de La Ville de Dijon (Paris, 1856)
34. Whitaker S. Flow in porous media I: A theoretical derivation of Darcy's law. *Transp. Porous Media*. 1986; 1, 3. doi: 10.1007/BF01036523.
35. Amico SC, Lekakou C. Axial impregnation of a fiber bundle. Part 1: Capillary experiments. *Polym. Compos.* 2002; 23(2), 249. doi: 10.1002/pc.10429.
36. Ashari A, Vahedi Tafreshi H. General capillary pressure and relative permeability expressions for through-plane fluid transport in thi n fibrous sheets. *Colloids Surf.* 2009; A 346(1–3), 114. doi: 10.1016/j.colsurfa.2009.06.001.
37. Dane JH, Hofstee C, Corey AT. Simultaneous measurement of capillary pressure, saturation, and effective permeability of immiscible liquids in porous media. *Water Resour. Res.* 1998; 34(12), 3687. doi: 10.1029/1998WR900026.
38. Babchin AJ, Bentsen R, Faybishenko B, Geilikman MB. On the capillary pressure function in porous media based on relative permeabilities of two immiscible fluids: Application of capillary bundle models and validation using experimental data. *Adv Colloid Interface Sci.* 2016; 233:176-185. doi: 10.1016/j.cis.2015.07.001.
39. Zarandi MAF, Pillai KM, Kimmel AS. Spontaneous imbibition of liquids in glass-fiber wicks. Part I: Usefulness of a sharp-front approach. *AIChE J*. 2018: 64(1), 294. doi: 10.1002/aic.15965.
40. Reches M, Mirica KA, Dasgupta R, Dickey MD, Butte MJ, Whitesides GM. Thread as a matrix for biomedical assays. *ACS Appl Mater Interfaces*. 2010; 2(6):1722-8. doi: 10.1021/am1002266.
41. Vasilakis N, Papadimitriou KI, Morgan H, Prodromakis T. High-performance PCB-based capillary pumps for affordable point-of-care diagnostics. *Microfluid Nanofluidics*. 2017; 21(6):103. doi: 10.1007/s10404-017-1935-2.
42. Safavieh R, Tamayol A, Juncker D. Serpentine and leading-edge capillary pumps for microfluidic capillary systems. *Microfluid. Nanofluid*. 2015; 18, 357. doi: 10.1007/s10404-014-1454-3.
43. Schaumburg F, Berli CLA. Assessing the rapid flow in multilayer paper-based microfluidic

devices. *Microfluid. Nanofluid*. 2019; 23(98), 98. doi: 10.1007/s10404-019-2265-3.

44. Yang L-J, Yao T-J., Tai Y-C. The marching velocity of the capillary meniscus in a microchannel*. J. Micromech. Microeng*. 2004; 14, 220. doi: 10.1088/0960-1317/14/2/008.
45. Goedecke N, Eijkel J, Manz A. Evaporation driven pumping for chromatography application. *Lab Chip*. 2002; 2(4):219-23. doi: 10.1039/b208031c.
46. Nie C, Frijns AJ, Mandamparambil R, den Toonder JM. A microfluidic device based on an evaporation-driven micropump. *Biomed Microdevices*. 2015; 17(2):47. doi: 10.1007/s10544-015-9948-7.
47. Liu H, Zhang X, Hong Z, Pu Z, Yao Q, Shi J, Yang G, Mi B, Yang B, Liu X, Jiang H, Hu X. A bioinspired capillary-driven pump for solar vapor generation. *Nano Energy*. 2017; 42, 115. doi: 10.1016/j.nanoen.2017.10.039.
48. Berry SB, Lee JJ, Berthier J, Berthier E, Theberge AB. Droplet Incubation and Splitting in Open Microfluidic Channels. *Anal Methods*. 2019; 21;11(35):4528-4536. doi: 10.1039/c9ay00758j.
49. Dosso FD, Tripodi L, Spasic D, Kokalj T, Lammertyn J. Innovative hydrophobic valve allows complex liquid manipulations in a self-powered channel-based microfluidic device. *ACS Sensors.* 2019; 4(3), 694-703. doi: 10.1021/acssensors.8b01555.
50. Elizalde E, Urteaga R, Berli CLA. Rational design of capillary-driven flows for paper-based microfluidics. *Lab Chip*. 2015; 15(10), 2173. doi: 10.1039/C4LC01487A.

Chapter 3 **| *At-home saliva sampling in healthy adults using CandyCollect, a lollipop-inspired device***

Reproduced in part from Wan-chen Tu, Anika M. McManamen,* Xiaojing Su, Ingrid Jeacopello, Meg G. Takezawa, Damielle L. Hieber, Grant W. Hassan, Ulri N. Lee, Eden V. Anana, Mason P. Locknane, Molly W. Stephenson, Victoria A. M. Shinkawa, Ellen R. Wald, Gregory P. DeMuri, Karen Adams, Erwin Berthier, Sanitta Thongpang[#], Ashleigh B. Theberge[#], "At-Home Saliva Sampling in Healthy Adults Using CandyCollect, a Lollipop-Inspired Device." Analytical Chemistry. 2023;**95**(27):10211-10220.*

** Equal contribution*
[#]Co-corresponding authors

WCT, AMM, XS, ERW, GPD, KNA, EB, ST, and ABT conceptualized the research. UNL designed CandyCollect devices. AMM, EVA, and WCT milled CandyCollect devices. DLH, EVA and MWS fabricated candy devices and prepared devices for human subject research. WCT, AMM, XS, MGT, and GWH reviewed the literature that informed the study. WCT, AMM, and XS designed biological experiments. WCT, AMM, XS, and IJ conducted biological experiments and data collection. KNA advised on work with human subjects study design and regulatory protocols. IJ, MGT, GWH, MPL, and VAMS recruited participants, set up the REDCap platform to screen participant eligibility and administer survey questions, packaged and shipped CandyCollects to research participants, and communicated with participants. WCT, AMM, XS, EB, ST, and ABT interpreted the data. WCT, AMM, XS, MPL, ST, and ABT wrote sections of the manuscript. WCT, AMM, XS, and MPL made figures for the manuscript. ERW and GPD provided expertise on clinical relevance and sampling bacteria in saliva. WCT, AMM, XS, MPL, ERW, GPD, KNA, EB, ST, and ABT edited and revised the manuscript, and all authors ap-proved the manuscript. ABT and ST supervised the research.

Abstract

Respiratory infections are common in children, and there is a need for user-friendly collection methods. Here, we performed the first human subjects study using the CandyCollect device, a lollipop inspired saliva collection device.[1] We showed the CandyCollect device can be used to collect salivary bacteria from healthy adults using *Streptococcus mutans* and *Staphylococcus aureus* as proof-of-concept commensal bacteria. We enrolled healthy adults in a nationwide (USA) remote study in which participants were sent study packages containing CandyCollect devices and traditional commercially available oral swabs and spit tubes.

Participants sampled themselves at home, completed usability and user preference surveys, and mailed the samples back to our laboratory for analysis by qPCR. Our results showed that for participants in which a given bacterium (*S. mutans* or *S. aureus*) was detected in one or both of the commercially available methods (oral swab and/or spit tubes), CandyCollect devices had a 100% concordance with the positive result (n=14 participants). Furthermore, the CandyCollect device was ranked the highest preference sampling method among the three sampling methods by 26 participants surveyed (combining survey results across two enrollment groups). We also showed that the CandyCollect device has a shelf life of up to 1 year at room temperature, a storage period that is convenient for clinics or patients to keep the CandyCollect device and use it any time. Taken together, we have demonstrated that the CandyCollect is a user-friendly saliva collection tool that has the potential to be incorporated into diagnostic assays in clinic visits and telemedicine.

3.1 Introduction

Infectious respiratory pathogens are a major health challenge worldwide. Children, in particular, are frequently affected by respiratory diseases.[2] The Covid-19 pandemic has illustrated the importance of global pandemic preparedness, and in particular the need to develop more comfortable and user-friendly sampling methods to test for pathogens. We developed a lollipop-inspired saliva collection device called CandyCollect to enable user-friendly sampling in both children and adults (Figure 3.1). Here, we conducted a human subjects study as a proof-of-concept to demonstrate functionality of the CandyCollect device for capturing bacteria from healthy adults and evaluate the comfort and user experience in comparison to standard saliva collection methods.

As previously reported, the CandyCollect is a saliva sampling device designed to collect *Streptococcus pyogenes* for the diagnosis of Group A streptococcus (GAS) pharyngitis, commonly referred to as strep throat.[1] Strep throat is most commonly seen in children.[3] It is easily treatable with antibiotics when diagnosed, however diagnosis can be thwarted by invasive sampling methods which discourage children (and adults) from successfully completing the sampling process and may result in decreased yields.[4] The gold standard method for diagnosing strep throat is a pharyngeal swab coupled with bacterial culture,[5,6] however, qPCR has become a new tool that can be implemented in diagnosis of strep throat, allowing saliva sampling as a means for diagnosis.[7,8] Current methods for saliva sampling include spit tubes (e.g., SpeciMAX Stabilized Saliva Collection Kit), drooling (e.g., SalivaBio Saliva Collection Aid), swabs (e.g., Eswab™) and cotton rolls (e.g., Salivette®, SalivaBio Oral Swab). In recent years, others have also developed lollipop-inspired devices, such as Self-LolliSponge™ (with lemon-aromatized cap), and non-conventional sampling devices using absorbing materials, e.g. V-Chek™ test card and Whistling™ midstream test.[9-13] The CandyCollect device was designed to facilitate easy, non-invasive, at-home sampling of saliva, particularly for children, which is then shipped to a lab for analysis and diagnosis.[1] The device sampling mimics the action of eating a lollipop, featuring a polystyrene stick with an open microfluidic channel for bacterial capture and isomalt candy that functions as a timer to ensure sufficient sampling time.

Here we demonstrate the versatility and functionality of the CandyCollect device through experimentation and at-home human research studies using commensal bacteria *Streptococcus mutans* and *Staphylococcus aureus* for proof-of-concept. Commensal bacteria exist in the microbiome of healthy hosts.[14,15] Using commensal bacteria as our analytes of interest, as

opposed to *S. pyogenes*, which we reported previously,[1] allowed us to enroll healthy participants for our human subjects research. In doing this, our target population was much broader than the limited population of those with strep throat, allowing greater diversity and easier enrollment of participants. This also provided the opportunity to test different bacteria and access the versatility of CandyCollect devices as a broader microbial sampling method. *S. mutans* and *S. aureus* were specifically selected as analytes due to their high prevalence in the healthy adult population.[16-19] The prevalence of *S. mutans* and *S. aureus* has been reported to vary between 80-87% and 18-39% in healthy adults, respectively.[16-19] In-lab experiments demonstrated the CandyCollect device can capture these commensal bacteria, and, through elution and qPCR, quantify their concentration. Our human subjects study established two key findings regarding the CandyCollect device: (1) the CandyCollect device was the preferred sampling method among participants compared to conventional sampling methods, and (2) the CandyCollect device captures *S. mutans* and *S. aureus*.

3.2 Methods

3.2.1 CandyCollect devices fabrication

CandyCollect device stick fabrication: The CandyCollect devices were milled out of 2 mm and 4 mm polystyrene sheets (Goodfellow, Cat# 235-756-86 and 700-272-86, respectively) using a DATRON computer numerically controlled (CNC) milling machine (Datron) (Appendix Figure B1). Devices were then sonicated in isopropanol (IPA) (FisherScientific, A451-4) and 70% v/v ethanol (FisherScientific, Decon™ Labs, 07-678-004).

Plasma treatment of CandyCollect devices: Devices were plasma treated with oxygen using the Zepto LC PC Plasma Treater (Diener Electronic GmbH, Ebhausen, Germany). The

protocol for plasma treatment is consistent with our previous publication, but in brief, gas was removed from the chamber down to a pressure of 0.20 mbar, oxygen gas was supplied up to 0.25 mbar for 2 minutes and then a 70 W voltage was applied for 5 minutes.[1] Following plasma treatment, devices for spike sample experimentation were ready for use.

Preparation of CandyCollect devices for human subjects study: Candy was applied to CandyCollect sticks in a kitchen following the hygiene guidance outlined in the Washington State Cottage Food Operations Law (RCW 69.22.040(2b-f(ii-iv))). Lab members who prepared CandyCollect were trained in food safety, had a Food Worker Card (WA State), and wore gloves and a mask during food preparation. The isomalt candy was prepared as described in our previous paper.[1] In brief, isomalt was gradually added to water. Food coloring was added with the last portion of isomalt. Once dissolved the isomalt was then heated to either 171 °F (dissolve time <20 min) or 165 °F (dissolve time >20 min). Once target temperature is reached, the pot containing isomalt was quickly placed in room temperature water to initiate cooling. At this time strawberry candy flavoring was quickly added to the mixture, and the isomalt poured onto a marble slab to set. After plasma treatment, CandyCollect polystyrene sticks for the human subjects study were cleaned using hot water and dish soap. Small portions of the isomalt candy were remelted and applied to the CandyCollect sticks using a silicone mold. Once the candy was applied to the sticks, the candy was cooled, the device mass was recorded, and the CandyCollect devices were placed into polypropylene bags and heat sealed. Devices were stored in food preparation containers with a desiccant (Amazon, Cat# B00DYKTS9C) until being sent to participants. CandyCollect devices used in this study had masses ranging from 1.2-1.9 grams on both days (Appendix Table B1-2).

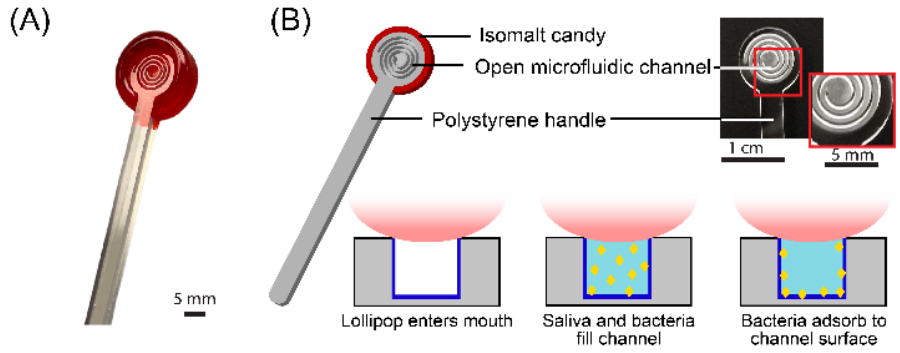

Figure 3.1. (A) The photo of the CandyCollect device. The CandyCollect device is composed of a polystyrene stick with a microfluidic channel and red isomalt candy. The open-fluidic channel is designed to prevent the tongue from removing the collected bacteria, also accumulating bacteria during the sampling time. The candy flavoring functions as a built-in timer for sampling time (i.e., dissolving time of the candy). (B) This figure is reproduced from Lee et al. [1] (Figure 1B) with permission from the Royal Society of Chemistry.

3.2.2 Bacteria culture

Liquid media preparation: The *S. mutans* culture media (trypticase soy yeast extract medium) was prepared based on the method from DSMZ website.20 The *S. aureus* culture media (Tryptic Soy Agar/Broth) was prepared based on the protocol from ATCC.21 The *S. pyogenes* culture media was prepared following the protocol from Gera & McIver, 2013.[22] All liquid media were autoclaved at 121 °C for 30 min, cooled to room temperature, and stored at 4 °C.

Agar plate preparation: 7.5g agar (BD Difco™ Dehydrated Culture Media: Potato Dextrose Agar, Fisher Scientific, Cat# DF0013-17-6) was added to the 500 mL of liquid media, then autoclaved at 121 °C for 30 min. 15 mL of liquid media with agar was added to petri dishes, left to cool overnight, and stored at 4°C until needed for.

S. mutans, *S. aureus*, and *S. pyogenes* maintenance in agar plate: *S. mutans* was prepared from *Streptococcus mutans* Clarke (American Type Culture Collection, ATCC®, Cat# 25175™). 880

µL of liquid media was added to freeze-dried *S. mutans*, and the bacteria suspension was transferred into a 10 mL tube. Additional liquid media was added for a total volume of 8.8 mL. *S. aureus* was prepared from *Staphylococcus aureus* subsp. aureus Rosenbach (American Type Culture Collection, ATCC®, Cat# 25923™). Freeze-dried *S. aureus* was rehydrated in 910 µL of liquid media. *S. pyogenes* was prepared from *Streptococcus pyogenes* Rosenbach (American Type Culture Collection, ATCC®, Cat# 700294™). Freeze-dried *S. pyogenes* was rehydrated with 1 mL liquid media, and then transferred to another conical tube containing 4.4 mL of liquid media. To maintain the bacteria, *S. mutans*, *S. aureus*, and *S. pyogenes* were streaked on their own agar plates by sterile disposable inoculating loops (Globe Scientific, Fisher Scientific, Cat# 22-170-201). The agar plates were incubated at 37 °C with 5% carbon dioxide overnight, then stored at 4°C until needed for experimentation.

3.2.3 In-lab capture of bacteria

Incubation of *S. mutans*, *S. aureus*, and *S. pyogenes* in liquid media: To ensure a pure culture, fresh *S. mutans*, *S. aureus*, and *S. pyogenes* from agar plates were inoculated in liquid media and cultured at 37 °C with 5% carbon dioxide in the incubator one day prior to an experiment.

Capturing, fixing, and staining bacteria: The procedures for capturing, fixing, and staining bacteria in liquid media are detailed in our previous paper.[1] In brief, after culturing overnight, the bacteria suspensions were homogenized with vortexing and added to each CandyCollect device at a volume of 50 µL (devices negative controls were loaded with 50 µL of PBS). Bacteria were incubated in the device for 10 min. For devices that were imaged, bacteria were fixed with 4% paraformaldehyde (PFA) for 15 min, and 50 µL of Alexa FluorTM 488 Wheat Germ Agglutinin

(WGA, InvitrogenTM, Fisher Scientific, Cat# W11261, 1 mg/mL) at 1:500 dilution (v/v) was added to the channel for staining *S. aureus* and *S. pyogenes*; 50 µL of 1:200 (v/v) WGA was added for staining *S. mutans*. An additional three devices were evaluated for a mixture of *S. mutans*, *S. aureus* and *S. pyogenes*, each at a concentration of 10^4 CFU/mL to match physiological bacterial concentration for detection of bacteria in a mixture.

3.2.4 Fluorescence imaging and quantification

Fluorescent images of *S. mutans*, *S. aureus*, and *S. pyogenes* were obtained on a Zeiss Axiovert 200 with a 10× (0.30 NA) objective coupled with Axiocam 503 mono camera (Carl Zeiss AG, Oberkochen, Germany). Four regions of interest were randomly chosen from each device to avoid bias from any regions. The contrast was adjusted uniformly and integrated densities of three regions of interest from each image were quantified using Fiji (ImageJ) software. The details about imaging and quantification for both bacteria followed the protocol from the previous paper.[1]

3.2.5 Elution of S. mutans, S. aureus, and S. pyogenes from CandyCollect devices

The buffer used to elute bacteria captured on CandyCollect devices was phosphate buffered saline (PBS) (Gibco™, Cat# 10010023) with 5% Proteinase K (Thermo Scientific™, Cat# EO0491). 300 µL elution buffer and 100 µL of 0.1 mm Zirconia/Silica beads (BioSpec Products, Cat# 11079101Z) were added in 14 mL round bottom tubes (Corning, Falcon®, 352001) containing CandyCollect devices. After incubating the tubes at 37 °C for 10 min and vortexing for 50 s, CandyCollect devices were left in the elution buffer at 4 °C for 90 min. The bacteria suspension and beads were then transferred from the 14 mL round bottom tubes to 2 mL screw cap

microtubes (ThermoFisher, Cat# 3490). The samples were beat-beaten in a MiniBeadBeater (BioSpec Products, Bartlesville, OK USA), and stored at -20 °C before analysis.

Additional elution buffers evaluated included (1) ESwab™ buffer (Becton, Dickinson and Company, Cat# R723482) with 5% Proteinase K; (2) ESwab™ buffer with 5% ethanol; (3) phosphate buffered saline (PBS) with 2% SDS (sodium dodecyl sulfate); and (4) ESwab™ buffer with 2% SDS. The elution procedures were the same as mentioned above.

3.2.6 Isolation, purification, and enrichment of genomic DNA from S. mutans, S. aureus, and S. pyogenes

DNA was isolated from bacterial lysates using the Mag-MAX™ Total Nucleic Acid Isolation Kit (ThermoFisher Scientific, Cat# AM1840) according to the "Purify the nucleic acid" protocol supplied by the manufacturer. In brief, 115 µL of sample was added to the provided processing plate. 60 µL of 100% IPA was added to each well containing a sample and the plate was shaken for 1 min. 20 µL of bead mix was then added to each well, and the plate was shaken for 5 min to allow DNA to bind to the beads. Beads were captured using a magnetic 96-well separator (Thermofisher, Cat# A14179) and supernatant was discarded. Four washes (two using Wash Solution 1 and additional two using Wash Solution 2 provided by the kit) were performed with shaking for 1 min each and supernatant was discarded between each wash. After final wash, beads were dried and then 23 µL of 65°C elution buffer was added to each sample to elute DNA from the beads. By using these methods, DNA was five-fold concentrated compared to the unprocessed bacterial lysates. The purified bacterial genomic DNA was used as a template in the qPCR assay.

3.2.7 Quantitative PCR assay for detection of S. mutans, S. aureus, and S. pyogenes

The species-specific genes, *S. mutans* gtfB (accession number M17361), encoding glucosyltransferases, and *S. aureus* nuc (accession number CP000046), encoding a thermonuclease, were used for qPCR detection of *S. mutans* and *S. aureus*, respectively. The primers/probe sequences for gtfB were adopted from Lochman et al., 2020,[23] the forward primer: 5'-CCT ACA GCT CAG AGA TGC TAT-3'; the reverse primer: 5'-GCC ATA CAC CAC TCA TGA ATT-3'; the probe: 5'-/56-FAM/TGG AAA TGA/ ZEN/CGG TCG CCG TTA T/3IABkFQ/ -3'. Primers/probe sequences for nuc were adopted from Wood et al., 2021 and Galia et al., 2019,[24, 25] with minor modifications to both forward and reverse primers, the forward primer (F1): 5'-GGC ATA TGT ATG GCA ATC GTT TC-3'; the reverse primer (R1): 5'-CGT ATT GTT CTT TCG AAA CAT T-3'; the probe sequence: 5'-/56-FAM/ATT ACT TAT AGG GAT GGC TAT C/3MGB-NFQ/ -3'. The modified primers were accessed for their specificity using NCBI Blast tool and verified by qPCR assay with purified DNA from *S. aureus*. Details can be found in Appendix Table B3 and Figure B2-3 and the discussion in the Appendix B. All primers and probes for *S. mutans* and *S. aureus* were ordered from IDT (Integrated DNA Technologies, Inc., Coralville, IA, USA). qPCR was performed using PerfeCTa® qPCR ToughMix (VWR, Cat# 97065-954). The 25 µL reaction volume included 5 µL of DNA template and 20 µL PerfeCTa® qPCR ToughMix with primers/probe in the qPCR assay. For *S. mutans* and *S. aureus* analysis, the final concentrations of both forward and reverse primers were 300 nM and 500 nM, respectively; the probe concentration for both bacteria was 250 nM. The details for the qPCR assay for *S. pyogenes* followed the protocol from our previous paper.[1] Briefly, the primers/probe sequences for spy1258 qPCR detection of *S. pyogenes* in our assay were: the forward primer: 5'-GCA CTC GCT ACT ATT TCT TAC CTC AA-3'; the reverse primer: 5'-GTC ACA

ATG TCT TGG AAA CCA GTA AT-3'; the probe sequence: 5'-FAM-CCG CAA C"T"C ATC AAG GAT TTC TGT TAC CA-3'-SpC6, "T" = BHQ1.1 For *S. pyogenes*, the primers were ordered from IDT, the probe was ordered from MilliporeSigma.[1] The 25 µL reaction volume included 10 µL of DNA template and 15 µL PerfeCTa® qPCR ToughMix with primers/probe in the qPCR assay. The final concentrations of both forward and reverse primers were 300 nM; the probe concentration was 100 nM. To quantify the DNA concentrations of samples, 1:10 serial dilution of purified genomic DNA ranging from 25 ng to 25 fg were used as standards for each plate. Each concentration of the standards was allotted into multiple 20 µL aliquots and stored at -80 °C (Appendix Figure B4), to ensure the same standards were used for all human subjects samples. No-template controls (NTC) for qPCR and device negative controls (see "in-lab capturing of bacteria") were also added to the plates. Amplification and detection were performed in 96-well PCR plates using CFX connect Real-Time PCR Detection System (Bio-Rad Laboratories, Hercules, CA, USA) in technical duplicate using the following protocol: 95 °C for 5 min followed by 40 cycles of 15 s at 95 °C and 30 s at 60 °C. The samples were considered positive when the Cq value is within the Cq of the standard curve.

3.2.8 Human subjects study

Participant characteristics: This study was approved by the University of Washington Institutional Review Board (IRB) under IRB-approved protocol STUDY00013842. Written informed consent was obtained prior to study procedures. A total of 28 healthy volunteers over the age of 18 were recruited using the University of Washington Institute of Translational Health Sciences (ITHS) "participate in research" website along with the study's website. Inclusion

criteria: healthy adults over the age of 18. Exclusion criteria: individuals who are allergic to sugar alcohols or individuals who currently reside in a correctional facility.

3.2.9 Human subjects' sample and feedback collection

The entire study was performed remotely using Research Electronic Data Capture (REDCap) for collection of participant information and survey responses (Appendix Table B4), and kits were mailed to study participants and returned to the study team by mail (Appendix Figure B5). Each kit contained six CandyCollects, six ESwab™ (Becton, Dickinson and Company, Cat# R723482), two SpeciMAX Stabilized Saliva Collection Kit (Spit tube) (Thermo Scientific™, Cat# A50697), and an instruction card. Based on the instruction card, participants collected samples for two days, and followed the same order of collection on both days: first, one SpeciMAX Stabilized Saliva Collection Kit, second, three ESwab™, and third, three CandyCollects. Collection for each method was instructed as follows: for the spit tube, participants spit approximately 1 mL of saliva into tubes provided by SpeciMAX Stabilized Saliva Collection kit; for ESwab™, participants sucked on the swab for 30 s and then kept the swab in the buffer provided by ESwab™; for the CandyCollect devices, participants were asked to suck on the lollipop until the candy was fully dissolved then left each CandyCollect device in an individual empty polypropylene 12 mL round bottom tube (Greiner Bio-one, Cat#163261) and record the time required for the candy to dissolve. The samples then were mailed back to our lab for analysis at the end of each day. An electronic survey was sent to each participant on the same day that they collected samples; the survey included CandyCollect dissolving times and any comments they wanted to leave about each of the sampling devices. After the Day 2 survey was completed, a user feedback survey was automatically sent to participants via REDCap. Participants were asked to rank the

different sampling methods as well as answer other specific questions related to the CandyCollect device.

We had two rounds of enrollment, targeting 15 participants per group (Figure 3.2). In group 1, 15 participants were recruited, but one of the participants did not return the kit and was lost to follow-up, so a total of 14 samples were returned and analyzed. Biological data from this group is presented in Figure 3.4. In group 2, 15 participants were recruited, however one participant was lost to follow-up and did not return their kit. A total of 14 kits were returned. Biological data from these samples is not presented in this paper as the samples are being used in an additional biological investigation.

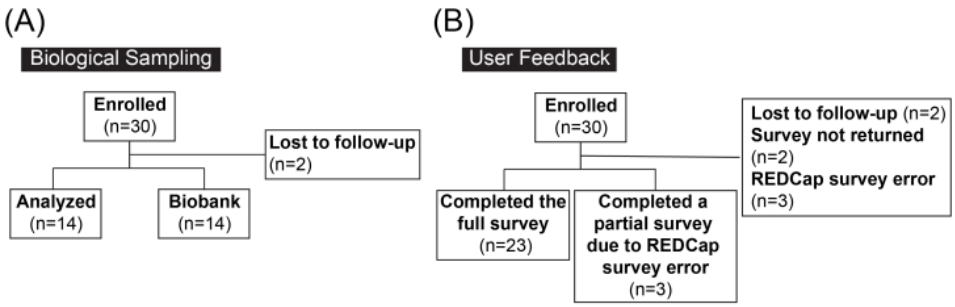

Figure 3.2. Participant flow diagram. (A) Human subjects samples for biological analysis. (B) User feedback surveys.

User feedback from groups 1 and 2 is presented in Figure 3.5. In group 1, all 14 participants answered the survey question corresponding to Figure 3.5A, however due to an electronic survey error, 3 of the 14 participants were unable to complete the survey questions in Figure 3.5B. In group 2, 12 of the 14 participants completed the survey questions in Figure 3.5. This resulted in a total of 26 participants responding to the question in Figure 3.5A and 23

participants responding to the question in Figure 3.5B. Protocol for sampling and surveys were identical for both groups.

3.2.10 Human subject sample processing

Participants stored their samples at ambient temperature, and they were picked up the following day using United Parcel Service (UPS) Next Day Air. Samples were stored at -20 °C upon receipt and transferred to -80 °C for longer term storage before processing. All laboratory procedures were performed in accordance with Biosafety Level-2 laboratory practices and the University of Washington Site-Specific Bloodborne Pathogen Exposure Control Plan. *S. mutans* and *S. aureus* on CandyCollect devices were eluted and lysed following the protocol stated above. To avoid unnecessary freeze-thaw cycles, ESwab™ and SpeciMAX Stabilized Saliva Collection Kits samples were aliquoted into 20 µL aliquots and stored at -80 °C. For ESwab™ and SpeciMAX Stabilized Saliva Collection Kits samples, DNA was isolated using MagMAX™ Total Nucleic Acid Isolation Kit (ThermoFisher Scientific, Cat# AM1840) according to the protocol "Disruption of liquid samples" supplied by the manufacturer. Briefly, 175 µL of aliquoted samples were transferred to each bead beating tube provided in the kit followed by the addition of 230 µL of Ly sis/Binding solution. Bead beating was carried out via MiniBeadBeater (mentioned above) twice for 30 s, then each tube was centrifuged at 16,000 g for 3 min. Afterward, genomic DNA of S. mutans and S. aureus was isolated and enriched following the protocol stated above and quantified using qPCR with a detection limit of 25 fg.

3.2.11 Human subject data analysis

Conversion factor: DNA content reported by the qPCR analysis was converted to estimated copy number of bacterial DNA/mL to facilitate comparisons between the three methods of saliva collection: CandyCollect, ESwab™, and SpeciMAX Stabilized Saliva Collection Kits. A conversion factor to derive bacterial concentrations/DNA content was calculated for each method, taking into consideration the variations in the collection and processing.

In brief, qPCR results from the CFX connect Real-Time PCR Detection System were reported in ng of DNA corresponding to the 5 µL samples loaded into the machine. Dilutions corresponding to the purification and enrichment of samples (see Methods section "Isolation, purification, and enrichment of genomic DNA from *S. mutans*, *S. aureus*, and *S. pyogenes*") were used to derive the DNA content of samples input into the purification and enrichment procedure. Estimates for sample dilution during sampling were employed to further convert the qPCR output reading to ng DNA per mL saliva. These sample dilution estimates are as follows: Spit tube, we assumed participants provided 1 mL of saliva as instructed into a tube containing 1 mL of stabilization solution; ESwab™, we assumed 130 µL of saliva is captured during sampling which was then stored in 1 mL of ESwab™ buffer; CandyCollect, we assumed 50 µL of saliva was captured by device. To report copy number of bacterial DNA/mL, based on the genome sizes of the bacteria (2.6 fg / genome for *S. mutans*, 3.0 fg /genome for *S. aureus*),[26, 27] detected DNA values (ng) were converted to the equivalent bacteria number and the data were reported estimated copy number of bacterial DNA/mL.

Statistics: Statistical analysis was performed using GraphPad Prism 9 software. One-way analysis of variance (One-way ANOVA) was chosen to compare groups and Tukey's multiple comparison tests were further used in evaluating significance of pairwise comparisons.

3.2.12 Shelf life test

The shelf life experiment followed the protocol established in our previous work.[1] In brief, the CandyCollect devices were plasma treated (see Methods section "CandyCollect device fabrication") in descending order 1 year (369 days), 4 months (137 days), 3 months (105 days) and 0 days (control) prior to the experiment with n = 3 replicated devices per time point and concentration. This allowed for all devices to be tested on the same day. Each time point was tested in triplicate at four concentrations of *S. pyogenes*, 10^3, 10^4, 10^5 and 10^9 CFU/mL, in addition to negative controls (concentration 0 CFU/mL).

3.3 Results and Discussion

3.3.1 Capture, Elution, and qPCR detection of S. mutans *and* S. aureus *from CandyCollect Devices*

In testing the capture ability of CandyCollect device with bacteria other than *S. pyogenes*, which was reported in our previous work,[1] finding an elution method that worked for all bacteria of interest, *S. pyogenes*, *S. mutans*, and *S. aureus*, was important to establish the versatility of the device. Effective elution is crucial for accurate analysis by qPCR. Various elution buffers were accessed for high elution rates. Fluorescence images were first quantified to assess the elution efficiency of the elution buffers (Figure 3.3A and Appendix Figure B6), with high elution efficiency resulting in less fluorescent signal after elution. While some elution buffers demonstrated low

elution efficiency (ESwab™ buffer with 5% ethanol, PBS with 2% SDS, and ESwab™ buffer with 2% SDS), those that demonstrated high elution efficiency (PBS with 5% Proteinase K and ESwab™ buffer with 5% Proteinase K) were then evaluated through qPCR. Several elution buffers were further eliminated when qPCR results demonstrated some of elution buffers contained qPCR inhibitors (data not shown), thus preventing downstream analysis of CandyCollect samples. We selected PBS with 5% Proteinase K as the elution buffer for the CandyCollect device as it was the buffer with the highest observed elution rates: approximately 90% of *S. mutans* and 95% of *S. aureus* were removed from CandyCollect (Figure 3.3Ai and 3.3Aii).

We also established the qPCR assays for analyzing DNA content from eluted *S. mutans* and *S. aureus* samples (see Methods section "Quantitative PCR assay for detection of *S. mutans*, *S. aureus*, *and S. pyogenes*" and Supplementary Information), which yielded good linear relationships between the DNA content from both eluted bacteria samples and bacterial concentrations incubated on the device (Figure 3.3B). The elution buffer and qPCR assay were also tested on a solution containing a mixture of *S. mutans*, *S. aureus* and *S. pyogenes* from CandyCollect devices (Figure B7). The result showed that PBS with 5% Proteinase K was able to elute the samples containing multiple bacteria (Figure B7).

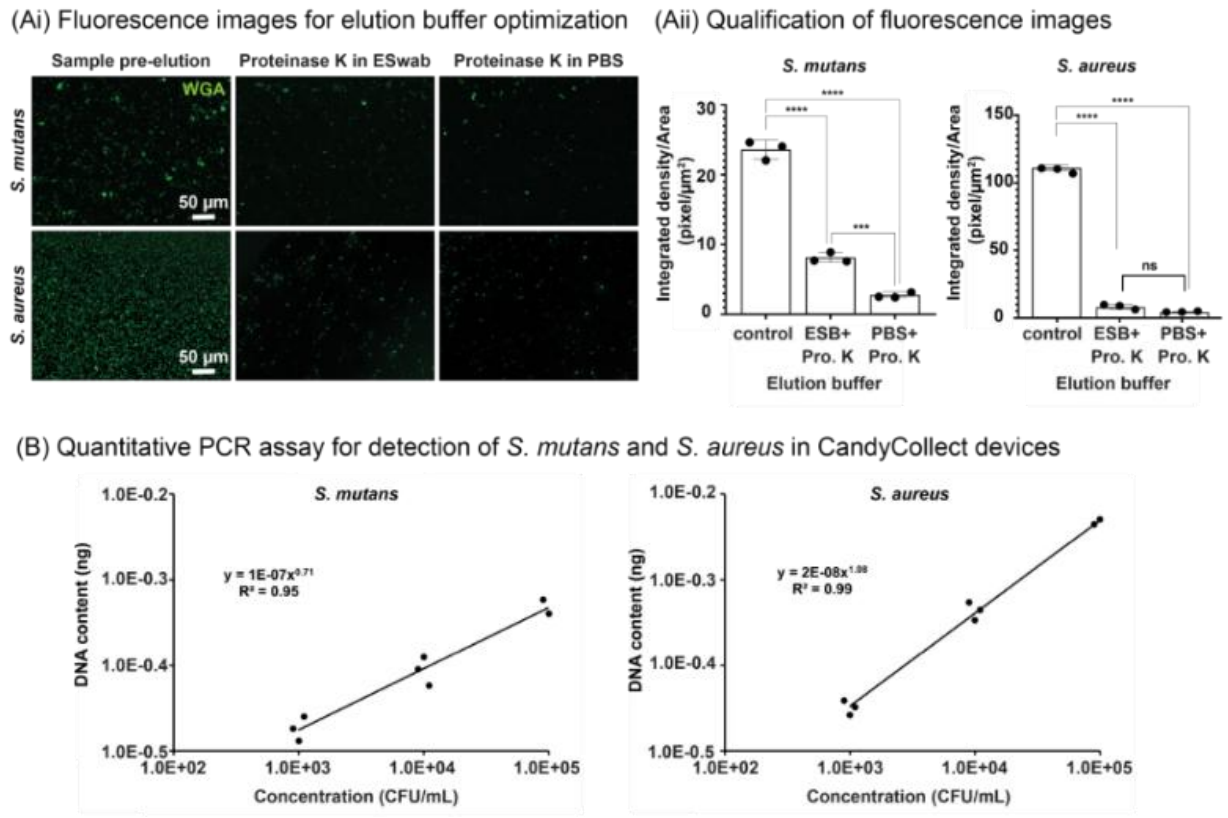

Figure 3.3. CandyCollect efficiently captures *S. mutans* and *S. aureus* and facilitates quantitative bacterial detection by qPCR. (Ai) Fluorescence microscopy images of *S. mutans* and *S. aureus* before elution (left), and after elution with Proteinase K in ESwab™ buffer (ESB) (middle) and with Proteinase K (Pro. K) in PBS (right). (Aii) Quantification of fluorescence microscopy images. Each data point represents data from one CandyCollect device and is the average of the integrated density per area of 12 (10000 µm^2) regions of interest (ROI) from 4 images of the CandyCollect device (3 ROIs per image). The bar graph represents the mean ± SEM of n = 3 CandyCollect devices. Data sets were analyzed using one-way ANOVA with Tukey's multiple comparison test; p-values are indicated for pairwise comparisons: ***p=0.0009, ****p<0.0001. (B) Reported concentration of *S. mutans* (left) and *S. aureus* (right) from qPCR analysis of bacteria eluted from CandyCollect devices using proteinase K in PBS as the CandyCollect elution buffer. Bacteria were incubated in-lab at concentrations of 10^3, 10^4 and 10^5 CFU/mL. *S. mutans* and *S. aureus* were fluorescently labeled with WGA.

3.3.2 Analysis of Human Subjects Samples via qPCR Demonstrates Feasibility of CandyCollect Devices for Salivary Commensal Bacteria Capture

We compared the CandyCollect device to two commercially available methods for oral sample/saliva collection, ESwab™ (oral swab) and SpeciMAX Stabilized Saliva Collection Kits (spit tube). Participants were instructed to provide a sample using the three methods as follows: CandyCollect (suck the samples until candy/flavor is gone), ESwab™ (suck 30 seconds), and Spit tube (collect 1 mL saliva). Although capture of bacterial pathogens is the ultimate goal for the CandyCollect device, commensal bacteria—bacteria present in healthy hosts—were selected as a proof-of-concept analytes to evaluate the device in order to maximize the population available for enrollment in this initial study. Individuals have different populations of commensal bacteria in their oral microbiome. As such, *S. mutans* and *S. aureus* are not universally present in the population, so we did not expect to detect these bacteria in samples from all participants. In general, *S. mutans* is more prevalent in the population compared to *S. aureus*, at 80-87% and 18-39% prevalence, respectively.[16-19] As such, it is unsurprising that more participants had detectable *S. mutans* than *S. aureus*.

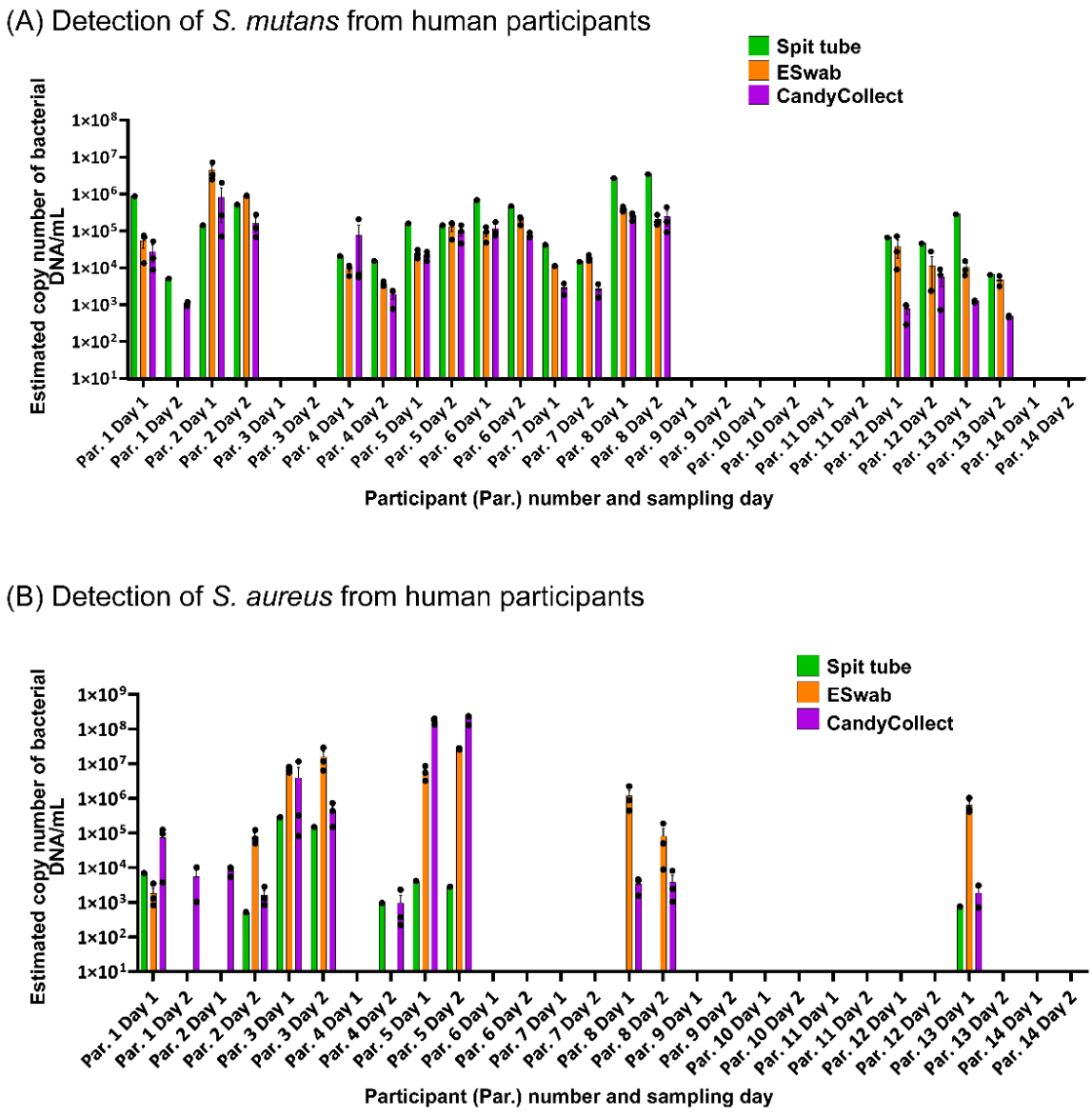

Figure 3.4. *S. mutans* and *S. aureus* can be captured on CandyCollect devices from all the participants who had positive results from spit tube and/or ESwab™ samples. CandyCollect, ESwab™, and SpeciMAX Stabilized Saliva Collection Kits (Spit tube) were sent to 14 research participants for a proof-of-concept test. The concentrations of (A) *S. mutans* and (B) *S. aureus* from participants' saliva, collected over two days by three different methods, were analyzed via qPCR and converted to estimated copy number of bacterial DNA/mL in the original saliva sample (see Methods section "Human subject data analysis" for detailed description of calculations). Each dot represents the average of two qPCR technical duplicates from one sample (three samples were collected for the CandyCollect device and ESwab™, and one for the Spit tube each day). Bar graphs represent the mean ± SEM of n = 3 CandyCollect devices or ESwab™. Participants only completed one spit tube per day.

Importantly, for participants in which a given bacterium (*S. mutans* or *S. aureus*) was detected in one or both of the commercially available methods (ESwab™ and Spit tubes), CandyCollect devices had a 100% concordance with the other positive results (Figure 3.4). As expected in human subjects studies, there was some variability in positive/negative results across sampling methods and across sampling days. For example, *S. aureus* was detected in Participant 8 on both Day 1 and 2 in the ESwab™ and CandyCollect samples, but not in Spit tubes sample. In Participant 4, on Day 2, S. aureus was detected in the spit tube and the CandyCollect samples, but not in the ESwab™ sample. While we cannot identify the exact cause of this variability, it is noteworthy that the CandyCollect device did not fail to capture *S. mutans* or *S. aureus* when they were collected by either of the two commercially available methods. In Figure 3.4, we have reported the data as estimated copy number of bacterial DNA/mL in the original saliva sample; this concentration is an estimate based on an estimated volume of saliva collected by the CandyCollect device and ESwab™ (as described in the Methods section). However, due to approximations in the collection volume these concentrations are less relevant than the presence or absence of the bacteria.

3.3.3 User Feedback Indicates CandyCollect Devices are the Preferred Saliva Sampling Tool

Of the 26 participants that completed the electronic survey, 65% of them selected CandyCollect as the best method of saliva collection (Figure 3.5A). Of the 23 participants who completed the detailed survey questions (Figure 3.5B), 70% of the participants ranked CandyCollect as being the best sampling experience, 65% chose it as the most sanitary sampling method, 87% selected it as being the least disgusting and uncomfortable, and 57% selected it as being the least invasive. (Note on sample size in Figure 5: Figure 5A represents n=26 and Figure

5B represents n=23 due to an electronic survey error wherein 3 participants failed to receive all survey questions (see Methods section "Human subjects' sample and feedback collection"). Overall, the CandyCollect device was selected by the majority of participants as the preferred saliva collection method (Figure 3.5A) and sampling experience (Figure 3.5B).

3.3.4 Shelf Life Tests: CandyCollect Devices Capture S. pyogenes after 1 Year of Storage

Bacterial adhesion to the polystyrene channel of the CandyCollect device is facilitated by an increase in the hydrophilicity and wettability caused by oxygen plasma treatment of the surface.[1,28-29] Hydrophilicity has been observed to decay over time, 30 potentially reducing the efficacy of bacterial capture by the CandyCollect device. Previously, we established through quantification of fluorescence images, that there was no notable difference in bacterial adhesion to CandyCollect devices plasma treated 0, 3, 7 and 14 days before bacterial incubation, and devices plasma treated 0 and 62 days before bacterial incubation.[1] Here, we have expanded on this research by evaluating CandyCollect devices over longer time frames, which is required for the device to be effective in a commercial setting. Devices from all time points—0 days, 3 months, 4 months and 1 year—were able to collect bacteria (Figure 3.6 and Appendix Figure B8). Although there is a significant difference between the integrated density per area in the images from the 0 days and 1-year devices (Figure 3.6B), there is only a 25% reduction in bacteria captured after 1 year of storage. In the future, longer lasting surface treatment can be used, such as treatments used for commercially available cell cultureware, which typically has a multiyear shelf life.

While *S. mutans* and *S. aureus* are well established commensal microbes, it is important to note that the location of these bacteria within the oropharyngeal space might differ from the location of pathogens of interest. GAS-related strep throat is an infection of the back of the

throat. *S. mutans* is a commensal bacterium of the oral cavity and particularly the gingiva (i.e., gums).[31, 32] *S. aureus* is located primarily in the anterior nares and is also found in other places in the respiratory tract (e.g., mouth, nose, and throat).[33] Nevertheless, independent of the primary location of each microbe, it is known that these bacteria are present in saliva.[34, 35] The present study lays the foundation for microbial collection from human subjects using the CandyCollect device, and it is important to evaluate the device in subsequent clinical studies for each pathogen of interest.

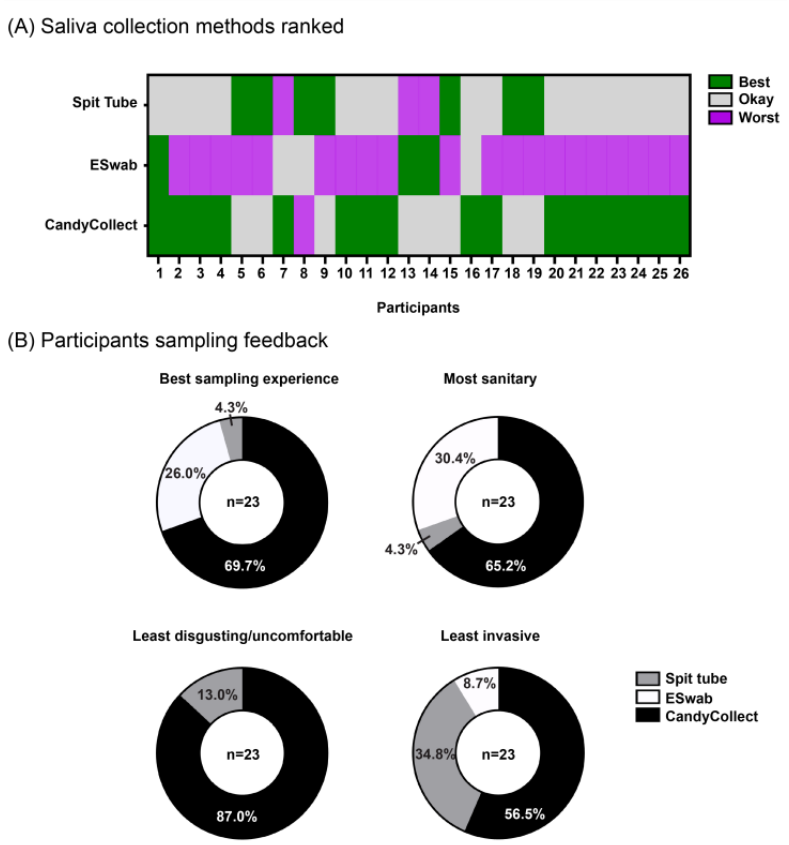

Figure 3.5. Participant feedback shows overall preference for CandyCollect devices. (A) Participants were asked to rank the three sampling methods (CandyCollect, ESwab™, and Spit Tube) in terms of best overall sampling method to worst overall sampling method. (B) Participants were asked to select one sampling method that most accurately fits the above descriptions (best sampling experience, most sanitary, least disgusting/uncomfortable, and least invasive). The CandyCollect device was the most frequently selected sampling method for all of the above user feedback questions.

We acknowledge that this pilot study was performed with a relatively small sample size; the goal was to establish the potential of the CandyCollect device in healthy adults before progressing to individuals with respiratory illness. We have ongoing studies with larger sample sizes in adults and children with respiratory illness. These additional studies also include user feedback surveys, and we will determine if the feedback from these larger cohorts is consistent with the feedback from this initial cohort.

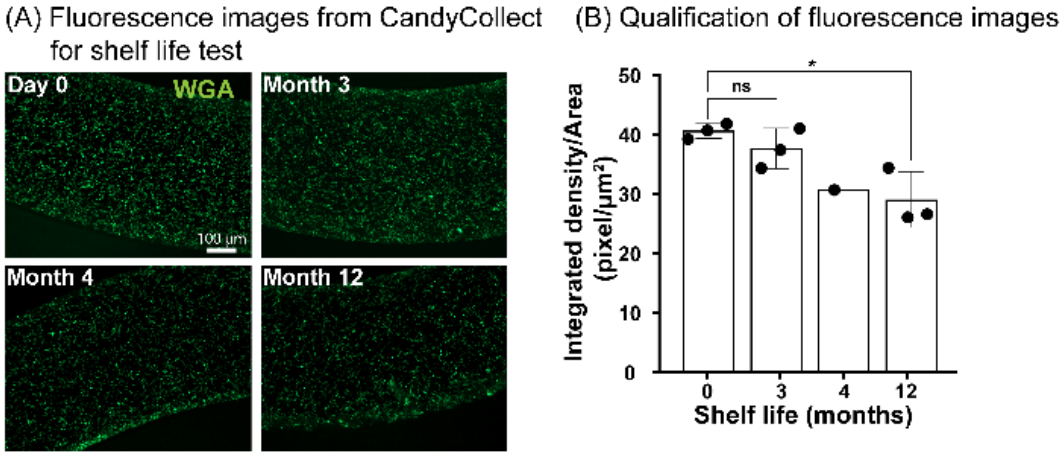

Figure 3.6. Shelf life tests demonstrate that CandyCollect devices effectively capture *S. pyogenes* after 1 year of storage. Devices were plasma treated and stored at room temperature for 0 days (control group), 3 months, 4 months, and 1 year. (A) Fluorescence microscopy images indicate capture of *S. pyogenes* after 1 year of storage is similar to the control, with ~25% decrease in bacteria captured. (B) Quantification of the integrated density per area (pixel/µm^2). Data sets were analyzed using one-way ANOVA and Tukey's multiple comparison tests (*$p<0.05$). No significant difference between 0 days (control group) and 3 months of storage was found. Note: depicted images are from CandyCollect devices incubated with *S. pyogenes* at a concentration of $1x10^9$ CFU/mL for 10 minutes. Each data point represents an individual CandyCollect device (4 images were taken per device, and the data point plotted is the average); the bars represent the mean ± SEM of n=3 CandyCollects. *S. pyogenes* was fluorescently labeled with WGA.

3.4 Conclusion

In this work, we used two commensal bacteria, *S. mutans* and *S. aureus*, as proof-of-concept bacteria to demonstrate the abilities of the CandyCollect device in capturing salivary bacteria in healthy adults. The results showed that (1) the CandyCollect device can effectively capture com-mensal bacteria from healthy participants in a home set-ting, (2) samples are stable through standard shipping at room temperature and the bacteria can be eluted and quantified using qPCR, (3) most users ranked CandyCollect as their first choice for oral sampling method (compared to standard oral swabs and spit tubes), (4) the CandyCollect device is functional after storage times of up to one year. For more reproducible clinical characterization work and commercial implementation, simple manufacturing can be set up by using rapid injection molding as the design is fully amenable to injection molding.[36] The present study opens up several exciting areas of future work as a new tool for at-home and in-clinic sampling that is intuitive, convenient, and child friendly. Currently, we are conducting a study using CandyCollect with patients age 5-17 with GAS pharyngitis. In addition, future work includes extending the capabilities of CandyCollect to viruses, mycobacteria, and fungal pathogens.

2.5 References

1. Lee UN, Su X, Hieber DL, Tu W-c., McManamen AM, Takezawa MG, Hassan GW, Chan TC, Adams KN, Wald ER, DeMuri GP, Berthier E, Theberge AB, Thongpang S. CandyCollect: at-home saliva sampling for capture of respiratory pathogens. *Lab Chip*. 2022; 22 (18), 3555-3564. doi: 10.1039/d1lc01132d.
2. Zar HJ, Ferkol TW. The global burden of respiratory disease—Impact on child health. *Pediatr. Pulmonol*. 2014; 49, 430-434. doi: 10.1002/ppul.23030.
3. Bisno AL. Acute Pharyngitis. *N. Engl. J. Med*. 2001; 344, 205-211. doi: 10.1056/NEJM200101183440308.

4. Kaitz M, Sabato R, Shalev I, Ebstein R, Mankuta D. Children's noncompliance during saliva collection predicts measures of salivary cortisol. *Dev. Psychobiol*. 2012; 54, 113-123. doi: 10.1002/dev.20580.
5. Shulman ST, Bisno AL, Clegg HW, Gerber MA, Kaplan EL, Lee G, Martin JM, Van Beneden C. Clinical Practice Guideline for the Diagnosis and Management of Group A Streptococcal Pharyngitis: 2012 Update by the Infectious Diseases Society of America. *Clin. Infect. Dis*. 2012; 55, e86-e102. https://doi.org/10.1093/cid/cis629.
6. Piasio RN, Turner N, Wheeler A. Methods and devices for testing saliva. WIPO (PCT) 2010/0273.177 A1, 2007.
7. DeMuri G, Wald ER. Detection of Group A Streptococcus in the Saliva of Children Presenting With Pharyngitis Using the cobas Liat PCR System. *Clin. Pediatr.* 2020; 59, 856–858. doi: 10.1177/0009922820920936.
8. Comber L, Walsh KA, Jordan K, O'Brien KK, Clyne B, Teljeur C, Drummond L, Carty PG, De Gascun CF, Smith SM, Harrington P, Ryan M, O'Neill M. Alternative clinical specimens for the detection of SARS-CoV-2: A rapid review. *Rev. Med. Virol.* 2021; 31, e2185. doi: 10.1002/rmv.2185.
9. Heat inactivation of respiratory viruses in raw saliva for nu-cleic acid extraction. ThermoFish-er.https://assets.thermofisher.com/TFS-Assets/BID/Application-Notes/heat-inactivation-viruses-nucleic-acid-extraction-app-note.pdf (accessed 2022/12/29).
10. Saliva Collection and Handling Advice. 3 rd Edition. Sali-metrics. https://www.researchgate.net/profile/Nirmala-Svsg/post/Saliva-collection-in-rats/attachment/59d633c579197b807799173e/AS%3A3 76127236395008%401466687129091/download/Saliva_Collection_Handbook.pdf (accessed 2022/12/29).
11. Melo Costa M, Benoit N, Dormoi J, Amalvict R, Gomez N, Tissot-Dupont H, Million M, Pradines B, Granjeaud S, Almeras L. Salivette, a relevant saliva sampling device for SARS-CoV-2 detection. *J. Oral Microbiol*. 2021; 13, 1920226. doi: 10.1080/20002297.2021.1920226.
12. Ottaviano E, Parodi C, Borghi E, Massa V, Gervasini C, Centanni S, Zuccotti G; LollipopStudy Group; Bianchi S. Saliva detection of SARS-CoV-2 for mitigating company outbreaks: a surveillance experience, Milan, Italy, March 2021. *Epidemiol Infect*. 2021; 30, 149:e171. doi: 10.1017/S0950268821001473.
13. De Meyer J, Goris H, Mortelé O, Spiessens A, Hans G, Jansens H, Goossens H, Matheeussen V, Vandamme S. Evaluation of Saliva as a Matrix for RT-PCR Analysis and Two Rapid Antigen Tests for the Detection of SARS-CoV-2. *Viruses.* 2022; 30, 14(9):1931. doi: 10.3390/v14091931.
14. Martín R, Miquel S, Ulmer J, Kechaou N, Langella P, Bermúdez-Humarán LG. Role of commensal and probiotic bacteria in human health: a focus on inflammatory bowel disease. Microb Cell Fact. 2013; 23, 12:71. doi: 10.1186/1475-2859-12-71.

15. Kreth J, Giacaman RA, Raghavan R, Merritt J. The road less traveled - defining molecular commensalism with Streptococcus sanguinis. *Mol Oral Microbiol*. 2017; 32(3):181-196. doi: 10.1111/omi.12170.
16. McCormack MG, Smith AJ, Akram AN, Jackson M, Robertson D, Edwards G. Staphylococcus aureus and the oral cavity: an overlooked source of carriage and infection? *Am J Infect Control*. 2015; 43(1):35-7. doi: 10.1016/j.ajic.2014.09.015.
17. Ohara-Nemoto Y, Haraga H, Kimura S, Nemoto TK. Occurrence of staphylococci in the oral cavities of healthy adults and nasal oral trafficking of the bacteria. *J Med Microbiol*. 2008 ;57(Pt 1):95-99. doi: 10.1099/jmm.0.47561-0.
18. Pannu P, Gambhir R, Sujlana A. Correlation between the salivary Streptococcus mutans levels and dental caries experience in adult population of Chandigarh, India. *Eur J Dent.* 2013; 7(2):191-195. doi: 10.4103/1305-7456.110169.
19. Lee YJ; Kim M-A; Kim J-G; Kim J-H Detection of Streptococcus mutans in human saliva and plaque using selective media, polymerase chain reaction, and monoclonal antibodies. *Oral Biol Res.* 2019; 43, 121–129. doi: 10.21851/obr.43.02.201906.121
20. Koblitz J, Halama P, Spring S, Thiel V, Baschien C, Hahnke RL, Pester M, Overmann J, Reimer LC. MediaDive: the expert-curated cultivation media database. *Nucleic Acids Res*. 2023; 6, 51(D1):D1531-D1538. doi: 10.1093/nar/gkac803.
21. TCC Medium: 18 Tryptic Soy Agar/Broth (Soybean-Casein Digest Medium, USP) https://www.atcc.org/-/media/product-assets/ documents/microbial-media-formulations/1/8/atcc-medium-18.pdf? rev=832846e1425841f19fc70569848edae7 (accessed 2022/8/20).
22. Gera K, McIver KS. Laboratory growth and maintenance of Streptococcus pyogenes (the Group A Streptococcus, GAS). *Curr Protoc Microbiol*. 2013; 2, 30:9D.2.1-9D.2.13. doi: 10.1002/9780471729259.mc09d02s30.
23. Lochman J, Zapletalova M, Poskerova H, Izakovicova Holla L, Borilova Linhartova P. Rapid Multiplex Real-Time PCR Method for the Detection and Quantification of Selected Cariogenic and Periodontal Bacteria. *Diagnostics (Basel).* 2019; 22, 10(1):8. doi: 10.3390/diagnostics10010008.
24. Wood C, Sahl J, Maltinsky S, Coyne B, Russakoff B, Yagüe DP, Bowers J, Pearson T. SaQuant: a real-time PCR assay for quantitative assessment of *Staphylococcus aureus*. *BMC Microbiol*. 2021; 8, 21(1):174. doi: 10.1186/s12866-021-02247-6.
25. Galia L, Ligozzi M, Bertoncelli A, Mazzariol A. Real-time PCR assay for detection of Staphylococcus aureus, Panton-Valentine Leucocidin and Methicillin Resistance directly from clinical samples. AIMS Microbiol. 2019; 21, 5(2):138-146. doi: 10.3934/microbiol.2019.2.138.
26. Yano A, Kaneko N, Ida H, Yamaguchi T, Hanada N. Real-time PCR for quantification of Streptococcus mutans. *FEMS Microbiol Lett*. 2002; 19, 217(1):23-30. doi: 10.1111/j.1574-6968.2002.tb11451.x.

27. Yang S, Lin S, Kelen GD, Quinn TC, Dick JD, Gaydos CA, Rothman RE. Quantitative multiprobe PCR assay for simultaneous detection and identification to species level of bacterial pathogens. *J Clin Microbiol.* 2002; 40(9):3449-54. doi: 10.1128/JCM.40.9.3449-3454.2002.
28. Hemmatian T, Lee H, Kim J. Bacteria Adhesion of Textiles Influenced by Wettability and Pore Characteristics of Fibrous Substrates. *Polymers (Bas*el). 2021; 11, 13(2):223. doi: 10.3390/polym13020223.
29. Guruvenket S, Rao GM, Komath M, Raichur AM. Plasma surface modification of polystyrene and polyethylene. *Appl. Surf. Sci.* 2004; 236, 278–284. doi: org/10.1016/j.apsusc.2004.04.033.
30. Li J, Oh K, Yu H. Surface rearrangements of oxygen plasma treated polystyrene: surface dynamics and humidity effect. *Chin. J. Polym. Sci* 2005; 23, 187–196.
31. Duchin S, van Houte J. Relationship of Streptococcus mutans and lactobacilli to incipient smooth surface dental caries in man*. Arch Oral Biol.* 1978; 23(9):779-86. doi: 10.1016/0003-9969(78)90155-3.
32. Berlutti F, Catizone A, Ricci G, Frioni A, Natalizi T, Valenti P, Polimeni A. Streptococcus mutans and Streptococcus sobrinus are able to adhere and invade human gingival fibroblast cell line. *Int J Immunopathol Pharmacol*. 2010; 23(4):1253-60. doi: 10.1177/039463201002300430.
33. Nilsson P, Ripa T. *Staphylococcus aureus* throat colonization is more frequent than colonization in the anterior nares*. J Clin Microbiol*. 2006; 44(9):3334-9. doi: 10.1128/JCM.00880-06.
34. Köhler B, Bratthall D. Practical method to facilitate estimation of *Streptococcus mutans* levels in saliva. J Clin Microbiol. 1979; 9(5):584-8. doi: 10.1128/jcm.9.5.584-588.1979.
35. Petti S, Boss M, Messano GA, Protano C, Polimeni A. High salivary *Staphylococcus aureus* carriage rate among healthy paedodontic patients. *New Microbiol*. 2014; 37(1):91-6.
36. Lee UN, Su X, Guckenberger DJ, Dostie AM, Zhang T, Berthier E, Theberge AB. Fundamentals of rapid injection molding for microfluidic cell-based assays. Lab Chip. 2018; 30, 18(3):496-504. doi: 10.1039/c7lc01052d.

Chapter 4| *Capture of Group A Streptococcus by Open-Microfluidic CandyCollect Device in Pediatric Patients*

Reproduced in part from Wan-chen Tu, Ingrid H. Robertson,* Andrea Blom, Elena Alfaro, Victoria A. M. Shinkawa, Daniel B. Hatchett, Juan C. Sanchez, Anika M. McManamen, Xiaojing Su, Erwin Berthier, Sanitta Thongpang, Ellen R. Wald,[#] Gregory P. DeMuri,[#] Ashleigh B. Theberge.[#] Bioeng Transl Med. e70001 (2025). https://doi.org/10.1002/btm2.70001*

** Equal contribution*
[#]Co-corresponding authors

W-c. T. designed the sample processing protocol, carried out the sample analysis, performed data analysis, made figures for the manuscript, drafted the initial manuscript, and critically reviewed and revised the manuscript. I. J. fabricated the CandyCollect devices and prepared devices for human subject research, interpreted the data, drafted the initial manuscript, and critically reviewed and revised the manuscript. A. B. advised on study design and execution, enrolled and interacted with the participants, collected the samples and user surveys, accessioned and shipped the samples, interpreted the data, and critically reviewed and revised the manuscript. E. A. advised on study design and execution, advised on all regulatory aspects, drafted the study protocol and survey instruments, obtained Institutional Review Board (IRB) approval, interpreted the data, and critically reviewed and revised the manuscript. V. A. M. S., D. B. H., and J. C. S. fabricated the CandyCollect devices and prepared devices for human subject research, including designing experimental protocols/engineering designs, and critically reviewed and revised the manuscript. A. M. M. and X. S. designed the sample processing protocol and drafted, critically reviewed, and revised the manuscript. E. B. conceptualized the research, advised on study design and interpretation, and critically reviewed and revised the manuscript. A. B. T., G. P. D., E. R. W., and S. T. conceptualized the research, designed the study, oversaw study execution, interpreted the data, and critically reviewed and revised the manuscript. All authors approved the final manuscript as submitted and agreed to be accountable for all aspects of the work.

Abstract

State the purpose: Obtaining high-quality samples to diagnose streptococcal pharyngitis in pediatric patients is challenging due to discomfort associated with traditional pharyngeal swabs. This may cause reluctance to go to the clinic, inaccurate diagnosis, or inappropriate treatment for children with sore throat. Here, we determined the efficacy of CandyCollect, a lollipop-inspired open-microfluidic pathogen collection device, to capture Group A Streptococcus

(GAS) and compare user preference for CandyCollect, conventional pharyngeal swabs, or mouth swabs in children with pharyngitis and their caregivers.

Results: All child participants (30/30) were positive for GAS by qPCR on both the mouth swab and CandyCollect. Caregivers ranked CandyCollect as a good sampling method overall (27/30), and all caregivers (30/30) would recommend CandyCollect for children 5 years and older. Twenty-three of 30 children "really like" the taste and 24/30 would prefer to use CandyCollect if a future test were needed. All caregivers (30/30) and most children (28/30) would be willing to use CandyCollect at home.

Conclusion: All participants tested positive for GAS on all three collection methods (pharyngeal swab, mouth swab, and CandyCollect). While both caregivers and children like CandyCollect, some caregivers would prefer a shorter collection time. Future work includes additional studies with larger cohorts presenting with pharyngitis of unknown etiology and shortening collection time while maintaining the attractive form of the device.

4.1 Introduction

Group A Streptococcus (GAS) accounts for over 600 million cases of bacterial pharyngitis worldwide each year,[1] affecting 15% of school-aged children in developed countries. In developing nations the burden is markedly greater, with rates 5-10 times higher.[1] Though symptoms of GAS pharyngitis almost always resolve after 3-4 days, antibiotics are recommended to shorten the course of the infection, lessen spread, and prevent acute suppurative complications.[1] Accurate detection of GAS is imperative; untreated and recurring GAS infections can lead to severe outcomes, such as acute rheumatic fever, which causes carditis in 30-45% of cases and is the most common cause of acquired heart disease in children worldwide.[1]

A standard method for diagnosing GAS pharyngitis is with a rapid antigen detection test (RADT), which requires a posterior pharyngeal swab sample and provides a positive or negative result within minutes.[2] If the RADT is negative, a throat culture is performed on a posterior pharyngeal swab in order to detect false negatives, and laboratory analysis takes more time.[2,3] Another option is a molecular test (e.g., quantitative polymerase chain reaction (qPCR)), again requiring a posterior pharyngeal swab.[4] Pharyngeal swabs are uncomfortable, often acting as a deterrent for children and adults; however, it is important to confidently diagnose bacterial pharyngitis not only for the long-term health of the patient but also to avoid over-prescribing antibiotics.[1] DeMuri, et al. established that mouth swabs (sucked on like a lollipop) provide an adequate sample for the detection of GAS when sensitive methods such as PCR are used.[5]

With developments in PCR and RADTs using saliva instead of posterior pharyngeal swabs, more options are now available for salivary detection, such as spit tubes (OMNIgene™), passive drooling, mouth swabs (Eswab™), and cotton rolls (Salivette®).[6-8] The CandyCollect, a lollipop-inspired open-fluidic sampling device, was first introduced in our 2021 in-lab study that showed its ability to capture and accumulate *Streptococcus pyogenes* for analysis.[9] In 2022, we tested the device with a remote, at-home human subjects study in which the CandyCollect devices effectively captured commensal bacteria (*Streptococcus mutans* and *Staphylococcus aureus*) from healthy adults.[10] The CandyCollect devices were shipped to the lab in dry tubes under ambient conditions to be quantified using qPCR from the elution fluid.[10] Ours is not the only lollipop-inspired device; there are at least three other collection or testing devices with a similar lollipop form already on the market, although these alternative devices do not look like a traditional candy lollipop and also do not provide flavor. The Self-LolliSponge™ by Copan has the user keep the

sponge stick in their mouth for a “few minutes” with a lemon scented cap to improve the experience.[11] The V-Chek COVID-19 Saliva Antigen Test provides a “‘Lollipop’ Saliva Swab” that the user places in their mouth for 90 seconds and then attaches to a lateral flow assay cassette.[12] The Whistling COVID-19 Saliva Antigen Rapid Test combines an absorbent material attached to a handle that the user places in their mouth with an immunochromatographic assay.[12]

Obtaining high-quality samples to diagnose GAS pharyngitis in pediatric patients is important for treatment; however, the current collection tools are not child friendly. Here we aimed to demonstrate the feasibility of the CandyCollect device by collecting salivary samples from 30 pediatric patients aged 5-17 years with known GAS pharyngitis. Further we aimed to compare user preference for CandyCollect, conventional pharyngeal swabs, or mouth swabs among children with pharyngitis and their caregivers.

4.2 Method

4.2.1 Mouth swabs and CandyCollect devices

Swabs and media: The pharyngeal swab used in the clinical visit was a standard of care double swab, BBL™ CultureSwab™ Transport Systems by Copan (FisherScientific, Cat# B4320109). The white-capped Eswab™ with nylon flocked swabs and Liquid Amies media collection kits by Copan (FisherScientific, Cat# R723480) were used as mouth swabs.

CandyCollect device stick fabrication: The CandyCollect device is milled from a sheet of 4 mm polystyrene (Goodfellow, Cat# 700-272-86) using the DATRON Neo computerized numerical control (CNC) mill as previously described.[9] The Fusion file and an engineering drawing of the CandyCollect device are included in the Appendix C (Figure C1). After sanding rough edges,

devices were sonicated in isopropanol (IPA) (FisherScientific, A451-4) and 70% v/v ethanol (FisherScientific, Decon™ Labs, 07-678-004).

Plasma treatment of CandyCollect devices: A Zepto LC PC Plasma Treater (Diener Electronic GmbH, Ebhausen, Germany), using oxygen gas, increased hydrophilicity of the device surface. The process includes decreasing the chamber pr essure to 0.20-0.25 mbar and adding oxygen gas while 70 W voltage is applied for 5 minutes.[9,10]

Preparation of CandyCollect devices for human subjects study: CandyCollect devices were prepared as previously described with the exception of storage containers and candy mass.[9,10] Half of the patients (1-15) were sampled with CandyCollects made with 1.2-1.34 g isomalt candy, while the second half (16-30) were sampled with 0.45-0.57 g; procedures are duplicated here for convenience. In accordance with the kitchen hygiene guidelines of the Washington State Cottage Food Operations Law (RCW 69.22.040(2b-f(ii-iv))), candy was applied to CandyCollect sticks by lab members who are trained in food safety, have a Food Worker Card (WA State), and wore gloves and a mask during food preparation. Candy was prepared by gradually adding isomalt to water while heating to a target temperature of 171°C, then adding food coloring. Next, the isomalt mixture was cooled in a room temperature water bath while strawberry candy flavoring was added. Plasma treated CandyCollect sticks were cleaned using hot water and dish soap. After the sticks were dry, small amounts of isomalt candy were re-melted and added to silicone molds with the CandyCollect sticks. Once the candy was cooled, the mass was recorded, and the device was heat-sealed in a polypropylene bag. Devices were stored in Ziploc® storage bags with a food safe desiccant (Amazon, Cat# B00DYKTS9C) until being sent to UW-Madison for the clinical study.

4.2.2 Clinical Study Procedures

4.2.2.1 Subjects and Specimens

Caregiver-child dyads were recruited from an ambulatory care clinic that serves children in Madison, Wisconsin. Children were diagnosed with GAS pharyngitis using a traditional pharyngeal swab via RADT. The study protocol and procedures were reviewed and approved by the appropriate institutional review board (UW-Madison Health Sciences Institutional Review Board, #2021-1427). The study team implemented procedures in accordance with the ethical standards of the relevant human subjects research oversight committees (institutional, local, and national) and in accordance with the Helsinki Declaration of 1975, as revised in 2008. Study data were collected and managed using REDCap (Research Electronic Data Capture) hosted at the University of Wisconsin-Madison, School of Medicine and Public Health.[13,14]

A parent or legal guardian (aka "caregiver") provided verbal consent for their own participation in the study and caregiver permission for their child, and all children provided verbal assent. Eligible children needed to be able to suck on swabs and the CandyCollect devices and could not have a sensitivity to sugar-free products; additionally, a parent or legal guardian needed to be present and enroll in the study along with the child. Immediately after the clinic visit, in which the traditional pharyngeal swab was obtained, a research nurse guided participants through collecting four oral samples: two commercially available mouth swabs (Eswab™) for 10 seconds each and two CandyCollect devices until the candy was fully dissolved (Figure 4.1). The samples were stored at -80°C and shipped on dry ice prior to qPCR analysis. Race and ethnicity information was collected based on the requirements of NIH. Race and ethnicity information was

taken from the electronic health record, where it had previously been entered based on self-report by the parent/legal guardian.

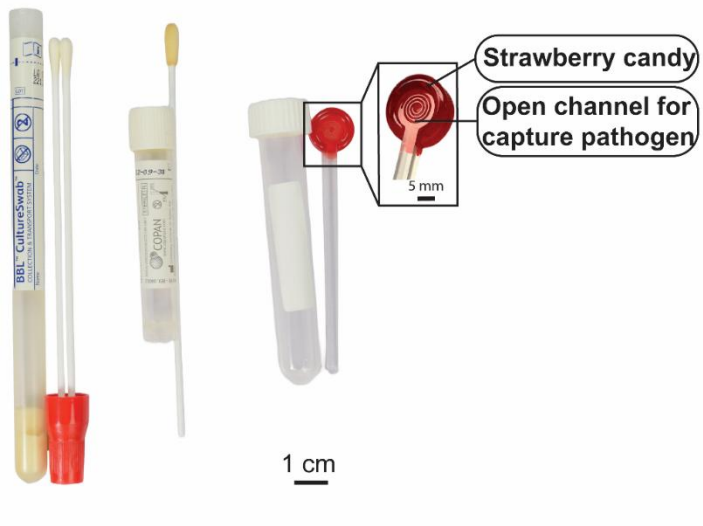

Figure 4.1. GAS sampling tools used in this study: pharyngeal (throat) swab, ESwab™ (mouth swab), and the CandyCollect device (from left to right). The components of the CandyCollect device include: 1) strawberry candy to facilitate pleasant user experience of the CandyCollect device and 2) open channels which capture bacterial pathogens.

4.2.2.2 Testing Preference Survey

After sample collection was complete, the research nurse gave a paper-based survey to both the child and their caregiver. All survey questions are included in Appendix C, Table C1-C2. The research nurse provided instructions about the Wong-Baker FACES® Pain Rating Scale to all child participants, explaining that each face represents a person who has no pain (hurt), or some, or a lot of pain (Appendix Figure C2).[15] The nurse asked the participants to choose the face that best describes the pain they experienced during each type of testing. The research nurse assisted children with completing the form if they needed help reading or understanding. The research nurse gave caregivers privacy in completing their surveys, to encourage honest responses, only

answering questions as needed. Participants were also asked to provide suggestions and free responses about the main reasons for their preferences. All free response questions are included in Appendix Table C3.

4.2.3 Specimen Processing and Laboratory Analysis

The detailed specimen processing and laboratory analysis procedures were previously described.[10] In brief, the mouth swab and CandyCollect sample collection was directed by a research nurse. Samples were stored in -20 °C and then transferred to storage at -80 °C within 12 days. Samples were shipped to the University of Washington on dry ice and then stored at -80 °C before processing. All laboratory procedures were performed in accordance with Biosafety Level-2 laboratory practices and the University of Washington Site-Specific Bloodborne Pathogen Exposure Control Plan. CandyCollect devices and mouth swabs were processed as previously described;[10] additional details are in the Appendix C. Briefly, the material on the CandyCollect device was eluted by phosphate-buffered saline (PBS) (Gibco™, Cat# 10010023) with 5% Proteinase K (Thermo Scientific™, Cat# EO0491); for mouth swab samples, *S. pyogenes* DNA was isolated using MagMAX™ Total Nucleic Acid Isolation Kit (ThermoFisher Scientific, Cat# AM1840) according to the protocol supplied by the manufacturer. After elution and lysis, the samples were also enriched and purified using MagMAX™ Total Nucleic Acid Isolation Kit following the protocol supplied by the manufacturer.[10]

qPCR was performed for the detection of *S. pyogenes* genomic DNA as previously described.[9, 10] The results were expressed as Cycle threshold (Ct, number of cycles until the sample was detected above the threshold). Any Ct value below or equal to Ct values for the lowest concentration of DNA standards (5 fg) on the same plate was considered positive; this cut-off was

determined from standard curves performed with genomic DNA isolated from *S. pyogenes* (Appendix Figure C4).[9]

Statistics: Statistical analysis was performed using GraphPad Prism 9 software. Paired t-tests were used to evaluate the significance of pairwise comparisons.

4.2.4 Preparation of positive and negative controls

Preparation of positive controls (via in-lab capture of *S. pyogenes*) and negative controls is described in our prior publications [9, 10] and the Appendix C. In brief, *S. pyogenes* was prepared from *Streptococcus pyogenes* Rosenbach (American Type Culture Collection, ATCC®, Cat# 700294™), and cultured in Todd-Hewitt Yeast broth.[16] *S. pyogenes* culture was inoculated one day prior to experiments. For positive controls, 50 µL of *S. pyogenes* culture media were added to the CandyCollect devices, and mouth swabs were soaked in the *S. pyogenes* culture media for 10 seconds. PBS was used as the negative control sample.

Figure 4.2. Subject demographics. Thirty participants, aged 5-14 years, were enrolled in this study. Of all the participants, 16 were females and 14 were males.

4.3 Results

4.3.1 Demographic Characteristics

In this study, 30 pediatric child-caregiver dyads were enrolled at a clinic in Madison, Wisconsin. Enrolled child participants were aged 5 to 14 years with GAS pharyngitis, which is consistent with the age range in which GAS pharyngitis is most common;[1] the mean age of participants was 8.8 years (Figure 4.2 and Appendix Table C4). More than 90% of child participants were white and not Hispanic. (Appendix Table C4).

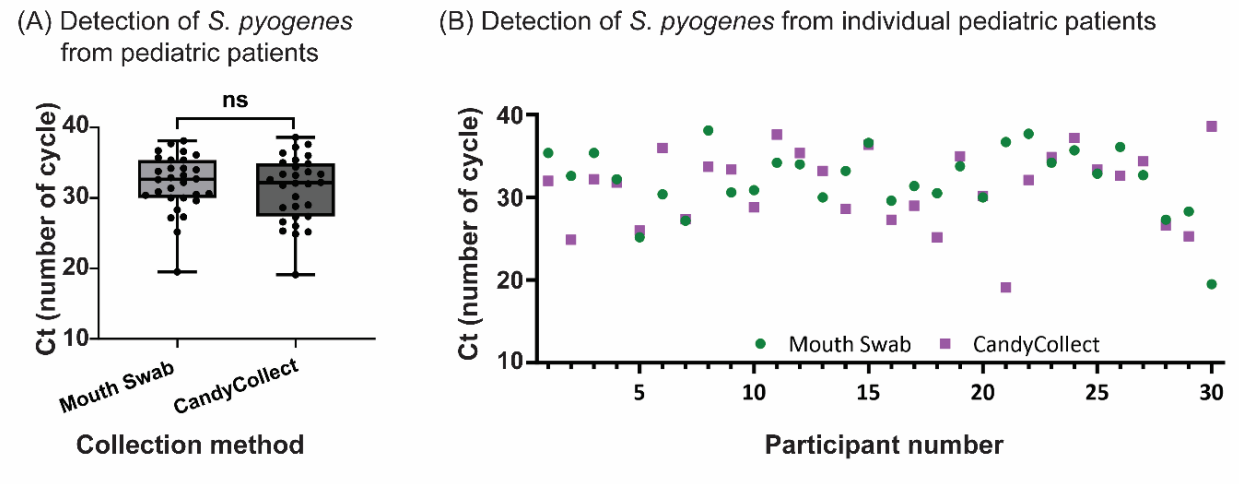

Figure 4.3. (A) Pooled cycle threshold (Ct) values of samples collected from 30 child participants with GAS pharyngitis with the mouth swabs (left, light grey) and CandyCollect devices ((right, dark grey). Ct from the two sampling methods of all 30 participants are not significantly different ($p>0.05$). (B) individual Ct values collected from the CandyCollect devices (purple, square) and mouth swabs (green, circle). Data are plotted by the Ct of the CandyCollect devices; the participant numbers were randomly re-numbered. Any Ct value below or equal to Ct values for the lowest concentration of DNA standards (5 fg) on the same plate was considered positive; this cut-off was determined from standard curves prepared with genomic DNA isolated from *S. pyogenes*; all points plotted are positive results.

4.3.2 qPCR analysis of GAS in CandyCollect devices and mouth swabs

Each sample was analyzed using qPCR and the Ct is shown in Figure 4.3. The samples collected by CandyCollect devices have an average Ct of 31.28 (range=19.1-38.6) and mouth

swabs have an average Ct of 32.08 (range=19.5-38.1); the Ct from the two sampling methods of the 30 participants are not significantly different ($p>0.05$). Nine samples collected by CandyCollect devices have a higher Ct than the corresponding mouth swabs and the Ct of 13 samples collected by CandyCollect devices is lower than the corresponding mouth swabs. Two different versions of the CandyCollect device (with 0.5 g and 1.3 g candy) were used, with half of the participants using each size. The comparison of the Ct values from two different sizes of candy (15 participants each size), shown in Appendix Figure 3C, are not significantly different ($p>0.05$). There is also no notable correlation between the CandyCollect device consumption time and the Ct values (Figure 4.4).

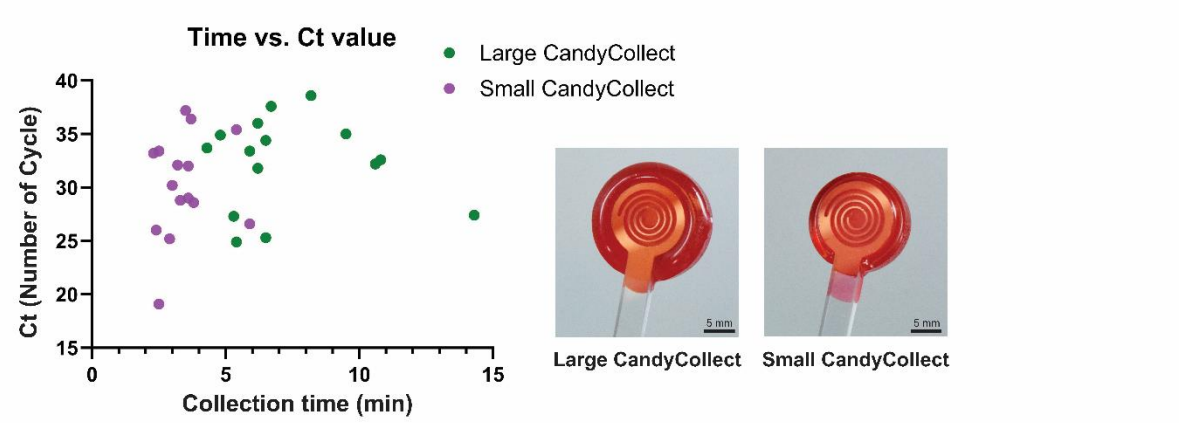

Figure 4.4. Collection time of CandyCollect devices vs. Ct values of samples collected from 15 participants using the large CandyCollect devices (Candy = 1.3 g, green) and from 15 participants using small CandyCollect devices (Candy = 0.5 g, purple).

4.3.3 User Feedback of CandyCollect devices and two other commercial collection tools

All 30 children and their caregivers completed feedback surveys. Twenty-nine of 30 children responded that they did not feel any pain or discomfort while using the CandyCollect devices; in comparison, more than half of participants felt pain/discomfort with the traditional throat swabs (Figure 4.5). Twenty-seven of 30 caregivers ranked the CandyCollect as a good

sampling method overall; 29/30 caregivers indicated that using the CandyCollect device was a pleasant experience for their child (Figure 4.5). The majority of children reported that the CandyCollect device is easy to use (17/30), and they "really like" the taste (n= 23/30) (Figure 4.6). The majority of caregivers reported that the appearance of the CandyCollect was appealing (n= 26/30) (Figure 4.6). When asked to consider using CandyCollect, mouth swab, or throat swab if they needed another GAS pharyngitis diagnostic test next week, more than a half of the children (24/30) and caregivers (17/30) preferred to use the CandyCollect device, with the remaining children and caregivers preferring the mouth swab; no participants selected the throat swab (Figure 4.6). For caregivers of children who consumed the 0.5 g CandyCollect device (consumption time range 2.3-5.9 min; 3.3 min median), 12/15 preferred the CandyCollect device and 3/15 preferred the mouth swab; for caregivers of children who consumed the 1.3 g CandyCollect device (consumption time range 4.3-14.2 min; 6.5 min median), 5/15 preferred the CandyCollect device and 10/15 preferred the mouth swab. Almost all children (28 out of 30) and all caregivers (30 out of 30) stated that they would be willing to use the CandyCollect device at home (Figure 4.6). All caregivers report they would recommend using the CandyCollect device (Figure 4.6) for children 5 years and older. All survey questions are included in Appendix Table C1-C2.

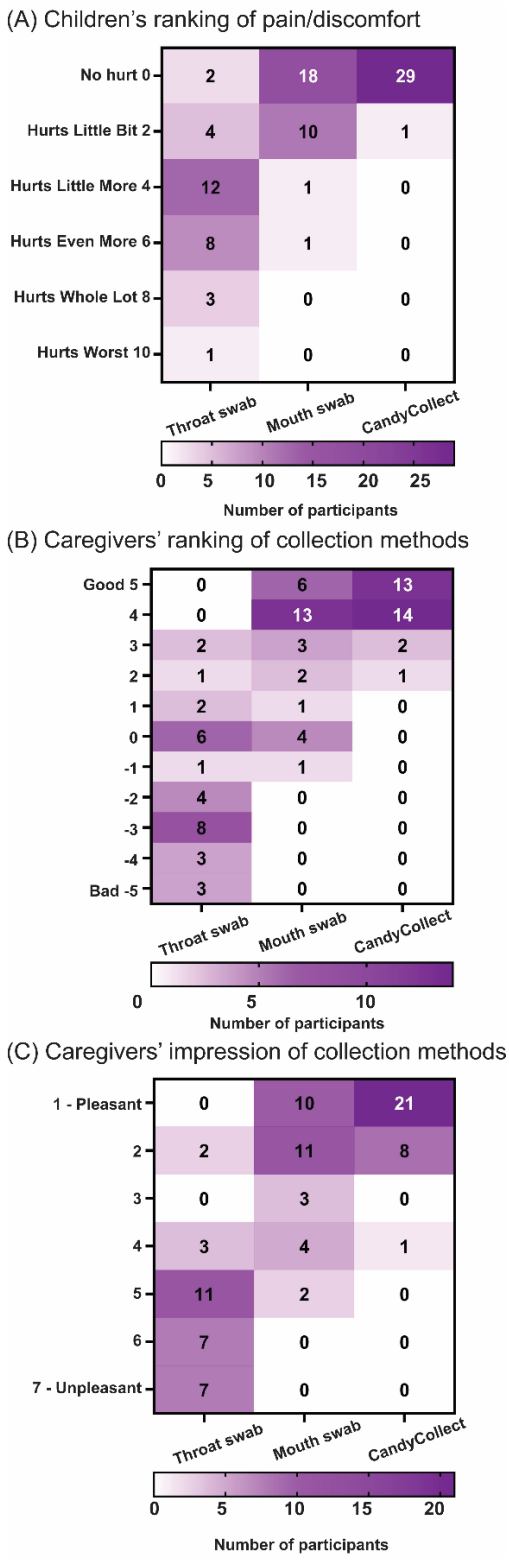

Figure 4.5. Survey responses to assess the comparison of three collection methods. All survey questions are included in Appendix Table C1 and C2: (A) Appendix Table C1 questions 1-3 (B) Appendix Table C2 questions 2, 4, and 6 (C) Appendix Table C2 questions 1, 3, and 5.

4.4 Discussion

The ultimate goal of the CandyCollect device is to capture bacterial pathogens for laboratory detection. In our previous in-lab study, we developed the CandyCollect device to capture *S. pyogenes* in saliva and established a qPCR assay to detect *S. pyogenes* eluted from CandyCollect devices.[9] We also used CandyCollect devices to capture commensal bacteria (*Streptococcus mutans* and *Staphylococcus aureus*) from healthy adults in a home setting as proof-of-concept human subjects research.[10] The present publication is the first human subjects research that used CandyCollect devices with pediatric patients. The results show that all 30 children diagnosed with GAS pharyngitis using a RADT were positive on CandyCollect devices and mouth swabs. As expected in studies of human subjects, there was some variability in the amount of bacteria (Ct value) across sampling methods and participants, which was also shown in a previous study comparing throat swabs and mouth swabs.[5]

From the user feedback surveys, many caregivers noted the CandyCollect device is less frightening for children than other sampling methods, especially in comparison to throat swabs. Several caregivers noted that the CandyCollect device is easy, fun, and non-invasive. Some caregivers indicated that the CandyCollect device could help children be less afraid of going to the doctor or even be excited to do the test. All survey free responses and suggestions are included in Appendix Table C3. When asked for suggestions to improve CandyCollect devices, the most common suggestion was to shorten the sampling time. We responded to this suggestion mid-study by using a CandyCollect device that afforded a shorter sampling time for the second half of participants. As noted in the Results, caregivers indicated a preference for either the CandyCollect device or the mouth swab, with no caregivers (and no children) preferring the throat

swab. Notably, more caregivers preferred their children to use CandyCollect devices rather than mouth swabs when their child used smaller CandyCollect devices with a faster dissolving time (12/15) in comparison to caregivers of children who used the larger CandyCollect devices with a longer dissolving time (5/15). Slightly more children also preferred using CandyCollect devices when they used faster-dissolving CandyCollect devices (13/15 vs. 11/15). Schuster et al., also reported the same reasoning for sampling preferences: 73% of participants preferred the nasal swab compared to saliva collection by drooling due to the faster sampling time.[17] We are currently working to modify the CandyCollect device so as to have faster dissolving candy.

There are three major limitations for this study. First, this pilot study was performed with a relatively small sample size; we have ongoing studies with larger sample sizes in adults and children with GAS and other respiratory illnesses. Second, participants were recruited from a single site with relatively homogenous demographics, although we have no reason to suspect that demographics influence capture of pathogens in saliva. Our ongoing work includes remote nationwide studies with enrollment demographics matching national distribution of race/ethnicities. Finally, to maximize the number of positive cases tested with CandyCollect devices in this feasibility study, we only included children who tested positive for GAS on pharyngeal swabs analyzed with RADT during their clinic visits; future studies will include children with pharyngitis of unknown etiology evaluated with standard clinical and research protocols.

4.5 Conclusion

The CandyCollect device, a user-friendly pathogen collection method, is specifically designed to make both in-clinic and at-home sampling more accessible for children. In our inaugural pediatric clinical study, we demonstrated the CandyCollect device successfully captured

GAS from 30 children in a clinical setting. Notably, a majority of the children and their caregivers expressed a preference for the CandyCollect device as their chosen method for collecting GAS (compared to traditional throat swabs and mouth swabs). This study represents a significant step towards facilitating collection of samples for the detection of GAS and other respiratory pathogens. Currently, we are modifying the CandyCollect device based on user feedback to optimize its performance and user experience. We will enroll more participants to achieve larger sample sizes of children with GAS pharyngitis and also include healthy children and/or children who test negative for GAS on the in-clinic RADT. We are also developing methods to integrate the CandyCollect device with RADT; initial work is reported in Sanchez et al.[18] The present study paves the way for several exciting research directions, including: (1) integrating existing lateral flow immunoassay techniques with the CandyCollect device to enhance the diagnostic capabilities at home and shorten the diagnostic time, and (2) expanding the range of pathogens that can be captured using the CandyCollect device.

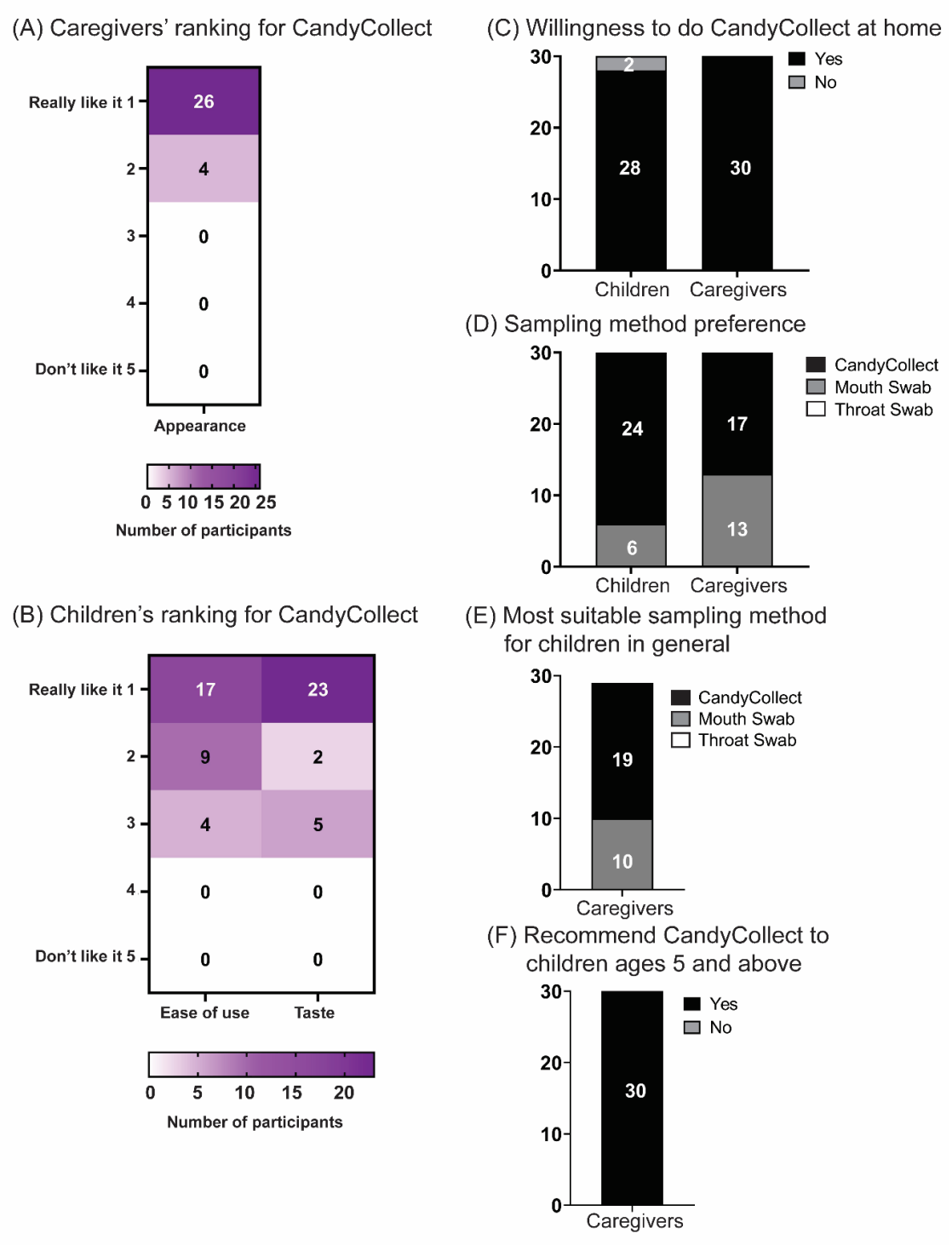

Figure 4.6. Survey responses to assess the ranking of CandyCollect devices and user preferences. All survey questions are included in Appendix Table C1 and C2. (A) Appendix Table C2 question 10 (B) Appendix Table C1 questions 6 and 7 (C) Appendix Table C1 question 5 and Appendix Table C2 question 9 (D) Appendix Table C1 question 4 and Appendix Table C2 question 7 (E) Appendix Table C2 question 8 (F) Appendix Table C2 question 11.

4.6 References

1. Walker MJ, Barnett TC, McArthur JD, et al. Disease Manifestations and Pathogenic Mechanisms of Group A Streptococcus. *Clinical Microbiology Reviews*. 2014;27(2):264-301. doi:10.1128/cmr.00101-13
2. Centers for Disease Control and Prevention Updated June 27, 2022. Accessed July10, 2023. https://www.cdc.gov/groupastrep/diseases-hcp/strep-throat.html#:~:text=Clinicians%20need%20to%20use%20either,the%20gold%20standard%20diagnostic%20test
3. Shulman ST, Bisno AL, Clegg HW, et al. Clinical Practice Guideline for the Diagnosis and Management of Group A Streptococcal Pharyngitis: 2012 Update by the Infectious Diseases Society of America*. Clinical Infectious Diseases*. 2012;55(10):e86-e102. doi:10.1093/cid/cis629
4. Ralph AP, Holt DC, Islam S, et al. Potential for Molecular Testing for Group A Streptococcus to Improve Diagnosis and Management in a High-Risk Population: A Prospective Study*. Open Forum Infect Dis*. 2019;6(4):ofz097. doi:10.1093/ofid/ofz097
5. DeMuri G and Wald ER. Detection of Group A Streptococcus in the Saliva of Children Presenting With Pharyngitis Using the cobas Liat PCR System*. Clin Pediatr (Phila).* 2020;59(9-10):856-858. doi:10.1177/0009922820920936
6. Bellagambi FG, Lomonaco T, Salvo P, et al. Saliva sampling: Methods and devices. An overview*. TrAC Trends in Analytical Chemistry*. 2020;124:115781. doi:https://doi.org/10.1016/j.trac.2019.115781
7. All-in-one system for the collection and rapid stabilization of microbial DNA and RNA. Accessed August 15, 2023. https://www.dnagenotek.com/row/products/collection-microbiome/omnigene-oral/OME-505.html
8. Melo Costa M., Benoit N, Dormoi J, et al. Al-meras, L. Salivette, a relevant saliva sampling device for SARS-CoV-2 detection. *J. Oral Microbiol*. 2021; 13, 1920226. doi: 10.1080/20002297.2021.1920226
9. Lee UN, Su X, Hieber DL, et al. CandyCollect: at-home saliva sampling for capture of respiratory pathogens*. Lab Chip*. 2022;22(18):3555-3564. doi:10.1039/d1lc01132d
10. Tu W-c, McManamen AM, Su X, et al. At-Home Saliva Sampling in Healthy Adults Using CandyCollect, a Lollipop-Inspired Device. *Analytical Chemistry*. 2023;95(27):10211-10220. doi:10.1021/acs.analchem.3c00462
11. Ottaviano E, Parodi C, Borghi E, et al. Saliva detection of SARS-CoV-2 for mitigating company outbreaks: a surveillance experience, Milan, Italy, March 2021. *Epidemiol Infect*. 2021;149:e171. doi:10.1017/s0950268821001473
12. De Meyer J, Goris H, Mortelé O, et al. Evaluation of Saliva as a Matrix for RT-PCR Analysis and Two Rapid Antigen Tests for the Detection of SARS-CoV-2. Viruses. 2022;14(9)doi:10.3390/v14091931

13. Harris PA, Taylor R, Thielke R, Payne J, Gonzalez N, Conde JG. Research electronic data capture (REDCap)—A metadata-driven methodology and workflow process for providing translational research informatics support. *Journal of Biomedical Informatics*. 2009;42(2):377-381. doi:10.1016/j.jbi.2008.08.010
14. Harris PA, Taylor R, Minor BL, et al. The REDCap consortium: Building an international community of software platform partners. *Journal of Biomedical Informatics*. 2019;95:103208. doi:10.1016/j.jbi.2019.103208
15. Wong-Baker FACES® Pain Rating Scale https://wongbakerfaces.org/
16. Gera K, McIver KS. Laboratory growth and maintenance of Streptococcus pyogenes (the Group A Streptococcus, GAS). *Curr Protoc Microbiol*. Oct 2 2013;30:9d.2.1-9d.2.13. doi:10.1002/9780471729259.mc09d02s30
17. Schuster JE, Potts J, Selvarangan R, Mast DK, Goldman JL. A COVID-19 Testing Preference Study in Schools. *Pediatrics.* 2023;152(Suppl 1) doi:10.1542/peds.2022-060352H
18. Sanchez JC, Robertson IH, Shinkawa VAM, et al. Integration of the CandyCollect device with a commercially available lateral flow immunoassay for GAS detection. medRxiv 2024, 2024.09.16, doi: https://doi.org/10.1101/2024.09.16.24312510

Chapter 5*|*Conclusion and Future Directions

This dissertation advances the foundational design of open microfluidic capillary flow systems and highlights the significant potential of open microfluidic technologies in patient-centered specimen collection devices.

Chapter 2 demonstrates that capillary trees with homothetically decreasing cross-sectional areas and incorporating absorbent paper pads at the terminal ends of the branches significantly extend the duration of high-flow pumping. This work opens new avenues for applying open microfluidics to challenging scenarios, such as sustaining the passive flow of viscous biological fluids like blood or saliva in open channels.

The collection of oral samples for diagnosing streptococcal pharyngitis is particularly important in pediatric populations. To address limitations of traditional pharyngeal swabs, our lab previously developed CandyCollect, an open microfluidic device for salivary pathogen collection, designed in the form of a lollipop to increase child compliance. Chapter 3 presents a proof-of-concept study showing that CandyCollect successfully captures various species of commensal oral bacteria from saliva from healthy adults nationwide. Chapter 4 validates CandyCollect as the preferred collection tool among children and caregivers. Clinical data from pediatric patients aged 5–14 years showed 100% concordance between CandyCollect samples and conventional sampling methods, supporting its clinical viability.

The increasing interest in applying open microfluidic systems to human health highlights the significance of the technologies presented in this work. The capillary-driven flow system, which utilizes open-channel tree structures integrated with paper pads, shows great potential for a range of biological applications, including *in vitro* cell culture and analytical assays involving

biofluids. Further development is needed to fully explore these applications—for example, using the capillary channels to separate plasma from whole blood, with the paper pad serving as an absorbent medium to collect the plasma.

CandyCollect, on the other hand, could be further refined by incorporating ingredients preferred by caregivers—such as replacing artificial food coloring with natural colorants—reducing sample collection time by enhancing capture and elution efficiency, and improving the sensitivity of downstream assays. Scalability challenges could be addressed through mass-production techniques like injection molding. Currently, the CandyCollect device is limited to saliva sample collection. To expand its utility as a point-of-care (PoC) diagnostic tool, it could be integrated with commercial rapid test kits, enabling both sample collection and detection in the at-home setting and to broaden its diagnostic utility.

Appendix

A. Appendix for Chapter 2

Reproduced in part from Jodie C. Tokihiro, Wan-chen Tu,* Jean Berthier,* Jing J. Lee, Ashley M. Dostie, Jian Wei Khor, Madeleine Eakman, Ashleigh B. Theberge,# Erwin Berthier,# "Enhanced capillary pumping using open-channel capillary trees with integrated paper pads." Physics of Fluids 35, 082120 (2023). https://doi.org/10.1063/5.0157801*

Table A1. Physical properties of the solvents. The term $\sqrt{\left(\frac{\gamma}{\mu}\right) 2\lambda cos\theta^*}$ is the coefficient of the extended Lucas-Washburn law and there is a slight difference between the value obtained from literature and from experiments.

Physical property	50% IPA	Nonanol	Pentanol
[a] Surface tension γ [mN/m]	24	28.5	25.4
[a] Viscosity μ [mPa•s]	3.2	11.2	3.75
[a,b] Contact angle ϑ [deg]	18	13	
$\gamma \cos \vartheta$ [mN/m]	22.8	27.8	
[c] $\gamma \cos \vartheta^*$ [mN/m]	14.6	17.9	
[d] Literature data $\sqrt{\left(\frac{\gamma}{\mu}\right) 2\lambda \cos\theta^*}$ [mm/s$^{1/2}$]	48.2	28.5	41.3
[e] Experimental data $\sqrt{\left(\frac{\gamma}{\mu}\right) 2\lambda cos\theta^*}$ [mm/s$^{1/2}$]	40	23-25	40

[a] air at room temperature[4-7]; [b] contact angle of the solvent on native PMMA; [c] $\cos \vartheta^*$ is the Cassie contact angle[8]; [d] calculated using values in the table on line 1 (γ), 2 (μ), 5 ($\gamma \cos \vartheta^*$), and λ = 259 µm[1,2]. [e] fit with the travel distance in the root channel (z_0).

Table A2. Characteristic dimensions of the homothetic channels

Dimension	Level 0 (root)	Level 1	Level 2	Level 3
Width [mm]	1.06	0.90	0.77	0.65
Depth [mm]	1.76	1.50	1.28	1.08
Wetted perimeter p_0 [mm]	4.13	3.51	3.00	2.53
[a]Friction length λ [μm]	259	220	187	159
Cross-sectional area S_0 [mm^2]	1.75	1.26	0.92	0.66

[a] obtained from previous publication.[1,2]

Table A3. Characteristics of Whatman #1 paper pads.

[a] Physical and geometrical properties	Symbol	Value	Unit
Permeability	K	2.3×10^{-6}	mm^2
Porosity	φ	0.7	-
Capillary pressure (IPA 50%)	P_{cap}	3300	Pa
Capillary pressure (nonanol)	P_{cap}	5500	Pa

[a] porosity and permeability are obtained from the literature[3], capillary pressures were determined by fitting K and φ to the experimental data.

Section 1. Dynamics of capillary flow in the open-channel capillary tree

Root channel. We derive first the dynamics in the root channel. Neglecting the evanescent initial inertial regime,[9,10] the balance between capillary force F_{cap} and wall friction F_{drag} leads to

$$F_{cap} = p\,\gamma\,cos\theta^* = F_{drag} = p\,z_0\bar{\tau} = p\,z_0\left(\mu\frac{V_0}{\lambda}\right), \tag{S1}$$

where $\bar{\tau}$ is the average friction, p the total channel perimeter in a cross section, V_0 the average velocity (which is a function of time and/or travel distance), λ the average friction length, μ the viscosity, γ the surface tension, and θ^* the generalized Cassie angle[11] (in order to take into account the free surface of the open channel and accommodate for the potential of non-monolithic channels comprising different materials on the floor and walls). Then we have the relation between travel distance and time

$$\frac{d\,z_0^2}{dt} = \frac{2\,\lambda\,\gamma\,cos\theta^*}{\mu}, \tag{S2}$$

And finally

$$z_0 = \sqrt{\frac{2\,\lambda\,\gamma\,cos\theta^*}{\mu}}\,\sqrt{t} \tag{S3}$$

Note that the time at which the flow reaches the bifurcation at a distance L_0 from entrance, is

$$t_0 = \frac{\mu}{2\lambda\,\gamma\,cos\theta^*}\,L_0^2 = \frac{L_0^2}{C} \quad \text{(S4)}$$

where $C = \frac{2\,\lambda\,\gamma\,cos\theta^*}{\mu}$.

Tree branches. After the first bifurcation, at the level *n*, we must use a formulation that uses the pressures and write the pressure equilibrium along a fluidic path[1,12–15]

$$p_0\,L_0\,\mu\frac{V_0}{\lambda_0}\frac{1}{S_0} + \cdots + p_n\,z_n\,\mu\frac{V_n}{\lambda_n}\frac{1}{S_n} = \frac{p_n\,\gamma\,cos\theta_n^*}{S_n}, \quad \text{(S5)}$$

where z_n here is the travel distance in the n^{th} ramification, S_n the cross-sectional area and V_n the velocity in the daughter branch ($V_n = \frac{dz_n}{dt}$). Relation (S5) indicates that the capillary pressure is equal to the pressure associated to the friction along a path starting from the root channel to the n^{th} channel. Using the relations linked to the homothetic ratio α, we have for the cross-sectional perimeters are

$$p_n = \alpha p_{n-1} = \cdots = \alpha^{n-1}p_1 = \alpha^n p_0, \quad \text{(S6)}$$

and the cross-sectional areas are

$$S_n = \alpha^2 S_{n-1} = \cdots = \alpha^{2(n-1)}S_1 = \alpha^{2n}S_0 \quad \text{(S7)}$$

Moreover, the friction lengths are homothetic because they are proportional to the hydraulic diameter of the channel

$$\lambda_n = \alpha\lambda_{n-1} = \cdots = \alpha^{n-1}\lambda_1 = \alpha^n\lambda_0 \quad \text{(S8)}$$

Hence the ratio $\frac{p_i}{\lambda_i}$ is constant for all indices *i* from *0* to *n*, equal to $\frac{p_0}{\lambda_0}$. Moreover, the Cassie angles are everywhere the same, i.e., $\theta^* = \theta_1^* = \cdots = \theta_n^*$. Substituting (S6), (S7) and (S8) in (S5) yields

$$\alpha^{2n}L_0\,V_0 + \alpha^{2(n-1)}\,L_1\,V_1 + .. + \alpha^2 L_{n-1}V_{n-1} + \,z_n\,V_n = \frac{p_n}{p_0}\frac{\gamma}{\mu}\lambda_0\,cos\theta^* \,= \alpha^n\frac{\gamma}{\mu}\lambda_0\,cos\theta^* = \alpha^n\frac{C}{2}\ . \quad \text{(S9)}$$

Using the mass conservation equation,

$$V_0 = (2\,\alpha^2)V_1 = (2\,\alpha^2)^2\,V_2 \,= \cdots = (2\,\alpha^2)^n\,V_n, \quad \text{(S10)}$$

and remarking that $V_n = \frac{dz_n}{dt}$, (S9) becomes a differential equation in z_n that can be integrated to obtain a quadratic polynomial in z_n

$$z_n^{\,2} + 2[(2\alpha^4)^n L_0 \,+\, (2\,\alpha^4)^{n-1}\,L_1 + \cdots + \,2\alpha^4 L_{n-1}]z_n = \alpha^n C\,(t - t_{n-1})\,, \quad \text{(S11)}$$

Denoting $A_n = (2\alpha^4)^n L_0 + (2\,\alpha^4)^{n-1} L_1 + \cdots + 2\alpha^4 L_{n-1} = (2\alpha^4)^n L_0 \Sigma_{n-1}$, where $\Sigma_{n-1} = \left[1 + \frac{L_1}{2\alpha^4 L_0} + \cdots + \frac{L_{n-1}}{(2\,\alpha^4)^{n-1} L_0}\right]$, the solution is

$$z_n = A_n \left[-1 + \sqrt{1 + \frac{\alpha^n C}{A_n^2}\,(t - t_{n-1})}\right] \qquad \text{(S12)}$$

Note that the travel distance given by relation (S12) is not of the conventional Lucas-Washburn form ($z \approx \sqrt{t}$), but of the form $z \approx -A + \sqrt{A^2 + \alpha^n C t}$.

Section 2. Dynamics of capillary flow in the paper pads (coupled to that in the open-channel capillary tree)

When reaching the extremities of the tree branches, the liquid start wicking the paper pads. The motion wicking of the pads is governed by Darcy's law [16,17]

$$V_p = -\frac{K}{\mu\phi}\nabla P = \frac{K}{\mu\phi}\frac{P_{cap}-P_j}{z_p}. \quad \text{(S13)}$$

where P_{cap} is the capillary pressure of the paper and P_j the pressure at the junction channel-paper pad. K is the permeability of the pad and φ its porosity. The index p refers to the paper. The triplet (P_{cap}, K, φ) characterizes the paper strip.[18,19]

Three assumptions are used in the present model. First, the paper pads are homogeneous, i.e., there are no regions of higher or lower porosity. Hence, degree of saturation (local percentage of liquid) is assumed the same everywhere in the paper pad.[20,21] As a consequence, the capillary pressure P_{cap} is constant everywhere, and there is no smearing of the advancing contact line, which is described in the literature as a sharp front approach.[22] Second, it is assumed that the dilatation of the paper fibers with the penetrating the liquid is negligible, so that the porosity φ is constant everywhere in the pad. Third, the cellulose fibers do not absorb the wicking liquid, so that the mass conservation is independent of the time. Then equation (S13) can be cast under the form

$$\frac{d(z_p)^2}{dt} = \frac{2K}{\mu\phi}\left(P_{cap} - P_j\right). \quad \text{(S14)}$$

In order to solve equation (S14), the pressure P_j mut be determined. According to (S5)

$$P_j = p_0\, L_0\, \mu \frac{V_0}{\lambda_0}\frac{1}{S_0} + \cdots + p_n\, L_n\, \mu \frac{V_n}{\lambda_n}\frac{1}{S_n}, \quad \text{(S15)}$$

where *n* is the channel level at the junction with the paper pads. Using again (S6), (S7), (S8) and (S10), the pressure P_j can be expressed as

$$P_j = p_0\, L_0\, \mu \frac{V_0}{\lambda_0}\frac{1}{S_0}\left(1 + \frac{L_1}{L_0}\frac{1}{2\,\alpha^4} + \cdots + \frac{L_n}{L_0}\frac{1}{(2\,\alpha^4)^n}\right) = p_0\, L_0\, \mu \frac{V_0}{\lambda_0}\frac{1}{S_0}\Sigma_n \quad . \quad \text{(S16)}$$

Using the mass conservation equation, the velocity V_0 can be expressed in function of the velocity in the paper

$$V_0 S_0 = 2^n \phi V_p S_p\,, \quad \text{(S17)}$$

where S_p is the total cross-sectional area of the pad. We consider two types of paper pads: rectangular and conical (triangular). We can group together the two geometries by writing

$$S_p = S_{p,0} + 2\beta\, h_p\, z_p\,, \quad \text{(S18)}$$

where z_p is the penetration distance, h_p is the thickness of the paper pad, $S_{p,0}$ the cross section of the paper at the junction—there can be a sharp increase of section between the last channels of the tree and the pads— and β the cone semi-angle. In the case of a rectangular pad, $\beta = 0$. In the case of a cone, the wetted cross-section in the paper pad is assumed to have a perfectly rounded interface.

Successively substituting (S18) in (S17) and (S17) in (S16) yields the expression of the pressure P_j in function of V_p and z_p

$$P_j = \frac{p_0 L_0}{\lambda_0 S_0} \mu \Sigma_n 2^n \phi V_p \left(\frac{S_{p,0}}{S_0} + \frac{2\beta h_p z_p}{S_0}\right). \quad \text{(S19)}$$

For simplifying the notations, let us note $a_n = 2^n \Sigma_n K \frac{p_0 L_0}{\lambda_0 S_0}$, $\delta = \frac{S_0}{2\beta h_p}$ and $b = \frac{2K}{\mu\phi} P_{cap}$. The two first parameters a_n and δ have the dimension of a length, while the unit for b is mm^2/s. Substituting (S19) in (S14), and using the relation $V_p = \frac{dz_p}{dt}$, produce the differential equation for the penetration distance z_p

$$\frac{d(z_p)^2}{dt}\left(1 + \frac{a_n}{\delta}\right) + 2a_n \frac{S_{p,0}}{S_0} \frac{dz_p}{dt} - b = 0. \quad \text{(S20)}$$

The solution is

$$z_p = \frac{a_n}{\left(1+\frac{a_n}{\delta}\right)} \frac{S_{p,0}}{S_0} \left(-1 + \sqrt{1 + \left(\frac{S_0}{S_{p,0}}\right)^2 \frac{b\left(1+\frac{a_n}{\delta}\right)\tau}{a_n^2}}\right), \quad \text{(S21)}$$

where □ = t - t_n is the time taken from the entrance of the pad (□ = 0, z_p = 0). Note that, for rectangular pads, $\delta = \infty$, ($\frac{1}{\delta} = 0$), and (S21) becomes

$$z_p = a_n \frac{S_{p,0}}{S_0} \left(-1 + \sqrt{1 + \left(\frac{S_0}{S_{p,0}}\right)^2 \frac{b\,\tau}{a_n^2}} \right) . \qquad \text{(S22)}$$

For rectangular pads, it is verified that, if the capillary pressure P_{cap} in the paper is very high (the parameter b is large), (S22) can be simplified, and the travel distance in the paper is $z_p \approx \sqrt{bt} = \sqrt{\frac{2K\,P_{cap}}{\mu\phi} t}$, which is simply the Lucas-Washburn law for paper alone, obtained by direct integration of (S14) with P_j = 0. In this case, the influence of the tree completely disappears.

In the general case, deriving (S21) in respect to time, the velocity of the fluid in the pad is

$$V_p = \frac{S_0}{S_{p,0}} \frac{b}{2a_n \sqrt{1+\left(\frac{S_0}{S_{p,0}}\right)^2 \frac{b\left(1+\frac{a_n}{\delta}\right)\tau}{a_n^2}}} . \qquad \text{(S23)}$$

Using the mass conservation equation (S17), the velocity in the root channel when the liquid wicks the paper is given by

$$V_{root} = 2^n V_p \phi \frac{S_p}{S_0} = \phi \left(\frac{S_{p,0}}{S_0} + \frac{z_p}{\delta}\right) \frac{S_0}{S_{p,0}} \frac{b}{2a_n \sqrt{1+\left(\frac{S_0}{S_{p,0}}\right)^2 \frac{b\left(1+\frac{a_n}{\delta}\right)\tau}{a_n^2}}} , \qquad \text{(S24)}$$

where z_p is given by (S21). At the precise time when the fluid contacts the pad (= 0, z_p = 0), relation (S24) yields $V_{root,0} = \frac{\phi\, b}{2a_n}$, and replacing a_n and b by their expressions, $\frac{P_{cap}}{\Sigma_n} = \frac{p_0 L_0}{S_0}\frac{\mu\, V_{root,0}}{\lambda_0}$, which is the expression of the pressure P_0 at the end of the root channel when the velocity is $V_{root,0}$.

Let us consider the case of conical pads. The penetration distance z_p can be removed from (S24) by using (S21)

$$V_{root} = \frac{2^{n-1}\phi\, b}{a_n}\frac{\left(\delta + a_n\sqrt{1+D\tau}\right)}{(\delta + a_n)\sqrt{1+D\tau}}, \qquad \text{(S25)}$$

where $D = \left(\frac{S_0}{S_{p,0}}\right)^2 \frac{b\left(1+\frac{a_n}{\delta}\right)}{a_n^2}$.

The unit of D is 1/s. In the case of rectangular pads, the derivation of V_{root} yields

$$V_{root} = \frac{2^{n-1}\phi\, b}{a_n}\frac{1}{\sqrt{1+D_r\tau}}, \qquad \text{(S27)}$$

where $D_r = \left(\frac{S_0}{S_{p,0}}\right)^2 \frac{b}{a_n^2}$

Table A4. Summary of coefficients used in the different solvents

Coefficient	Unit	IPA 50%	Nonanol	Pentanol
a	mm	0.0026	0.0026	0.0026
d	mm	1.6	1.6	1.6
a/d	-	0.002	0.002	0.002
Sp_0/Sp	-	0.38	0.38	0.38
b	mm^2/s	3.7	1.8	
Viscosity μ	mPa.s	3.2	11.2	3.75
Capillary pressure P_{cap}	Pa	2072	4116	
2^nS_n	-	11.34	11.34	
Surface tension γ	mN/m	24	28.5	
Contact angle ϑ	degrees	18	13	
Cassie contact angle ϑ^*	degrees	55.5	52.0	
Capillary force $\gamma \cos \vartheta^*$	mN/m	13.6	17.5	
Washburn coefficient $\sqrt{\left(\frac{\gamma}{\mu}\right) 2\lambda \cos\theta^*}$	$mm/s^{1/2}$	47.0	28.5	
Washburn coefficient from fit with experiments $\sqrt{\left(\frac{\gamma}{\mu}\right) 2\lambda \cos\theta^*}$	$mm/s^{1/2}$	38	25	

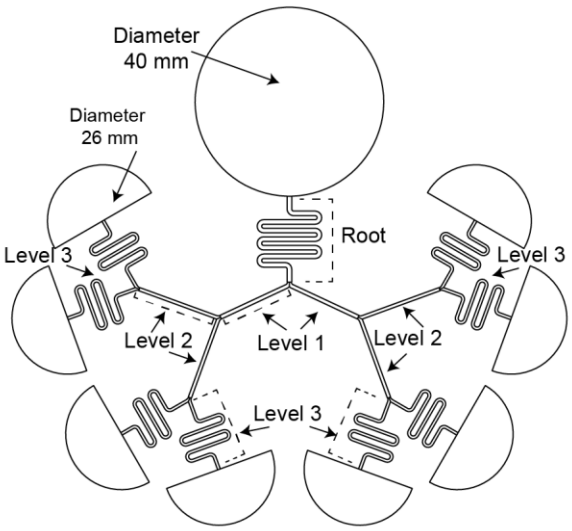

Level (L)	Length (mm)	Width (mm)	Depth (mm)
0 (root)	98.0	1.06	1.76
1	18.2	0.90	1.50
2	20.1	0.77	1.28
3	58.8	0.65	1.08

Figure A1. Engineering drawing of device with dimensions.

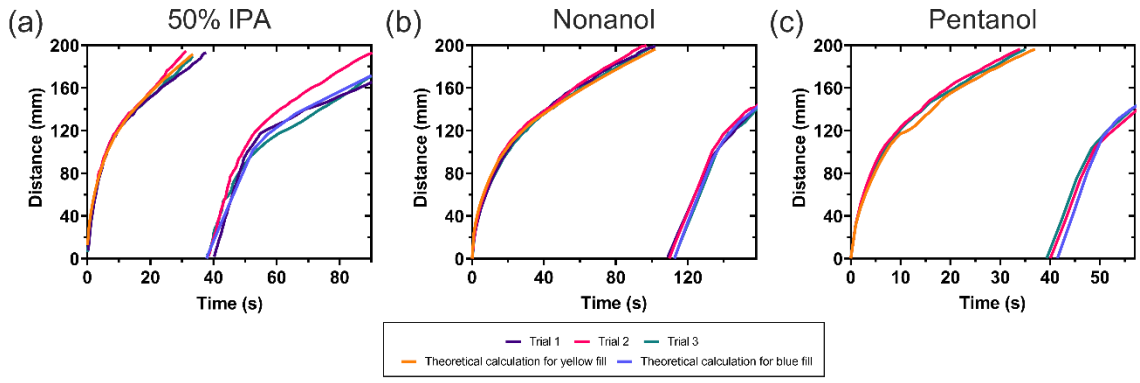

Figure A2. Raw data plots of all trials for (a) 50% IPA and (b) nonanol (c) pentanol of distance traveled over time.

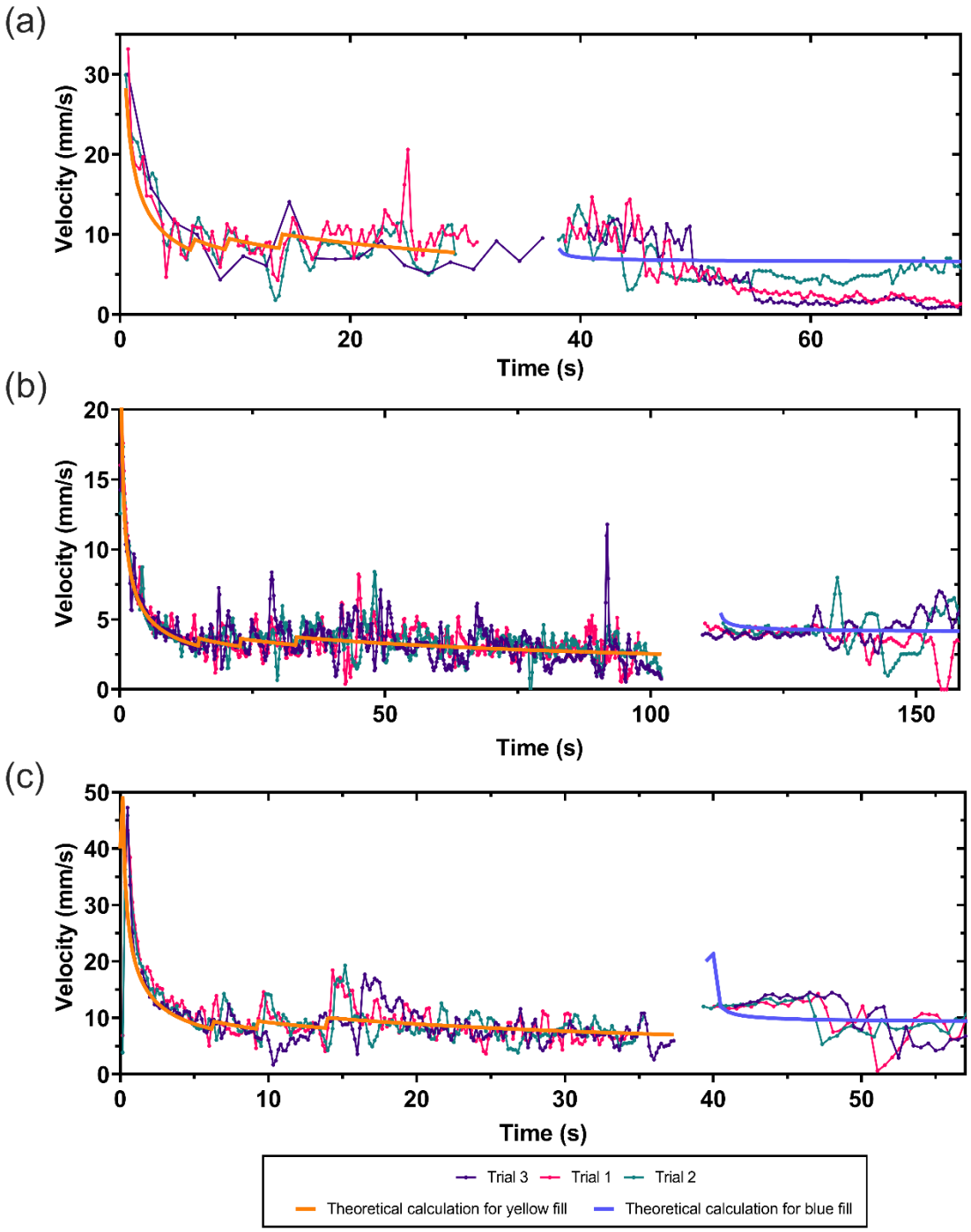

Figure A3. Raw data plot of all trials for (a) 50% IPA and (b) nonanol (c) pentanol of velocity over time.

References

[1] J. J. Lee, J. Berthier, A. B. Theberge, and E. Berthier, Langmuir 35, 10667 (2019).

[2] J. J. Lee, J. Berthier, K. E. Kearney, E. Berthier, and A. B. Theberge, Langmuir 36, 12795 (2020).

[3] M. Boodaghi and A. Shamloo, AIChE J. 66, e16756 (2020).

[4] A. A. Mohammad, K. H. A. E. Alkhaldi, M. S. AlTuwaim, and A. S. Al-Jimaz, J. Chem. Thermodyn. 74, 7 (2014).

[5] S. Kim, P. A. Thiessen, E. E. Bolton, J. Chen, G. Fu, A. Gindulyte, L. Han, J. He, S. He, B. A. Shoemaker, J. Wang, B. Yu, J. Zhang, and S. H. Bryant, Nucleic Acids Res. 44, (2016).

[6] J. Berthier, K. A. Brakke, D. Gosselin, A.-G. Bourdat, G. Nonglaton, N. Villard, G. Laffite, F. Boizot, G. Costa, and G. Delapierre, Microfluid. Nanofluidics 18, 919 (2015).

[7] J. J. Lee, J. Berthier, K. A. Brakke, A. M. Dostie, A. B. Theberge, and E. Berthier, Langmuir 34, 5358 (2018).

[8] J. Berthier, K. A. Brakke, and E. Berthier, Open Microfluidics, 1 (2016).

[9] C. H. Bosanquet, Philos. Mag. Ser. 6 45, 525 (1923).

[10] D. Quéré, Europhys. Lett. 39, 533 (1997).

[11] J. Berthier, K. A. Brakke, and E. Berthier, Microfluid. Nanofluidics 16, 779 (2014).

[12] H. Mehrabian, P. Gao, and J. J. Feng, Phys. Fluids 23, 122108 (2011).

[13] D. Yang, M. Krasowska, C. Priest, M. N. Popescu, and J. Ralston, J. Phys. Chem. C 115, 18761 (2011).

[14] F. F. Ouali, G. McHale, H. Javed, C. Trabi, N. J. Shirtcliffe, and M. I. Newton, Microfluid. Nanofluidics 15, 309 (2013).

[15] J.-C. Baret, M. M. J. Decré, S. Herminghaus, and R. Seemann, Langmuir 23, 5200 (2007).

[16] H. Darcy, Les Fontaines Publiques de La Ville de Dijon, (Paris, 1856).

[17] S. Whitaker, Transp. Porous Media 1, 3 (1986).

[18] S. C. Amico and C. Lekakou, Polym. Compos. 23, 249 (2002).

[19] A. Ashari and H. Vahedi Tafreshi, Colloids Surfaces A Physicochem. Eng. Asp. 346, 114 (2009).

[20] J. H. Dane, C. Hofstee, and A. T. Corey, Water Resour. Res. 34, 3687 (1998).

[21] B. AJ, B. R, F. B, and G. MB, Adv. Colloid Interface Sci. 233, 176 (2016).

[22] M. A. F. Zarandi, K. M. Pillai, and A. S. Kimmel, AIChE J. 64, 294 (2018).

B. Appendix for Chapter 3

Reproduced in part from Wan-chen Tu, Anika M. McManamen,* Xiaojing Su, Ingrid Jeacopello, Meg G. Takezawa, Damielle L. Hieber, Grant W. Hassan, Ulri N. Lee, Eden V. Anana, Mason P. Locknane, Molly W. Stephenson, Victoria A. M. Shinkawa, Ellen R. Wald, Gregory P. DeMuri, Karen Adams, Erwin Berthier, Sanitta Thongpang#, Ashleigh B. Theberge#, "At-Home Saliva Sampling in Healthy Adults Using CandyCollect, a Lollipop-Inspired Device." Analytical Chemistry. 2023;95(27):10211-10220.*

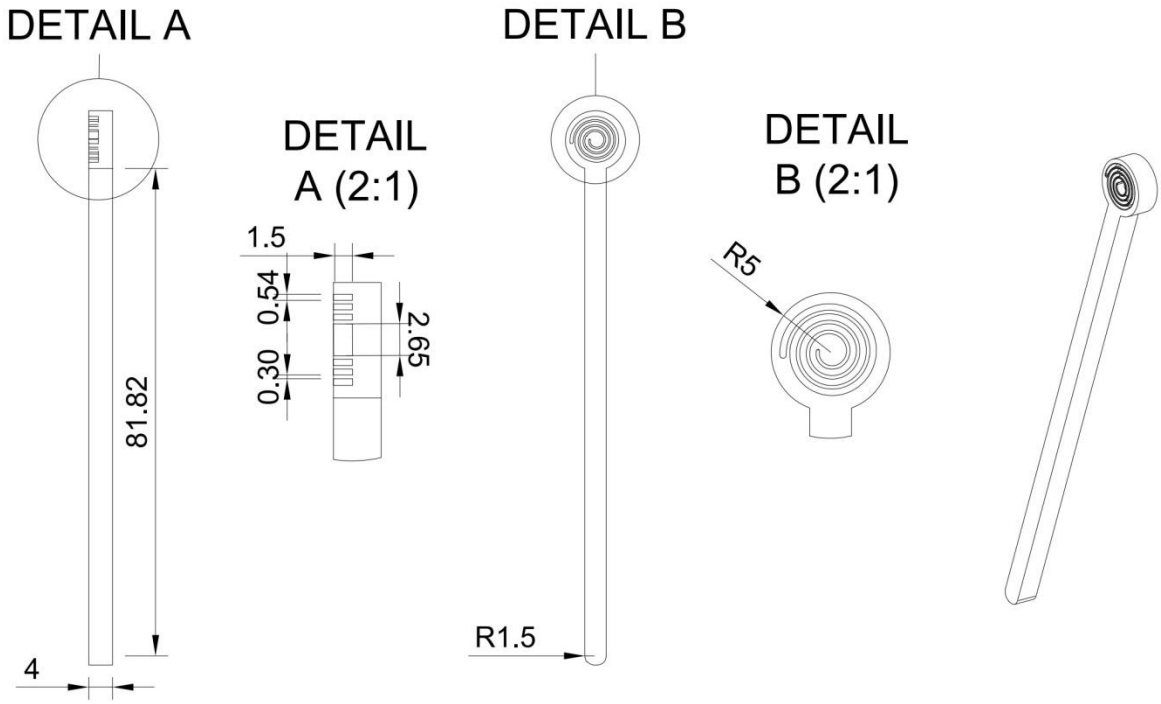

Figure B1. Schematic of the CandyCollect device dimensions. All dimensions are in mm.

Table B1. Mass, diameter, thickness, and dissolving time of CandyCollects in Figure 3.4 (Day 1)

Participant	Mass (g)	Diameter (mm)	Thickness (mm)	Time (min)
1	1.34	16	4	4:35
	1.24	16	4	4:16
	1.37	16	4	5:00
2	1.26	16	4	2:48
	1.21	16	4	3:31
	1.38	16	4	3:51
3	1.34	16	4	4:13
	1.33	16	4	5:01
	1.28	16	4	4:16
4	1.37	16	4	4:50
	1.23	16	4	4:21
	1.40	16	4	4:34
5	1.34	16	4	4:25
	1.30	16	4	4:51
	1.40	16	4	4:31
6	1.32	16	4	5:02
	1.39	16	4	5:37
	1.31	16	4	4:19
7	1.24	16	4	8:32
	1.41	16	4	7:00
	1.32	16	4	7:52

8	1.30	16	4	7:58
	1.39	16	4	8:22
	1.34	16	4	4:43
9	1.40	16	4	2:48
	1.23	16	4	2:10
	1.36	16	4	2:12
10	1.86	16	5	3:14
	1.86	16	5	2:34
	1.90	16	5	2:45
11	1.33	16	4	5:04
	1.37	16	4	3:58
	1.37	16	4	4:54
12	1.40	16	4	2:37
	1.34	16	4	2:06
	1.21	16	4	2:39
13	1.24	16	4	4:35
	1.33	16	4	4:32
	1.21	16	4	4:25
14	1.32	16	4	5:41
	1.32	16	4	5:24
	1.32	16	4	5:31

Table B2. Mass, diameter, thickness, and dissolving time of CandyCollects in Figure 3.4 (Day 2)

Participant	Mass (g)	Diameter (mm)	Thickness (mm)	Time (min)
1	1.7	16	5	4:45
	1.72	16	5	4:33
	1.83	16	5	5:00
2	1.80	16	5	3:51
	1.76	16	5	2:49
	1.77	16	5	3:29
3	1.70	16	5	5:46
	1.72	16	5	6:20
	1.72	16	5	5:54
4	1.84	16	5	5:50
	1.79	16	5	5:00
	1.76	16	5	4:59
5	1.77	16	5	6:01
	1.75	16	5	5:20
	1.72	16	5	4:48
6	1.82	16	5	4:53
	1.88	16	5	5:01
	1.9	16	5	4:21
7	1.81	16	5	9:08
	1.83	16	5	10:34
	1.77	16	5	9:49

8	1.74	16	5	4:53
	1.81	16	5	6:18
	1.90	16	5	4:18
9	1.86	16	5	2:47
	1.81	16	5	2:34
	1.89	16	5	2:39
10	1.31	16	4	2:08
	1.24	16	4	2:57
	1.37	16	4	3:10
11	1.89	16	5	5:35
	1.77	16	5	6:02
	1.76	16	5	6:49
12	1.83	16	5	4:37
	1.81	16	5	4:49
	1.77	16	5	4:59
13	1.86	16	5	5:37
	1.77	16	5	6:11
	1.88	16	5	6:35
14	1.81	16	5	5:32
	1.9	16	5	6:22
	1.79	16	5	6:36

S. aureus primer modification and verification

The primer/probe sequences for the *S. aureus* qPCR assay were referenced from Galia et al., 2019[1] with minor modifications for both forward and reverse primers. Probe sequence remains the same as in Galia et al., 2019[1] except using FAM as a reporter dye. The forward primer sequence was modified based on the NCBI database for *S. aureus* sequence (25923) (GenBank accession no. CP000046); the reverse primer sequence modification was based on the ATCC Genomes database for *S. aureus* (25923). All primer/probe sequences are listed in Table S3 below. Primer validation is shown in Figure B2-3.

Table B3. The sequences of *S. aureus* primers and probe. The original forward (F0), reverse (R0) primers, and probe are adopted from Galia et al., 2019; in this study, modified forward and reverse primers were designated as F1 and R1.

Primers/probe	**sequences**	**Notes**
Forward (F0)	5'-GGCATATGTATGGCAATTGTTTC-3'	Galia et al. 2019[1]
Forward (F1)	5'-GGCATATGTATGGCAATCGTTTC-3'	This study
Reverse (R0)	5'-CGTATTGCCCTTTCGAAACATT-3'	Galia et al. 2019[1]
Reverse (R1)	5'-CGTATTGTTCTTTCGAAACATT-3'	This study
Probe	5'-/56-FAM/ATT ACT TAT AGG GAT GGC TAT C/3MGB-NFQ/-3'	Galia et al. 2019[1]

We first tested the original forward/reverse primer pair (F0/R0), from Galia et al., 2019,[1] for qPCR amplification and efficiency with SYBR Green chemistry. A 1:10 serial dilution of purified DNA from *S. aureus* was used as templates (10 ng to 10 fg/reaction). Purified DNA from *S. mutans* and *S. pyogenes* (10 ng/reaction) were used as negative controls. qPCR was run under the following thermal cycling conditions: 5 min at 95 °C followed by 40 cycles of 95 °C for 15 s and 60 °C for 30

s. Based on the amplification plot (Figure B2), qPCR with F0/R0 primer pair did not have a good dynamic range of detection and the reaction efficiency was low. In addition, two negative controls had strong fluorescence signals (data not shown). This prompted us to seek improvement in primer design. The modified forward primer sequence (F1) has only one nucleotide different from the F0; the modified reverse primer sequence (R1) has two nucleotides different from the R0 (Table B3). To validate the new primers, the new primer was paired with the original forward or reverse primers or another new primer: F0/R1, F1/R0, F1/R1, and was examined for qPCR amplification and efficiency as above. The F0/R1 primer pair had improved assay dynamic range and efficiency compared to the original F0/R0. The F1/R0 and F1/R1 primer pairs sets provided the best assay dynamic range and efficiency (Figure B2). It is noted that non-specific amplification can also be detected in the qPCR assays for these three pairs of primers. To increase specificity, F1/R0 and F1/R1 primer pairs were combined with the probe originally designed from Galia et al., 2019[1], and TaqMan master mix was used for the qPCR assay with purified DNA as above. The results showed that the F1/R1 primer pair had better sensitivity and wider assay dynamic range compared with F1/R0 pair (Figure B3A). The efficiency is 85%. Agarose gel electrophoresis showed a single PCR product (~70 bp, an expected amplicon size) in qPCR with both F1/R0 and F1/R1 primers/probe pairs indicating amplification specificity (Figure B3B). Based on these results, we proceeded to use F1/R1 primers in the qPCR assay together with the TaqMan probe for detection of *S. aureus* in this paper.

qPCR amplification plots and standard curves with SYBR green chemistry

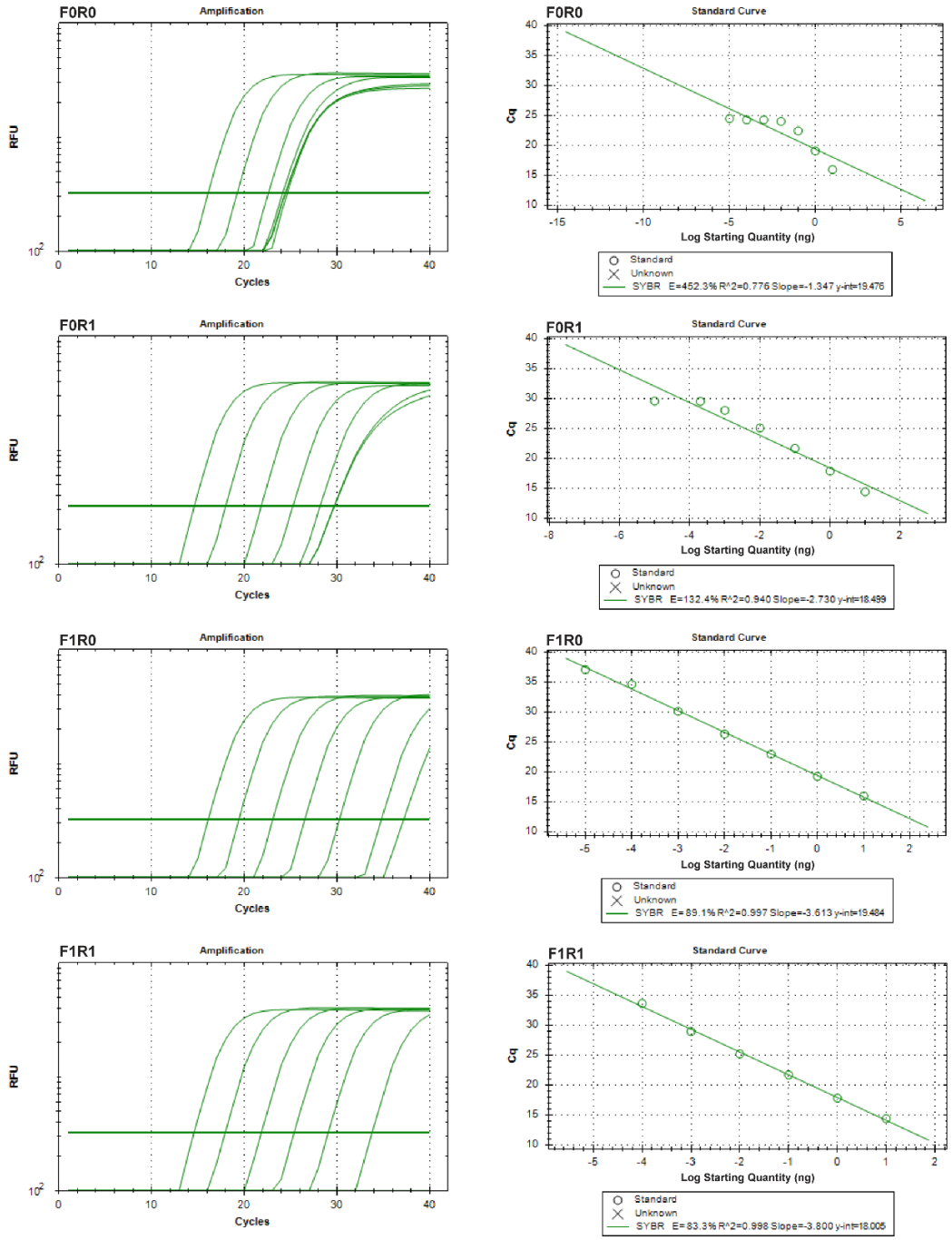

Figure B2. *S. aureus* primer validation by qPCR with SYBR Green chemistry. The qPCR amplification plots and standard curves were from different combinations of *S. aureus* forward and reverse primers. SYBR Green chemistry was used for detection. F0 and R0 are the original forward and reverse primers used in Galia et al. 2019[1]; F1 and R1 are modified forward and reverse primers, respectively.

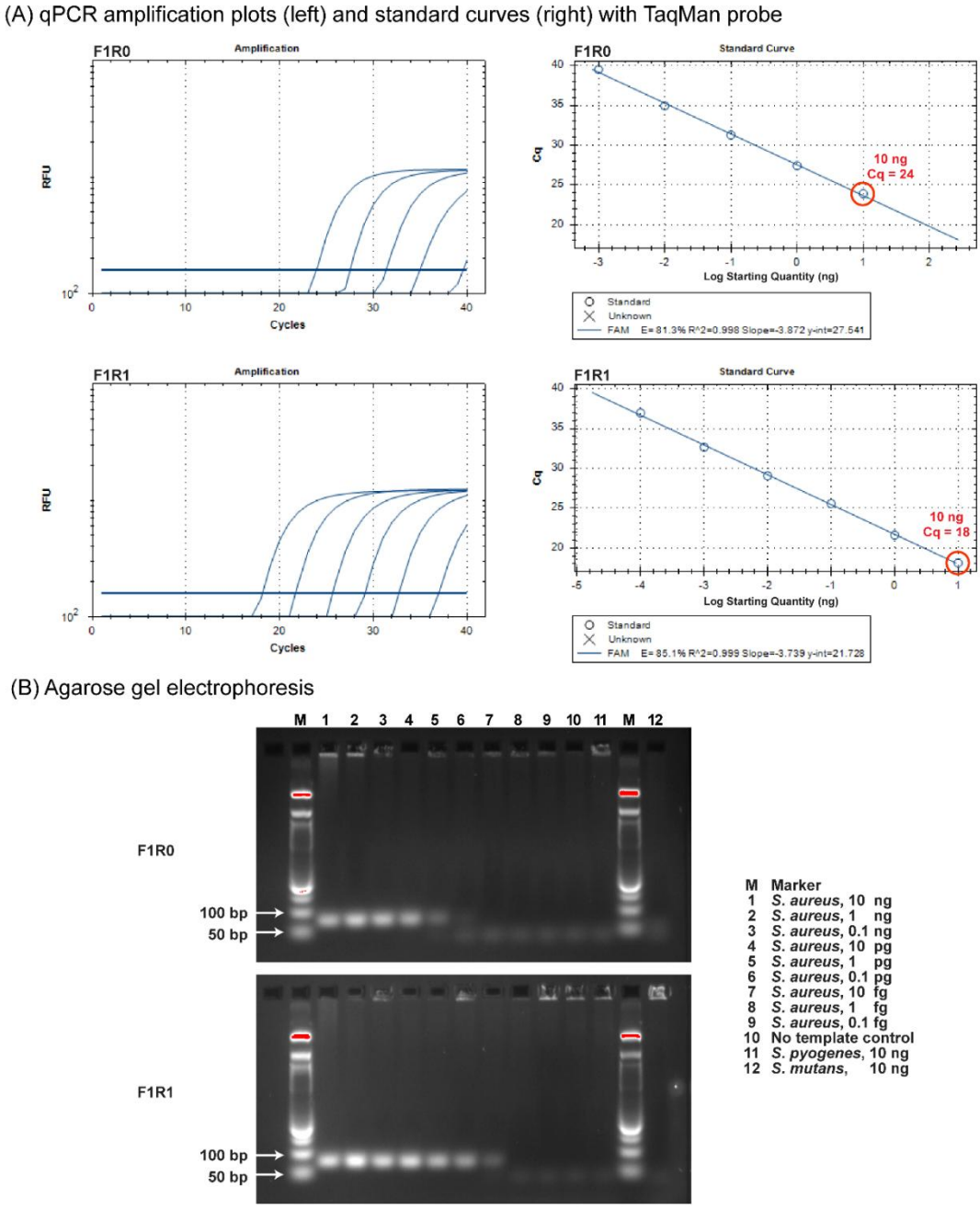

Figure B3. *S. aureus* primer validation by agarose gel electrophoresis and qPCR with TaqMan probe. The modified forward and reverse primers (F1/R1) with probe analysis used in this paper for *S. aureus* detection. (A) The qPCR amplification plots (left) and standard curves (right) of *S. aureus.* Probe was added in the qPCR assay. The result showed that the F1/R1 pair (bottom) had better sensitivity and wider dynamic range compared with F1/R0 pair (top). (B) Agarose gel electrophoresis demonstrated high selectivity of the qPCR assay. Agarose gel electrophoresis showed a single PCR product (~70 bp, expected amplicon size) in qPCR with both F1/R0 and F1/R1 primers/probe pairs (top: F1R0 and bottom: F1R1) indicating amplification specificity. The

templates were 1:10 serial dilution of DNA (10 ng to 0.1 fg /reaction) from *S. aureus* DNA (lane 1 to 9) and lane M is DNA ladder. No PCR products were shown in DNA samples from no template control (lane 10), *S. pyogenes* (lane 11) (10 ng), and *S. mutans* (lane 12) (10 ng). 3% agarose gel was used to separate DNA products from the qPCR reactions.

(A) *S. mutans* standard curves for human participant samples

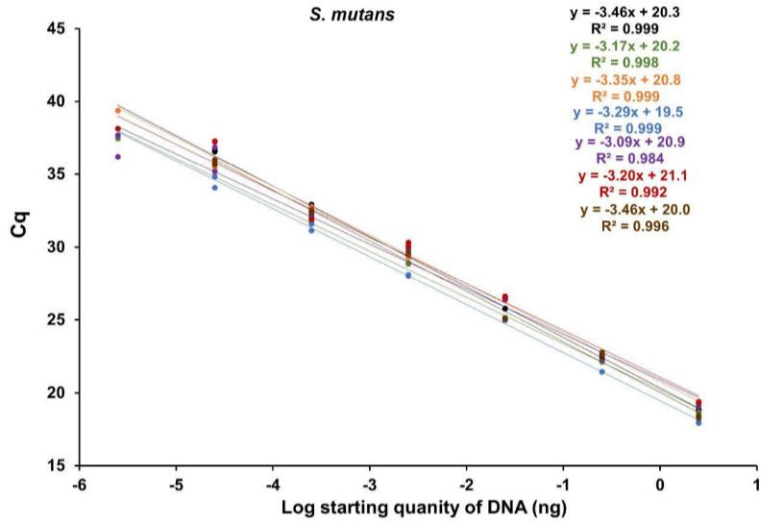

(B) *S. aureus* standard curves for human participant samples

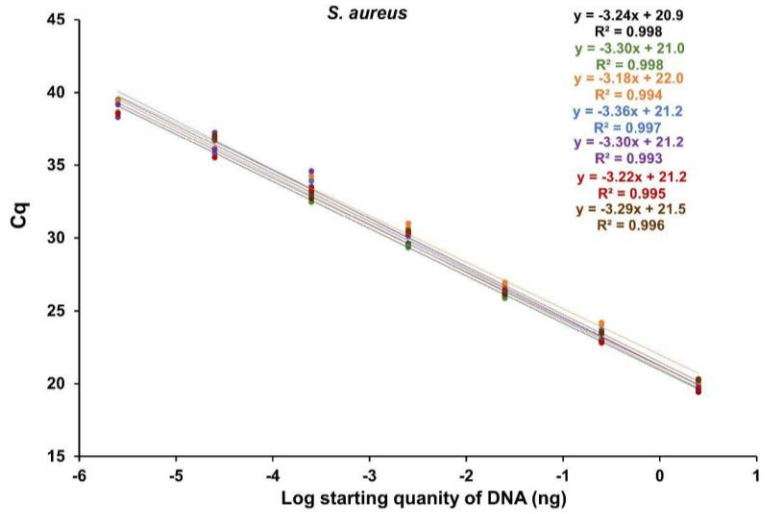

Figure B4. Standard curves for the (A) *S. mutans* and (B) *S. aureus* qPCR assays. 1:10 serial dilutions of genomic DNA ranging from 25 ng to 25 fg was used as template for qPCR. Each dot represents one technical duplicate (in cases where one point is visible the duplicates were identical). The standard curves in which Cq values were plotted against starting template DNA, were linear. qPCR slopes ranged from -3.09 to -3.46 for *S. mutans* and -3.18 to -3.36 for *S. aureus* across 7 independent experiments.

Table B4. Survey questions for user feedback

Was the CandyCollect easy to hold on to the handle?	(1 Very Bad - 5 Very Good)
Was the CandyCollect easy to suck on?	1 - 5
Does the CandyCollect look appealing (the color, the overall appearance)?	1 - 5
Did you like the taste of the CandyCollect?	1 - 5
Do you have a dry mouth today?	Yes No
Do you have a chronic condition such as Sjogren's syndrome that affects saliva production?	Yes No
If so, did you think your saliva production decreased during your participation in this study?	Yes No
Would you recommend these CandyCollect to children ages 4 and above?	Yes No
Please explain your choice from the previous question.	
How can we improve our CandyCollect for children? (Provide any suggestions) (optional)	
What was your preferred method of sampling?	CandyCollect ESwab Spitting Tube
What was the most suitable sampling method for children?	CandyCollect ESwab Spitting Tube
Please explain your choice from the question above	
What method provided the best sampling experience?	CandyCollect ESwab Spitting Tube
Rank the methods from easiest to hardest to use.	CandyCollect ESwab Spitting Tube
What method provided the best sampling experience?	CandyCollect ESwab Spitting Tube

Which method seemed the least invasive?	CandyCollect ESwab Spitting Tube
Which method was the least disgusting or uncomfortable?	Yes No
Which method was the most sanitary?	
Was it easy to follow the instructions?	1 – 5
How easy was it to complete the surveys and enroll in our study?	1 – 5
How can we improve our instructions and the survey section of this form? (Provide any suggestions) (optional)	

(A)

(B)

Figure B5. At-home saliva sampling devices for human subjects study. Self-saliva collection methods enable at-home sampling then shipping back to lab analysis. Three different collection methods included six CandyCollect devices, six ESwab™, and two SpeciMAX Stabilized Saliva Collection Kits (from left to right). (A) wrapped (B) unwrapped.

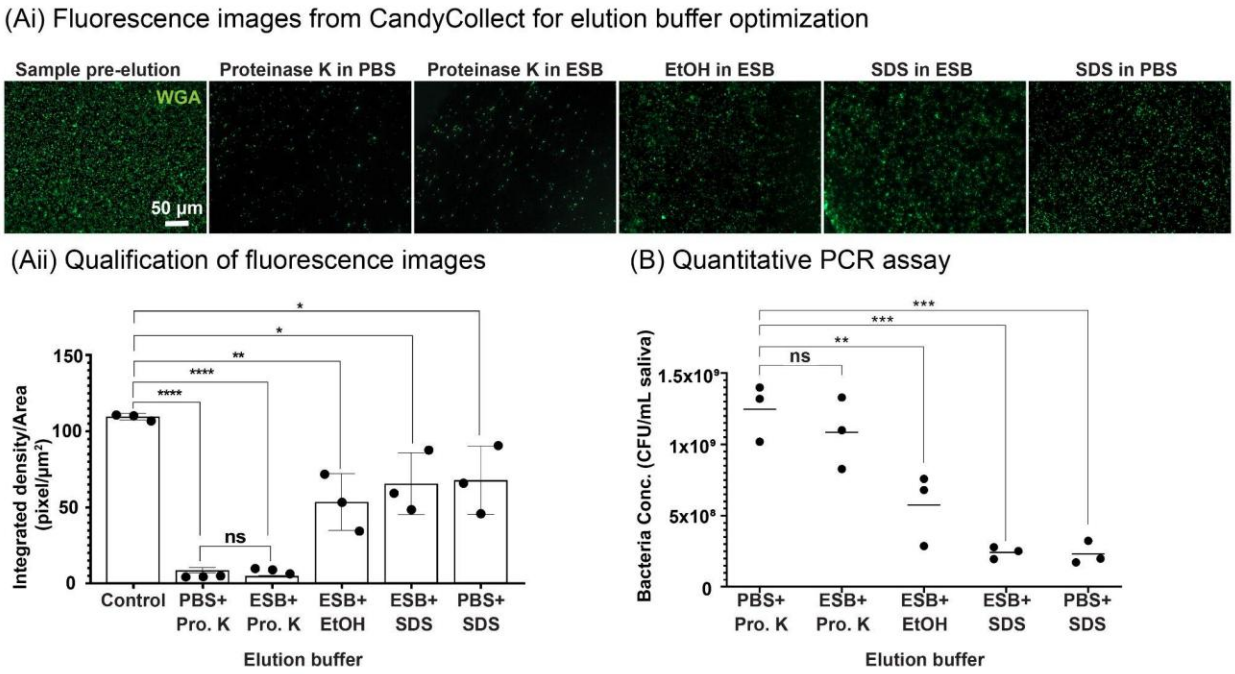

Figure B6. Additional elution experiments demonstrate that *S. aureus* captured by CandyCollect devices can be removed efficiently via elution buffers. (A) *S. aureus* at a concentration of $1x10^9$ CFU/mL was incubated on the CandyCollect device and eluted via five elution buffers. The image result suggests that only the Proteinase K in PBS and Proteinase K in ESwab buffer (ESB) could efficiently remove *S. aureus* on CandyCollect. *S. aureus* was green fluorescently labeled with WGA. (Aii) Quantification of the integrated density per area (pixel/μm^2). Each data point represents an individual CandyCollect; The bar graph represents the mean ± SEM of n = 3 CandyCollects. Data sets were analyzed using one-way ANOVA; p-values are indicated for pairwise comparisons between the control and different elution buffers: *p ≤ 0.1, **p ≤ 0.01, ****p ≤ 0.0001 (Tukey's multiple comparison tests). (B) Proteinase K in PBS and Proteinase K in ESwab buffer were the most efficient elution buffers based on the qPCR results. Quantification of *S. aureus* by qPCR. Each data point represents an individual CandyCollect. No significant differences were observed between Proteinase K in PBS and Proteinase K in ESwab buffer.

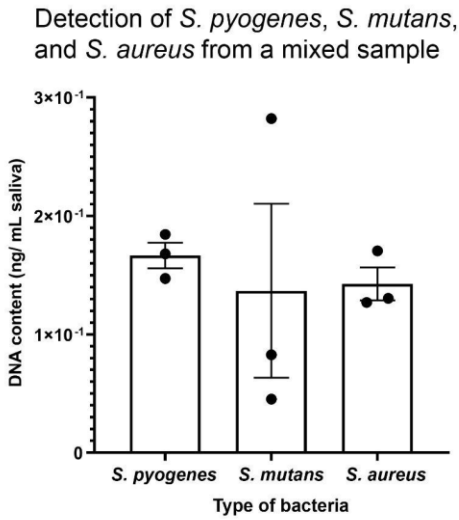

Figure B7. qPCR tests demonstrate that the mixture of three bacteria in saliva can be analyzed for their individual concentrations. Three bacteria, *S. pyogenes*, *S. mutans*, and *S. aureus*, were mixed at the concentration of 10^4 CFU/mL. Quantification of the three bacteria by qPCR. DNA contents were detected in a bacterial concentration-dependent manner. Each data point represents an individual CandyCollect; the bars represent the mean ± SEM of n=3 CandyCollects.

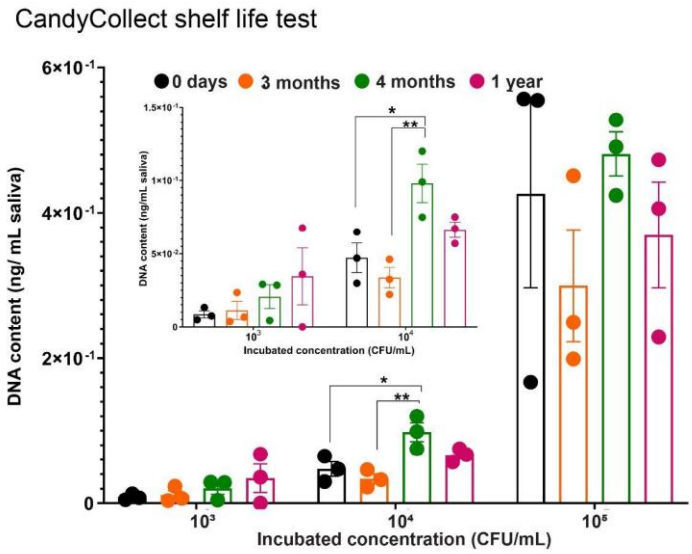

Figure B8. qPCR shelf life tests demonstrate that the CandyCollect device effectively captures *S. pyogenes* after 1 year of storage. CandyCollect devices were plasma treated and stored at room temperature for 0 days (control group), 3 months, 4 months, and 1 year. After the storage period, *S. pyogenes* was incubated on the CandyCollect devices, eluted, and analyzed by qPCR. Each data point represents an individual CandyCollect device; the bar graph represents the mean ± SEM of n = 3 CandyCollect devices. Data sets were analyzed using one-way ANOVA followed by Tukey's multiple comparisons test; p-values are indicated for pairwise comparisons between different storage times (*p<0.05 and **p<0.01). Note: one of the CandyCollect devices from 1 year shelf life 10^3 CFU/mL had no qPCR signal.

References

(1) Galia, L.; Ligozzi, M.; Bertoncelli, A.; Mazzariol, A. Real-time PCR assay for detection of *Staphylococcus aureus*, Panton-Valentine Leucocidin and Methicillin Resistance directly from clinical samples. *AIMS Microbiol.* **2019**, 5, 138-146.

C. Appendix for Chapter 4

Reproduced in part from Wan-chen Tu, Ingrid H. Robertson,* Andrea Blom, Elena Alfaro, Victoria A. M. Shinkawa, Daniel B. Hatchett, Juan C. Sanchez, Anika M. McManamen, Xiaojing Su, Erwin Berthier, Sanitta Thongpang, Ellen R. Wald,# Gregory P. DeMuri,# Ashleigh B. Theberge.# Bioeng Transl Med. e70001 (2025). https://doi.org/10.1002/btm2.70001*

Table C1. Survey questions for user feedback (children)

1	Circle a number below to show how much pain (discomfort) you felt during the THROAT SWAB. [Children were shown the Wong-Baker FACES® Pain Rating Scale, refer to Figure S2.]	0 No hurt 2 Hurts Little Bit 4 Hurts Little More 6 Hurts Even More 8 Hurts Whole Lot 10 Hurts Worst 99 Declined to answer
2	Circle a number below to show how much pain (discomfort) you felt during the MOUTH SWAB. [Children were shown the Wong-Baker FACES® Pain Rating Scale, refer to Figure S2.]	0 0 No hurt 2 2 Hurts Little Bit 4 4 Hurts Little More 6 6 Hurts Even More 8 8 Hurts Whole Lot 10 10 Hurts Worst 99 Declined to answer
3	Circle a number below to show how much pain (discomfort) you felt during the CANDYCOLLECT (lollipop). [Children were shown the Wong-Baker FACES® Pain	0 0 No hurt

	Rating Scale, refer to Figure S2.]	2 — 2 Hurts Little Bit 4 — 4 Hurts Little More 6 — 6 Hurts Even More 8 — 8 Hurts Whole Lot 10 — 10 Hurts Worst 99 — Declined to answer
4	If you needed to have another test for strep throat next week, which would you prefer?	1 — Throat Swab 2 — Mouth Swab 3 — CandyCollect (lollipop) 99 — Declined to answer
5	Would you be willing to do the CandyCollect (lollipop) at home?	1 — Yes 2 — No 99 — Declined to answer
6	Was the CandyCollect (lollipop) easy to suck on?	1 — 1 Very Easy 2 — 2 3 — 3 4 — 4 5 — 5 Very Hard 99 — Declined to answer
7	Did you like the taste of the CandyCollect (lollipop)?	1 — 1 Really like it

		2 | 2 3 | 3 4 | 4 5 | 5 Don't like it 99 | Declined to answer

Table C2. Survey questions for user feedback (caregivers)

<table>
<tr><td>1</td><td>Think back to the moment when your child was having the THROAT SWAB done by the clinic staff. Please provide your impressions of the THROAT SWAB by marking your impression on the scale between Pleasant and Unpleasant.</td><td><table><tr><td>1</td><td>1 - Pleasant</td></tr><tr><td>2</td><td>2</td></tr><tr><td>3</td><td>3</td></tr><tr><td>4</td><td>4</td></tr><tr><td>5</td><td>5</td></tr><tr><td>6</td><td>6</td></tr><tr><td>7</td><td>7 - Unpleasant</td></tr></table></td></tr>
<tr><td>2</td><td>How would you rate the THROAT SWAB overall?</td><td>Slider (number, Min: -5, Max: 5)
Slider labels: Bad, Good</td></tr>
<tr><td>3</td><td>Think back to the moment when your child was having the MOUTH SWAB done by the clinic staff. Please provide your impressions of the MOUTH SWAB by check marking your impression on the scale between Pleasant and Unpleasant.</td><td><table><tr><td>1</td><td>1 - Pleasant</td></tr><tr><td>2</td><td>2</td></tr><tr><td>3</td><td>3</td></tr><tr><td>4</td><td>4</td></tr><tr><td>5</td><td>5</td></tr><tr><td>6</td><td>6</td></tr><tr><td>7</td><td>7 - Unpleasant</td></tr></table></td></tr>
<tr><td>4</td><td>How would you rate the MOUTH SWAB overall?</td><td>Slider (number, Min: -5, Max: 5)
Slider labels: Bad, Good</td></tr>
<tr><td>5</td><td>Think back to the moment when your child was having the CandyCollect (lollipop) done by the clinic staff . Please provide your impressions of the CandyCollect (lollipop) by checkmarking your impression on the scale between Pleasant and Unpleasant.</td><td><table><tr><td>1</td><td>1 - Pleasant</td></tr><tr><td>2</td><td>2</td></tr><tr><td>3</td><td>3</td></tr></table></td></tr>
</table>

<table>
<tr><td></td><td></td><td><table>
<tr><td>4</td><td>4</td></tr>
<tr><td>5</td><td>5</td></tr>
<tr><td>6</td><td>6</td></tr>
<tr><td>7</td><td>7 - Unpleasant</td></tr>
</table></td></tr>
<tr><td>6</td><td>How would you rate the CandyCollect (lollipop) overall?</td><td>Slider (number, Min: -5, Max: 5)
Slider labels: Bad, Good</td></tr>
<tr><td>7</td><td>If your child needed to have another test for strep throat next week, which would you prefer?</td><td><table>
<tr><td>1</td><td>Throat Swab</td></tr>
<tr><td>2</td><td>Mouth Swab</td></tr>
<tr><td>3</td><td>CandyCollect (lollipop)</td></tr>
<tr><td>99</td><td>Declined to answer</td></tr>
</table></td></tr>
<tr><td>8</td><td>What do you think is the most suitable sampling method for children in general?</td><td><table>
<tr><td>1</td><td>Throat Swab</td></tr>
<tr><td>2</td><td>Mouth Swab</td></tr>
<tr><td>3</td><td>CandyCollect (lollipop)</td></tr>
<tr><td>99</td><td>Declined to answer</td></tr>
</table></td></tr>
<tr><td>9</td><td>Would you be willing to have your child do the CandyCollect (lollipop) at home?</td><td><table>
<tr><td>1</td><td>Yes</td></tr>
<tr><td>2</td><td>No</td></tr>
<tr><td>99</td><td>Declined to answer</td></tr>
</table></td></tr>
<tr><td>10</td><td>Does the CandyCollect (lollipop) look appealing (the color, the overall appearance)?</td><td><table>
<tr><td>1</td><td>1 Really like it</td></tr>
<tr><td>2</td><td>2</td></tr>
</table></td></tr>
</table>

<table>
<tr><td></td><td></td><td><table>
<tr><td>3</td><td>3</td></tr>
<tr><td>4</td><td>4</td></tr>
<tr><td>5</td><td>5 Don't like it</td></tr>
<tr><td>99</td><td>Declined to answer</td></tr>
</table></td></tr>
<tr><td>11</td><td>Would you recommend these CandyCollect (lollipop) to children ages 5 and above?</td><td><table>
<tr><td>1</td><td>Yes</td></tr>
<tr><td>2</td><td>No</td></tr>
<tr><td>99</td><td>Declined to answer</td></tr>
</table></td></tr>
</table>

Table C3. Free response question

Please explain your response	**How can we improve our CandyCollect (lollipop) for children? Provide any suggestions**
Not scary, pleasant color, tasty, soothing on throat	Shorter time, other flavors, not sure about the sugar free sweetener
Child friendly, appealing to children.	No ideas
It takes longer than a swab but it is way more pleasant and fun for the child.	I think it's a great idea. Only complaint is that it takes a little while-but my child didn't mind!
Compared to throat swab, more appealing/less scary. Could help kids be less afraid to go to the doctor in general.	Consider making handle white instead of clear to make it look more like a lollipop.
My child is 10 yr old: he was in tears on the way here dreading the throat swab test. The candy collect would not only provide test results but also perhaps soothe his sore throat.	My only suggestion would be having a few flavors?
It seems fun for kids.	N/A
N/A	No suggestions
Kids like lollipops so not scary	Not take as long
They would be old enough to follow instructions and not have to worry of choking. They would also enjoy it.	N/A
Great, non-invasive test for an already painful ailment.	If it goes forward-esp over the counter-very easy, detailed instructions are helpful.
N/A	N/A
The CandyCollect was easy and fast; he seemed to enjoy it and there was no pain-big plus!!! :)	Different flavors for kids to choose from
My child seemed to find it far more pleasant than the throat swab.	I can't think of any suggestions.

N/A	Avoiding food dye would be beneficial for many children.
This is a simple, appealing test for kids: the color, size, and flavor all seem like a lollipop.	Make sure that parents know whether it includes red artificial food dye. Some parents avoid red dye #40 and similar additions. Parents might feel reassured knowing the ingredients and whether vegetable dye is used.
Seems like the candy would be way more appealing than having a throat swab.	Variety of flavors
Great alternative to throat swab	Quicker collection
Easy for kids to suck on as it tastes good and kids like suckers	None
Child was excited to do the test.	Nothing
No discomfort, especially compared to throat swab.	None
I feel based on the time for it dissolve that it would be better for kids 5 and older. I think that is a great age to be able to do that and wait. My son has a strong gag reflex so I think this was great.	I don't have any suggestions for improvement. I think it was a great way to collect a sample and I really hope strep can be detected this way.
My child liked the flavor, enjoyed the concept. It takes a bit longer than the mouth swab though.	Maybe have it dissolve in less time.
Easy, non-invasive	Quicker process
The mouth swab was easy, but if it's not effective the Candycollect was just as good!	Maybe shorter suck time?!
It is more pleasant than throat swab by far- but was time consuming.	No suggestions
Much easier than throat swab.	N/A
Really liked the concept of the CandyCollect but the time was a little long. The mouth swab is quick and easy even though no flavor.	N/A

Great way to collect in a fun way for kids.	My only concern would be the length of time and how much swallowing they have to do if their throat is very sore, and if they aren't feeling well.
N/A	I don't have any feedback.
If it didn't take as long	Offer a variety of flavors (Grape, Bubblegum), too long to do test

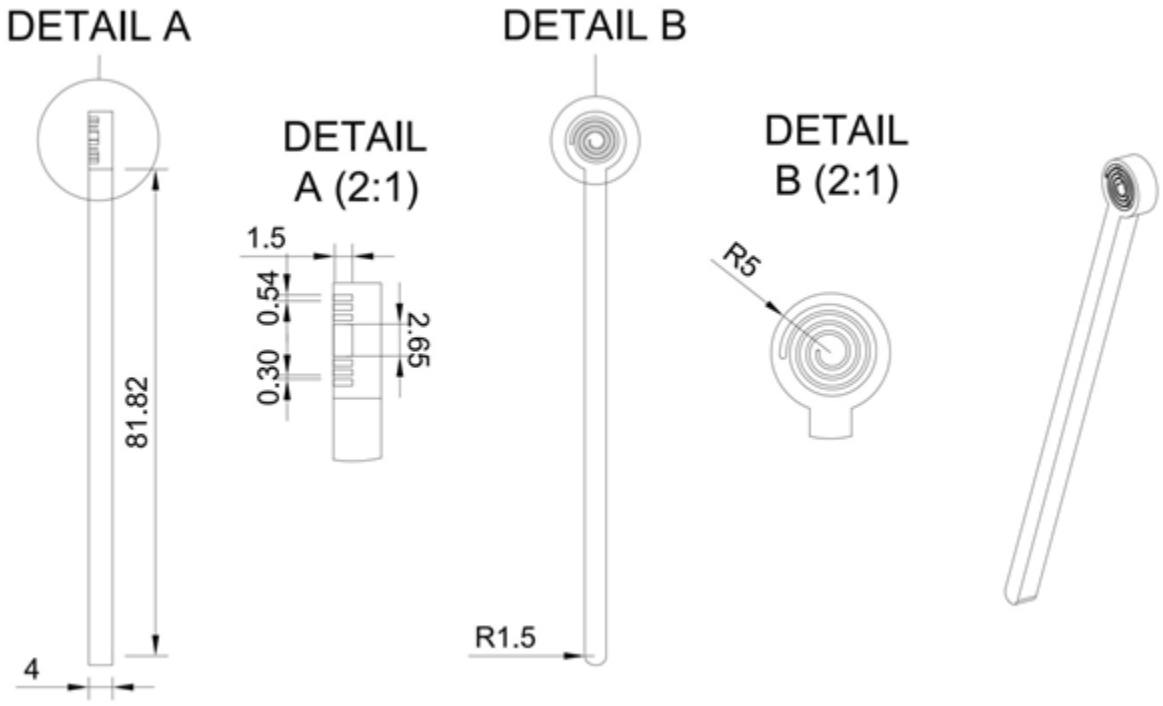

Figure C1. Schematic of the CandyCollect device dimensions. All dimensions are in mm. This figure is reproduced from Tu et al. [1] (Figure S1) with permission from the ACS publication (*Analytical Chemistry*).

Figure C2. Wong-Baker FACES® Pain Rating Scale.[2] Face 0 represents does not hurt at all; face 2 represents hurts just a little bit; face 4 represents hurts a little bit more; face 6 represents hurts even more; face 8 represents hurts a whole lot; face 10 represents hurts as much as you can imagine, although you do not have to be crying to have this worst pain.

Table C4. Study Participant Characteristics (Child Participants)

Characteristic	In this study No. (percentage)	In Dane County, Wisconsin[3]
Mean age	8.8 ± 2.5 years	
Female, n (%)	16 of 30 (53%)	49.9%
Race, n (%)		
American Indian or Alaska Native	0 (0%)	0.5%
Asian	1 (3%)	6.6%
Black or African American	1 (3%)	5.8%
Native Hawaiian or Other Pacific Islander	0 (0%)	0.1%
White	28 (93%)	84.1%
Ethnicity, n (%)		
Hispanic or Latino	1 (3%)	7.0%
Not Hispanic or Latino	29 (97%)	78.0%

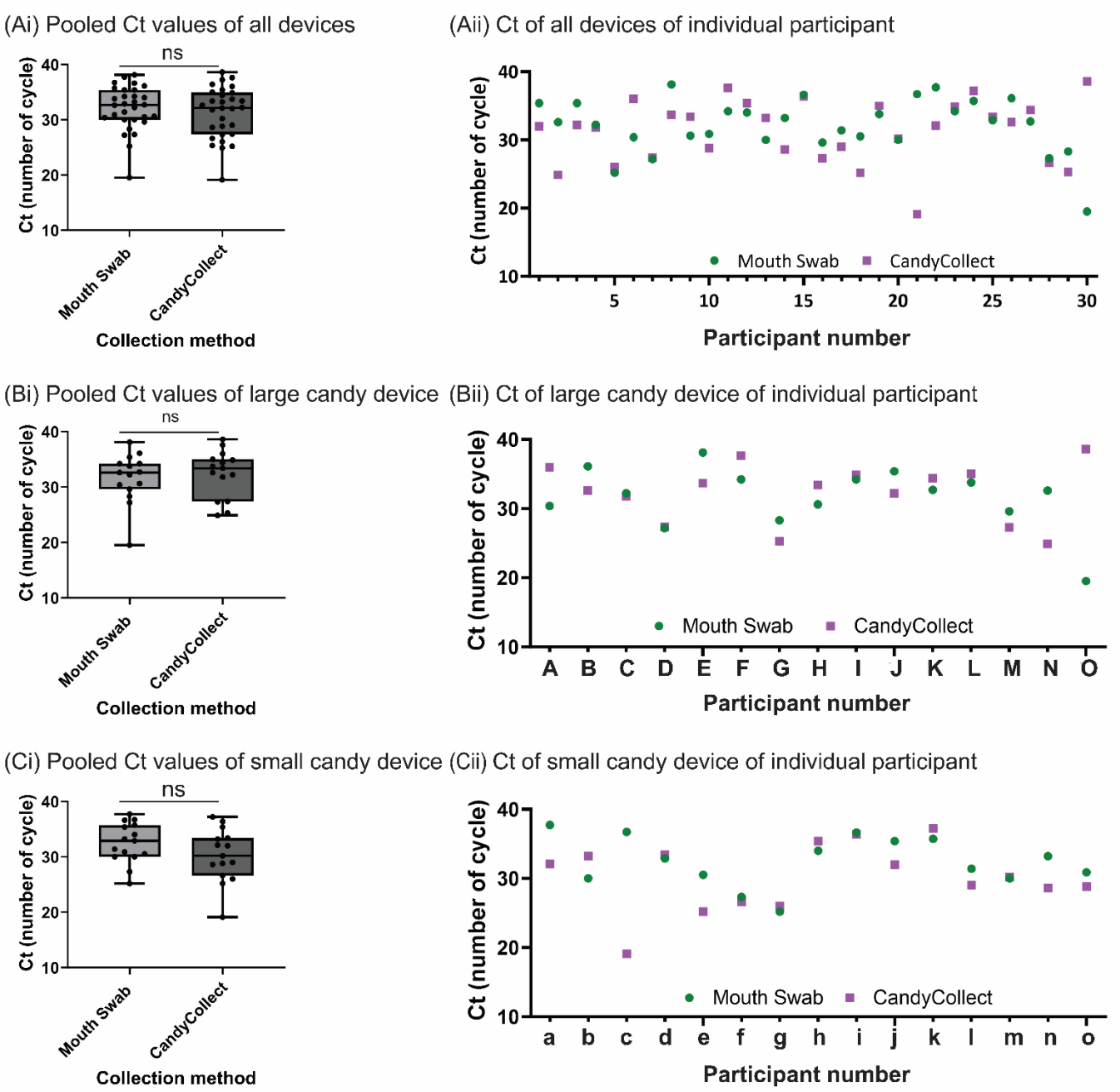

Figure C3. Pooled and individual cycle threshold (Ct) values of samples collected from mouth swabs and CandyCollect devices (A) all 30 child participants (B) from15 participants using the large CandyCollcet devices (Candy = 1.3g, green) and (C) from 15 participants using small CandyCollect devices (Candy = 0.5g, purple). Ct values from the two sampling methods are not significantly different ($p>0.05$). The participant numbers were randomly re-numbered.

Method (This section is reproduced from Lee et al. [3] and Tu et al. [1])

Bacteria culture

Liquid media preparation

For the THY liquid media, 30 g of Todd-Hewitt Broth (BD Bacto™ TH broth, Fisher Scientific, Cat# DF0492-17-6) and 2 g of Yeast Extract (United States Biological Corporation, Fisher Scientific, Cat# NC9796728) (THY) were added to 0.8 L distilled water and dissolved to completion. Additional distilled water was added for a total volume of 1 L. THY liquid media was autoclaved at 121 °C for 30 min, cooled to room temperature, and stored at 4 °C.

Agar plate preparation

7.5g agar (BD Difco™ Dehydrated Culture Media: Potato Dextrose Agar, Fisher Scientific, Cat# DF0013-17-6) was added to the 500 mL of liquid media, then autoclaved at 121 °C for 30 min. 15 mL of liquid media with agar was added to petri dishes, left to cool overnight, and stored at 4°C until needed for.

S. pyogenes maintenance in agar plate

Freeze-dried *S. pyogenes* was rehydrated with 1 mL liquid media, and then transferred to another conical tube containing 4.4 mL of liquid media. To maintain the bacteria, *S. pyogenes* were streaked on agar plates by sterile disposable inoculating loops (Globe Scientific, Fisher Scientific, Cat# 22-170-201). The agar plates were incubated at 37 °C with 5% carbon dioxide overnight, then stored at room temperature for up to 7 days.

In-lab capture of bacteria on CandyCollect devices and mouth swab

Incubation of S. pyogenes in liquid media

To ensure a pure culture, fresh *S. pyogenes* from agar plates were inoculated in liquid media and cultured at 37 °C with 5% carbon dioxide in the incubator one day prior to an experiment.

Preparation of positive and negative controls

After culturing overnight, the bacteria suspensions were homogenized with vortexing at a concentration of $1x10^4$ CFU/mL and added to each CandyCollect device at a volume of 50 µL and incubated for 10 minutes; for the mouth swab, the swab was soaked in homogenized bacteria suspensions for 10 seconds (PBS was used for device negative controls).

Specimen Processing and Laboratory Analysis

Research nurse stored the mouth swab (ESwab™) and CandyCollect samples at -20 °C for a few days after sampling at Madison, Wisconsin, and the samples were shipped to University of Washington using United Parcel Service (UPS) Next Day Air. Samples were stored at -80 °C before processing. All laboratory procedures were performed in accordance with Biosafety Level-2 laboratory practices and the University of Washington Site-Specific Bloodborne Pathogen Exposure Control Plan. To avoid unnecessary freeze-thaw cycles, mouth swab (ESwab™) samples were aliquoted into 20 µL aliquots and stored at -80 °C.

Elution of S. pyogenes from CandyCollect devices

The buffer used to elute bacteria captured on CandyCollect devices was phosphate buffered saline (PBS) (Gibco™, Cat# 10010023) with 5% Proteinase K (Thermo Scientific™, Cat# EO0491). 300 µL elution buffer and 100 µL of 0.1 mm Zirconia/Silica beads (BioSpec Products, Cat#

11079101Z) were added in 14 mL round bottom tubes (Corning, Falcon®, 352001) containing CandyCollect devices. After incubating the tubes at 37 °C for 10 min and vortexing for 50 s, CandyCollect devices were left in the elution buffer at 4 °C for 90 min. The bacteria suspension and beads were then transferred from the 14 mL round bottom tubes to 2 mL screw cap microtubes (ThermoFisher, Cat# 3490). The samples were beat-beaten in a MiniBeadBeater (BioSpec Products, Bartlesville, OK USA), and stored at -20 °C before analysis.

DNA isolation from mouth swab samples

DNA from mouth swab was isolated using MagMAX™ Total Nucleic Acid Isolation Kit (ThermoFisher Scientific, Cat# AM1840) according to the protocol "Disruption of liquid samples" supplied by the manufacturer. Briefly, 175 µL of aliquoted samples were transferred to each bead beating tube provided in the kit followed by the addition of 230 µL of Lysis/Binding solution. Bead beating was carried out via MiniBeadBeater (mentioned above) twice for 30 s, then each tube was centrifuged at 16,000 g for 3 min. Afterward, genomic DNA of *S. pyogenes* was isolated and enriched following the protocol stated above and quantified using qPCR with a detection limit of 5 fg.

Isolation, purification, and enrichment of genomic DNA from S. pyogenes

DNA was isolated from bacterial lysates using the MagMAX™ Total Nucleic Acid Isolation Kit (ThermoFisher Scientific, Cat# AM1840) according to the "Purify the nucleic acid" protocol supplied by the manufacturer. In brief, 115 µL of sample was added to the provided processing plate. 60 µL of 100% IPA was added to each well containing a sample and the plate was shaken for 1 min. 20 µL of bead mix was then added to each well, and the plate was shaken for 5 min to

allow DNA to bind to the beads. Beads were captured using a magnetic 96-well separator (Thermofisher, Cat# A14179) and supernatant was discarded. Four washes (two using Wash Solution 1 and additional two using Wash Solution 2 provided by the kit) were performed with shaking for 1 min each and supernatant was discarded between each wash. After final wash, beads were dried and then 23 µL of 65°C elution buffer was added to each sample to elute DNA from the beads. By using these methods, DNA was five-fold concentrated compared to the unprocessed bacterial lysates. The purified bacterial genomic DNA was used as a template in the qPCR assay.

Quantitative PCR assay for detection S. pyogenes

The details for the qPCR assay for *S. pyogenes* followed the protocol from our previous paper.[1] Briefly, the primers/probe sequences for *spy1258* qPCR detection of *S. pyogenes* in our assay were: the forward primer: 5'-GCA CTC GCT ACT ATT TCT TAC CTC AA-3'; the reverse primer: 5'-GTC ACA ATG TCT TGG AAA CCA GTA AT-3'; the probe sequence: 5'-FAM-CCG CAA C"T"C ATC AAG GAT TTC TGT TAC CA-3'-SpC6, "T" = BHQ1.1 The primers were ordered from IDT, the probe was ordered from MilliporeSigma. The 25 µL reaction volume included 10 µL of DNA template and 15 µL PerfeCTa® qPCR ToughMix with primers/probe in the qPCR assay. The final concentrations of both forward and reverse primers were 300 nM; the probe concentration was 100 nM. To quantify the DNA concentrations of samples, 1:10 serial dilution of purified genomic DNA ranging from 5 ng to 5 fg were used as standards for each plate. No-template controls (NTC) for qPCR and device negative controls were also added to the plates. Amplification and detection were performed in 96-well PCR plates using CFX connect Real-Time PCR Detection System (Bio-Rad Laboratories, Hercu-les, CA, USA) in technical duplicate using the following protocol: 95 °C for 5

min followed by 40 cycles of 15 s at 95 °C and 30 s at 60 °C. The samples were considered positive when the Ct value is within the Ct of the standard curve.

Threshold cycle (Ct) evaluation for positive results of human subject samples

To evaluate qPCR efficiency and specificity, a 1:10 serial dilution of purified genomic DNA (5 ng - 5 fg) isolated from *S. pyogenes* was used to construct a standard curve (Figure C6A and C6B) along with the following three different negative controls: 1. Device control - experiments were performed with CandyCollect devices running through all the procedures using PBS, instead of *S. pyogenes* suspension. 2. Other bacterial species controls - experiments were performed with *Streptococcus mutans* and *Staphylococcus aureus*. 3. qPCR control - elution buffer from the MagMAX™ Total Nucleic Acid Isolation Kit was used as non-template control (Figure C6C). While all DNA concentrations of DNA standard generate normal PCR amplification curves, all negative controls either did not show any amplification curve or resulted in the Ct value higher than 40, indicating PCR specificity. Furthermore, the efficiency of the qPCR standard is within 100-103 %. After resolving on 3% agar gel, a single band was shown for qPCR products from all tested concentrations of standards, further validating the specificity of qPCR amplification (Lee et al. Figure S4).[3] Clinical samples were run across three PCR plates, and a standard curve was run separately on each plate. The Ct values for the lowest concentration of DNA standards (5 fg) were 37.96, 38.88, and 38.23, and we compared the Ct values of the samples with the lowest Ct value of standard curve on the same plate. This number was used as a cut-off number for differentiating positive and negative detection. Any Ct value below or equal to Ct values for the lowest concentration of DNA standards (5 fg) on the same plate was considered positive, and all clinical samples were below the cycle threshold and therefore positive.

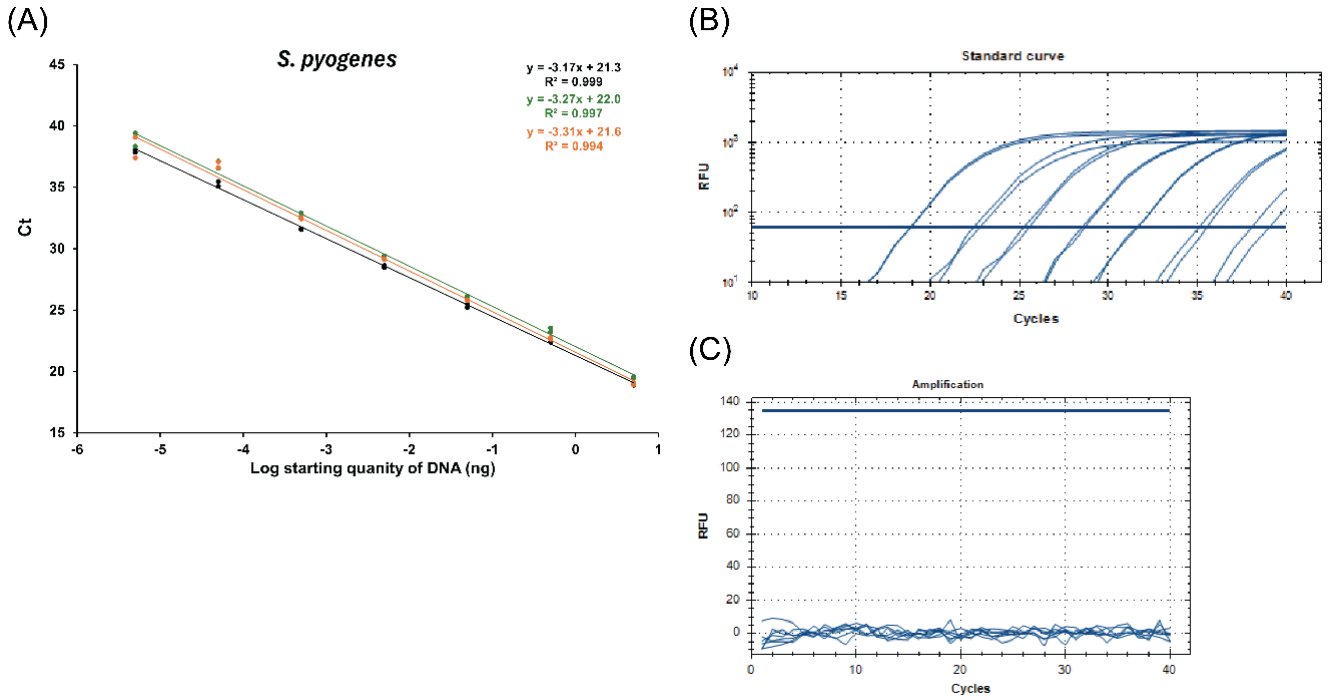

Figure C4. (A) Standard curves for the *S. pyogenes* qPCR assays. 1:10 serial dilutions of genomic DNA ranging from 5 ng to 5 fg were used as templates for qPCR. Each dot represents one technical duplicate (in cases where one point is visible the duplicates were identical). (B) The qPCR amplification plots of standard curve and (C) the qPCR amplification plots of negative controls from a representative of three qPCR plates.

References

1. Tu W-c, McManamen AM, Su X, et al. At-Home Saliva Sampling in Healthy Adults Using CandyCollect, a Lollipop-Inspired Device. *Analytical Chemistry*. 2023;95(27):10211-10220. doi:10.1021/acs.analchem.3c00462
2. Wong-Baker FACES® Pain Rating Scale https://wongbakerfaces.org/
3. United States Census Bureau. https://www.census.gov/quickfacts/fact/table/danecountywisconsin#. Accessed Novemebr 17, 2023.
4. Lee UN, Su X, Hieber DL, et al. CandyCollect: at-home saliva sampling for capture of respiratory pathogens. *Lab Chip.* 2022;22(18):3555-3564. doi:10.1039/d1lc01132d